UNIVERSITÄTSKLINIKUM HAMBURG-EPPENDORF

Institut für experimentelle Immunologie und Hepatologie

Prof. Dr. rer. nat. Gisa Tiegs

Cross-presentation capabilities of proximal tubular epithelial cells and the relevance in glomerulonephritis

Dissertation

zur Erlangung des Grades eines Doktors der Medizin
an der Medizinischen Fakultät der Universität Hamburg.

vorgelegt von:

Hakan Cicek
aus Flensburg

Hamburg 2023

Angenommen von der
Medizinischen Fakultät der Universität Hamburg am: 04.03.2024

Veröffentlicht mit Genehmigung der
Medizinischen Fakultät der Universität Hamburg.

Prüfungsausschuss, der/die Vorsitzende: Prof. Dr. Ulf Panzer

Prüfungsausschuss, zweite/r Gutachter/in: Prof. Dr. Gisa Tiegs

Content

1 Aims of this study

Glomerulonephritides are autoimmune-mediated glomerular diseases, the mechanisms of which are currently the subject of intensive research. It could be shown previously that $CD8^+$ T cells contribute to renal damage during glomerulonephritis. In addition, modulation of T cell activity by renal intrinsic antigen presenting cells (APCs) was shown to be essential for disease progression. Although APC functions are classically associated with immunological cell populations like dendritic cells (DCs) or macrophages, structural cells can also function as (non-professional) APCs. Accordingly, in 2019 it was shown, that proximal tubular epithelial cells (PTECs) can activate cluster of differentiation (CD)4^+ T cells, inducing an inflammatory phenotype and proliferation. The present study aimed to assess the ability of PTECs to exert such immunomodulatory functions towards $CD8^+$ T cells, and the possible relevance of this postulated ability in glomerulonephritis.

An important mechanism for the activation of naïve $CD8^+$ T cells is the capability of APCs to present exogenous antigen on major histocompatibility complex (MHC) class I molecules, which is called cross-presentation. In order to investigate the capability of PTECs to cross-present, in this study ribonucleic acid (RNA) and protein expression analyses of target genes/proteins associated with cross-presentation were conducted, in which the PTECs were compared to DCs as a population of professional and liver sinusoidal endothelial cells (LSECs) as a well-described population of non-professional APCs.

As internalization of exogenous antigen is a prerequisite for cross-presentation, the kinetic of model antigen uptake by PTECs was studied to pursue the question, if PTECs are able to internalize exogenous antigen in an active process.

Finally, this study aimed to assess the possibility of the modulation of $CD8^+$ T cells by PTECs as non-professional APCs in vivo, which could contribute to the pathogenesis of glomerulonephritis. As such an interaction requires cell-to-cell contact, an immunohistochemical staining was established to analyze the number and location of $CD8^+$ T cells in kidney sections of different murine models of glomerulonephritis.

In summary, this study aims to provide insights, that may help to identify PTECs as a population of tissue-resident non-professional APCs that may contribute to cell-mediated autoimmune cytotoxicity through their activation of $CD8^+$ T cells during glomerulonephritis.

2 Introduction

2.1 Glomerulonephritis

Glomerulonephritides are autoimmune-mediated renal inflammations, that can damage the glomeruli and the tubulointerstitium. They can be classified according to clinical presentation, aetiology or pathological findings. In clinical practice, the clinical manifestation is the first diagnostic tool to further classify the disease entity. Typical clinical presentations of glomerulonephritis are the nephritic and the nephrotic syndrome (Chadban and Atkins, 2005). The nephritic syndrome encompasses a symptom complex of proteinuria, hematuria and impairment of renal function, resulting in salt and water retention, possibly edema – especially of the eyelids – and hypertension. Urine samples show typically shaped erythrocytes (acanthocytes), caused by deformation occurring when the erythrocytes pass the glomerular filter (Lamba et al., 2020). The nephrotic syndrome summarizes proteinuria (>3.5 g per 1.73 m^2 body surface area in 24h, typically more pronounced than in nephritic syndromes), hypoalbuminemia, hyperlipidemia, and generalized edema. Additionally, due to the loss of antithrombotic factors and immunoglobulins (Igs) through the damaged glomerular filtration barrier, thrombophilia and susceptibility to infections can occur (Politano et al., 2020). However, glomerular diseases do not always present themselves clearly with one of these two syndromes, and mixed forms are possible. The most aggressive course of glomerulonephritis is the rapidly progressive or crescentic glomerulonephritis (cGN). It is mostly associated with a nephritic syndrome and can lead to renal failure within a few weeks. Furthermore, a glomerulonephritis can present itself as a chronic disease with persistent proteinuria and slowly progressing loss of renal function, and asymptomatic courses are possible, where only minor urinary abnormalities without further symptoms are present (Chadban and Atkins, 2005).

For further diagnosis, a kidney biopsy is often the decisive tool. Aetiologically, glomerulonephritis can be categorized into primary or secondary glomerulonephritis. Secondary glomerulonephritis has its underlying cause in systemic diseases such as systemic autoimmune disorders, infections or malignancy, that can lead to glomerular damage by the deposition of immune complexes or pathological complement activity (Lech and Anders, 2013, Tang and Lai, 2013, Couser, 2017). Typical diseases, that cause a secondary glomerulonephritis are systemic lupus erythematosus (SLE) (Almaani et al., 2017), antineutrophil cytoplasmic antibodies (ANCA)-associated

vasculitis (Berden et al., 2010) or an infection with streptococci (Sesso et al., 1986). Examples for primary glomerulonephritides are the IgA nephropathy, the dense deposit disease and the Goodpasture's disease (Floege and Amann, 2016). Besides these rather etiological classifications, glomerulonephritides are also classified according to the histological findings in conventional, electron or fluorescence microscopy or in immunohistochemistry. Histologically, the glomerular pathologies can be described as membranous, membranoproliferative or focal segmental glomerulonephritis or as minimal change disease (Alchi and Jayne, 2010, Floege and Amann, 2016, Vivarelli et al., 2017, Rosenberg and Kopp, 2017, Ronco et al., 2021). These are rather descriptive terms and various secondary diseases can manifest with each of these lesion pattern (Floege and Amann, 2016). However, primary forms of glomerulonephritis, named after the lesion pattern, are being diagnosed, not infrequently, because a secondary cause cannot be found or the cause is unknown. This approach is not without controversy, e.g., regarding the question if the minimal change disease and the focal segmental glomerulonephritis are two different diseases and if the primary membranoproliferative glomerulonephritis really exists (Cho et al., 2007, Fervenza et al., 2012). An exception to this is primary membranous glomerulonephritis, in which autoantigens have been identified as targets that cause the disease (Beck et al., 2009, Tomas et al., 2014). The use of phenotypical histological findings for disease definition and the ambiguities in disease delineation show, that underlying aetiologies and pathomechanisms are still only poorly understood in inflammatory glomerular diseases. Another possible histological finding in kidney biopsies is the formation of crescents. These crescents are caused by the proliferation of parietal epithelial cells, which leads to tubular obstruction, loss of nephron function and tubulointerstitial inflammation (Le Hir and Besse-Eschmann, 2003, Smeets et al., 2009). Crescent formation in >50% of the glomeruli defines the cGN, which requires rapid therapeutic intervention to prevent end stage kidney disease (Moroni and Ponticelli, 2014). According to the deposition pattern of immunoglobulins in fluorescence microscopy, the cGN is classified into three types: Type I shows linear deposition of immunoglobulins and is associated with the Goodpasture's disease, where antibodies against the non-collagenous domain of α3 type IV collagen of the glomerular basement membrane (GBM) are present, Type II is characterized by granular depositions and can be caused by various diseases, that are associated with the formation of immune complexes such as SLE or IgA vasculitis, Type III shows no depositions (also called

pauci) and is associated with ANCA-associated vasculitis (Moroni and Ponticelli, 2014).

Therapeutic regimes include basic measures such as blood pressure control, treatment of dyslipidemia with lifestyle modifications and statins, and symptomatic therapy of edema with diuretics. Anticoagulation and administration of vaccinations may be considered in patients with nephrotic syndrome and the loss of respective proteins. The immunosuppressive therapy encompasses corticosteroids, azathioprine, cyclophosphamide, calcineurin inhibitors and mycophenolate mofetil. However, these drugs are unspecific and severe side effects may include the occurrence of malignancies or severe infections (Rovin et al., 2021). Biologicals against B cells like Rituximab, which targets CD20, or Belimumab, which targets the B-cell activating factor, are more directed agents, but not as efficient as the conventional immunosuppressive drugs, are not yet part of the first line therapy and are used in combination with conventional immunosuppressants (Furie et al., 2020, Ronco et al., 2021). Further investigations into the disease pathology may lead to the development of other specific and more effective targeted therapies. End-stage kidney diseases require the application of dialysis or a kidney transplantation as ultima ratio (Rovin et al., 2021).

2.1.1 Mechanisms of immune-mediated glomerular damage

The contribution of immunoglobulins (Beck et al., 2009, Lech and Anders, 2013, Hellmark and Segelmark, 2014, Tomas et al., 2014, Couser, 2017, Goel et al., 2018, Alsharhan and Beck, 2021), the complement system (Berthoux et al., 2008, Smith et al., 2011, Fervenza et al., 2012, Pickering et al., 2013, Khalighi et al., 2016) and the coagulation system (Cunningham et al., 2000, Heuberger and Schuepbach, 2019) to the pathogenesis of glomerulonephritis is well known and has been studied in various previous works. As this study will focus on the modulation of $CD8^+$ T cell responses by kidney intrinsic cells, the current knowledge about the contribution of $CD8^+$ T cells and their modulation by kidney intrinsic cells to the pathogenesis of glomerulonephritis will be discussed in more detail in the following two chapters.

2.1.1.1 $CD8^+$ T cells

T cells can be divided into the $CD4^+$ and $CD8^+$ T cells, which can differentiate upon activation into effector $CD4^+$ T helper or cytotoxic $CD8^+$ T cells. Effector $CD4^+$ T helper

cells can stimulate the production of antibodies by B cells or attract neutrophils or macrophages and stimulate their expression of cytotoxic mediators, and thereby contribute to immune-mediated damage during glomerulonephritis (Reynolds et al., 2000, Summers et al., 2009, Kitching and Holdsworth, 2011, Hopfer et al., 2012, Hu et al., 2016). Effector cytotoxic $CD8^+$ T cells exert cell-mediated cytotoxicity by release of perforin and granzyme B (GzmB) or by binding to FAS, which leads to cleavage of caspase 3 in their target cells and induction of apoptosis (Barry and Bleackley, 2002). Thus, cytotoxic $CD8^+$ T cells play a pivotal role in adaptive immunity against intracellular infections and malignancy.

In a vast array of autoimmune disorders, the contribution of $CD8^+$ T cells has been shown or suggested, which can be mediated by direct cytotoxic effects and the attraction of other immune cells via chemokines, that are released from $CD8^+$ T cells (Walter and Santamaria, 2005). Regarding autoimmune-mediated renal damage, early studies reported periglomerularly located leukocytic infiltrates in renal biopsies of human and experimental glomerulonephritis and drew a correlation between these infiltrates and the formation of crescents and the disruption of the bowman's capsule (Boucher et al., 1987, Lan et al., 1992). Studies of human lupus nephritis showed renal infiltration of $CD8^+$ T cells, which were associated with crescent formation, rupture of bowman's capsule and poor response to therapy (Murata et al., 2002, Couzi et al., 2007). In anti-GBM glomerulonephritis $CD8^+$ T cells contribute to the disease pathology and the extent of the renal infiltration by $CD8^+$ T cells correlates with the severity of the disease (Merkel et al., 1996, Hu et al., 2016). Depletion of $CD8^+$ T cells in studies with murine anti-GBM glomerulonephritis models reduced the disease severity and prevented crescent formation (Kawasaki et al., 1992, Reynolds et al., 2002). In blood samples of patients with ANCA-associated vasculitis it could be shown that higher numbers of $CD8^+$ T cells aggravate the disease, which was hypothesized to be due to the activation of neutrophils by secretion of interferon (IFN)-γ (Iking-Konert et al., 2008). In renal biopsies of patients with ANCA-associated glomerulonephritis the number of macrophages and $CD8^+$ T cells correlated with the impairment of renal function and was associated with crescent formation (Kidder et al., 2017). Another study with murine experimental anti-myeloperoxidase (MPO) glomerulonephritis, which is a mouse model for ANCA-associated glomerulonephritis, could show that the depletion of $CD8^+$ T cell before disease triggering results in decreased disease activity and reduced number of $CD4^+$ T cells and macrophages, which could be explained by

reduced $CD8^+$ T cell mediated cytokine and chemokine production. Furthermore, transfer of MPO-specific $CD8^+$ T cells into T and B cell-deficient *Rag1*$^{-/-}$ mice before disease induction was sufficient for development of glomerular lesions and macrophage recruitment. Interestingly, in-vitro assays that were conducted in that study with MPO-specific $CD8^+$ T cells, could show a release of the cytotoxic enzyme GzmB, suggesting a possible role of direct cytotoxic effects by $CD8^+$ T cells in experimental anti-MPO glomerulonephritis (Chang et al., 2017). In another study using another antigen-specific model to study the role of $CD8^+$ T cells in glomerulonephritis, transgenic mice with podocytes, that express enhanced green fluorescent protein (EGFP), were transfected with EGFP-specific $CD8^+$ T cells. Podocytes form the third layer of the glomerular filtration barrier and are located inside of the bowman's capsule. Thus, the transfer of the EGFP-specific $CD8^+$ T cells alone did not result in glomerular damage as the bowman's capsule prevented access of $CD8^+$ T cells to podocytes. However, after the induction of severe glomerulonephritis, which led to the disruption of the bowman's capsule in some glomeruli, significantly higher glomerular damage could be observed in glomeruli of transgenic mice with EGFP-expressing podocytes, that had received EGFP-specific $CD8^+$ T cells. This effect was especially pronounced regarding podocyte apoptosis, suggesting that the direct contact of antigen-specific $CD8^+$ T cells could lead to direct $CD8^+$ T cell-mediated cytotoxicity, that drives glomerulonephritis (Chen et al., 2018). Most recently, the role of $CD8^+$ T cells in glomerulonephritis was studied in 2023 by Mueller et al. This study used blood samples and renal biopsies from patients with ANCA-associated glomerulonephritis to perform single cell analyses of T cells. In these analyses a clonally expansion of *Gzmb*$^+$ cytotoxic $CD8^+$ T cells could be observed. The same observation could be made in analyses of T cells from kidneys of mice with experimental cGN. Furthermore, *Cd8a*$^{-/-}$ mice and *Gzmb*$^{-/-}$ mice, which lack GzmB, showed ameliorated renal damage in experimental cGN. This correlated with reduced induction of apoptosis inducing cleaved caspase 3 in renal tissues of *Gzmb*$^{-/-}$ and *Cd8a*$^{-/-}$ mice. Thus, this study was not only able to show, that $CD8^+$ T cells contribute to renal damage during glomerulonephritis, but also gave hints, that the T cell response during glomerulonephritis is antigen specific and that direct cytotoxic effects, mediated by the secretion of GzmB by $CD8^+$ T cells, contribute to renal damage (Mueller et al., 2023).

2.1.1.2 Modulation of T cell responses by intrinsic kidney cells

Before T cells can fulfill their effector function, they first need to be activated. Activation requires costimulatory signals in addition to T cell receptor (TCR) signaling, which can be transduced by binding of the co-stimulatory molecules CD80 and CD86 to CD28 on T cells (Mueller et al., 1989). CD80 and CD86 are surface proteins on APCs, that are upregulated during inflammation and thus regulate T cell responses (Banchereau and Steinman, 1998, Banchereau et al., 2000, Hammer and Ma, 2013). The role of APCs is classically occupied by DCs or macrophages – leukocytic cell populations, of which DCs have been described as the most potent APCs (Banchereau and Steinman, 1998). Encounter of DCs with pathogenic antigen induces a maturation process, which leads to the migration of DCs to a draining lymph node and activation of antigen-specific T cells, that migrate to the site of the immune response (Banchereau and Steinman, 1998, Mellman and Steinman, 2001). However, under homeostasis APCs such as DCs can mediate tolerance to self or foreign antigens, which is an important mechanism to prevent autoimmunity or excessive immune reactions. If an APC induces immunity or tolerance, depends on additional stimuli such as the presence of pathogen associated products, that induce APC activation (Banchereau and Steinman, 1998, Banchereau et al., 2000, Hawiger et al., 2001, Théry and Amigorena, 2001, Joffre et al., 2012).

The kidney is populated by a vast number of DCs, that continuously take up glomerular filtrated antigen and present it to T cells, which under homeostasis leads to the induction of tolerance against harmless antigens (Kaissling and Le Hir, 1994, Woltman et al., 2007, Lukacs-Kornek et al., 2008). Interestingly, kidney-intrinsic DCs are reported to attenuate the course of glomerulonephritis in early stages of disease (Scholz et al., 2008). However, in the course of glomerulonephritis, DCs can become proinflammatory by regulation of the expression of co-stimulatory and co-inhibitory molecules in favor of stimulation and secretion of proinflammatory cytokines, and thus aggravate the course of disease. Additionally, proinflammatory monocytes infiltrate the kidney during glomerulonephritis and differentiate into proinflammatory DCs. Accordingly, depletion of DCs at an early stage of disease aggravates, whereas depletion at a later time point attenuates glomerulonephritis (Scholz et al., 2008, Heymann et al., 2009, Hochheiser et al., 2011). This attenuating effect of DC depletion at a later time point was shown by Heymann et al. using a mouse model for experimental glomerulonephritis, in which the disease is induced by injection of

ovalbumin (OVA)-specific $CD8^+$ T cells and activated OVA-specific $CD4^+$ T cells into transgenic mice, in which the podocytes express OVA. In that study, the depletion of DCs at a later time point (day 5) led to the disappearance of infiltrating leukocytes and a reduction of renal inflammation after just 40 hours. Thus, it was concluded, that kidney intrinsic DCs not only mediate the infiltration of $CD8^+$ T cells and other leukocytes into the kidney, but are also required to maintain the presence of infiltrating immune cells (Heymann et al., 2009).

2.2 Antigen cross-presentation

Antigen cross-presentation is a mechanism attributed to APCs by which exogenous antigen can be presented on MHC-I molecules, on which usually endogenous antigens are presented. Since infections and malignancy do not necessarily also affect APCs, whereby APCs could present the respective antigens as endogenous proteins on MHC-I, cross-presentation is an additional important mechanism for APCs to activate $CD8^+$ T cells (Sigal et al., 1999, den Haan and Bevan, 2001, Théry and Amigorena, 2001, Joffre et al., 2012).

Two pathways of antigen-cross presentation are described: the vacuolar and the endosome-to-cytosol pathway, with the significant difference between them being the antigen processing machinery and its location within APCs. Whilst in the vacuolar pathway antigen is processed in the lyso-/endosome via Cathepsin S (Shen et al., 2004), in the endosome-to-cytosol pathway the internalized antigen is translocated from endosomes into the cytosol, where it is processed by the proteasome. This proteasome-dependent endosome-to-cytosol pathway is described to be more important for cross-presentation, which seems plausible, because for sufficient T cell response, the epitopes generated by cross-presentation must be the same as the ones generated by the infected/malignant cell, which are generated via degradation by the proteasome and not by Cathepsin S (Embgenbroich and Burgdorf, 2018). Since it is more relevant, the endosome-to-cytosol pathway was investigated in this study and will be described in more detail in this chapter.

Processes, that are involved in this pathway, are antigen internalization, the translocation of antigen from endosomes into the cytosol, the proteasomal degradation of the antigen, the translocation of peptides back into endosomes, the alkalization of endosomes and peptide trimming in endosomes, which is followed by loading of the

peptides onto MHC-I molecules, which are then finally transportet to the cell surface to present the antigen-derived peptides.

APCs have various mechanisms of antigen internalization, such as pinocytosis, scavenger receptors and endocytosis via the mannose receptor (Watts, 1997, Burgdorf et al., 2007). However, targeting of the internalized antigens into the proper endosomal compartments with low lysosomal activity is essential for efficient antigen cross-presentation, as the antigens need to be stable and protected from rapid degradation after internalization (Delamarre et al., 2005, Chatterjee et al., 2012). In comparison to pinocytosis or endocytosis via scavenger receptors, this proper targeting occurs after antigen internalization by the mannose receptor, as it was shown that in comparison only antigen, that is internalized via the mannose receptor, is cross-presented to $CD8^+$ T cells and leads to their activation (Burgdorf et al., 2007, Chatterjee et al., 2012).

Furthermore, internalized antigens are protected from rapid degradation in cross-presenting APCs by a priori low lysosomal activity (Lennon-Duménil et al., 2002, Delamarre et al., 2005) as well as alkalization of the endosomes by the NADPH oxidase 2 (Nox2), which generates reactive oxygen species (ROS), that capture protons, thereby alkalizing endosomes and thus preventing the pH-dependent activation of lysosomal proteases (Savina et al., 2006, Mantegazza et al., 2008).

After internalization and trafficking into a non-degrading endosome, the antigen needs to be translocated into the cytosol for proteasomal degradation. There is strong evidence, that this transport is mediated through the endoplasmic reticulum (ER)-associated degradation (ERAD) machinery, that is also described to translocate misfolded proteins form the ER into the cytosol for degradation (Hiller et al., 1996, Ackerman et al., 2003, Ye et al., 2004, Lilley and Ploegh, 2004, Imai et al., 2005, Ackerman et al., 2006, Goldszmid et al., 2009, Krshnan et al., 2022). Closely associated with the ERAD is the AAA ATPase p97, and it could indeed be shown, that cross-presentation is p97-dependent (Ackerman et al., 2006, Zehner et al., 2011, Ménager et al., 2014). Interestingly, it was shown that mannose receptor ubiquitination, which is required for antigen transport into endosomes, also recruits p97 to antigen-containing endosomes, highlighting the interplay between antigen internalization and provision of the ERAD machinery for antigen export from endosomes during cross-presentation (Zehner et al., 2011). However, the question of the exact translocon has not yet been finally clarified. Derlin-1 and Sec61 are two membrane pore complexes, that are associated with the ERAD machinery (Lilley and Ploegh, 2004). Studies

particularly emphasize the role of Sec61 in antigen translocation across endosomal membranes into the cytosol (Koopmann et al., 2000, Imai et al., 2005, Ackerman et al., 2006, Zehner et al., 2015). Strong evidence could be provided by a recent work, in which specifically the recruitment of Sec61 to endosomal membranes was blocked using an intrabody, that trapped Sec61 in the ER. While the ERAD machinery as such was not affected by the intrabody, as demonstrated by preserved cytosolic degradation of TCRα and CD3δ, that are transported into the cytosol in an ERAD-dependent manner, cross-presentation was affected by lack of recruitment of Sec61 to endosomal membranes. The presentation of endogenous antigens on MHC-I, MHC-II-dependent antigen presentation and the activation of T cells by peptide-loaded DCs was not affected. In the same study, it could be shown, that downregulation of Derlin-1 does not impair cross-presentation (Zehner et al., 2015). However, another, although debated proposal for entering of internalized endosomal antigens into the cytosol includes the translocation of antigens not via a translocon but rather by endosomal leakage. The proposing study could show, that NOX2-generated ROS lead to lipid peroxidation and that lipid peroxidation leads to the entrance of endosomal peptides into the cytosol by leakage. Inhibition of NOX2 or lipid peroxidation showed an effect similar to inhibition of the proteasome and led to impaired cross-presentation. This leakage-dependent translocation especially effected large peptides and it was concluded, that lipid peroxidation-mediated endosomal leakage contributes to transendosomal antigen translocation complementary to Sec61 by translocating large peptides (Dingjan et al., 2016). However, the uncontrolled passage of endosomal components is reported to induce inflammasome activation, which in turn can lead to cell death. Thus, the idea of transendosomal antigen transport by unspecific leakage is contested (Hornung et al., 2008, Próchnicki et al., 2016, Embgenbroich and Burgdorf, 2018).

After the antigen is transported into the cytosol, it can be degraded into peptides, which is a necessary step, since on MHC-I whole proteins cannot be presented but derived peptides. Whilst the peptides, that will be presented on MHC-I can be generated by the proteasome, another type of proteasome, called the immunoproteasome is constitutively expressed on higher levels in APCs compared to regular cells. The expression of this immunoproteasome can be upregulated under inflammatory conditions such as in the presence of IFN-γ . IFN-γ mediates the synthesis of the three alternative proteasomal subunits low-molecular-weight protein (LMP) 2, LMP7 and

multicatalytic endopeptidase complex subunit (MECL) 1, which are incorporated into the proteasome after synthesis. In contrast to the proteasome, the immunoproteasome enables the generation of peptides, that are more efficient in triggering immune responses (immunodominant peptides) (Aki et al., 1994, Chen et al., 2001, Palmowski et al., 2006, Guimarães et al., 2018). After degradation the peptides are translocated back into endosomes for loading onto MHC-I molecules. Such transport is described to occur dependent on the transporter associated with antigen processing (TAP), especially for antigens internalized by endocytosis (Kovacsovics-Bankowski and Rock, 1995, Ackerman et al., 2003, Guermonprez et al., 2003, Burgdorf et al., 2008, Merzougui et al., 2011). However, TAP-independent entering of peptides into phagosomes, which can be subsequently cross-presented, has been described previously, suggesting the possibility of another, although less efficient transporter for peptide translocation, that may also affect endosomes (Merzougui et al., 2011, Lawand et al., 2016).

After reentering the endosome, the peptides are trimmed by the insulin-regulated aminopeptidase (IRAP) (Saveanu et al., 2009) and finally loaded onto MHC-I molecules to be present to $CD8^+$ T cells on the cell surface of APCs.

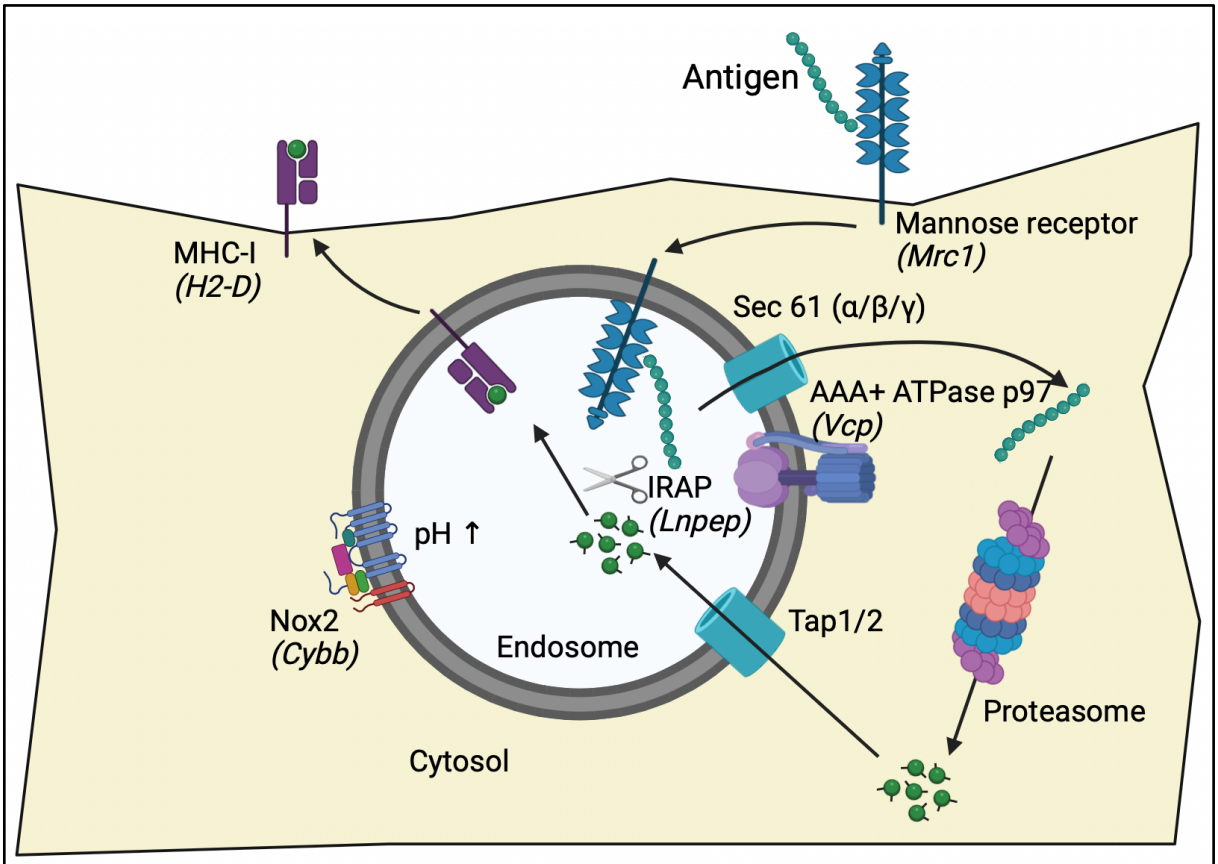

Figure 1: The endosome-to-cytosol pathway of antigen cross-presentation
Depiction of proteins, associated with the endosome-to-cytosol pathway of cross-presentation for soluble antigens. Gene names are written in brackets below in italics. Soluble antigen is internalized via the mannose receptor into non-degrading endosomes, which are alkalized by Nox2 for antigen stability. After translocation from the endosome into the cytosol via the ERAD under contribution of the ATPase p97 and Sec61, the antigen is degraded by the proteasome. Afterwards, the antigen is translocated back into an endosome by Tap and trimmed by IRAP, before being loaded onto MHC-I. Finally, the antigen is presented on MHC-I on the cell surface.
Based on a figure from (Embgenbroich and Burgdorf, 2018). Created with BioRender.com.

2.3 Non-professional antigen presenting cells

The presentation of exogenous antigens is an APC function and thus in classical immunology limited to leukocytes such as DCs or macrophages. However, since this first concept of APC biology, later studies could show, that also non-immunological, structural cell populations such as epithelial, endothelial or stromal cells are capable to present exogenous antigen, either on MHC-II or by cross-presentation on MHC-I (Krausgruber et al., 2020, Harryvan et al., 2021). As these cells perform APC functions, but do not belong to the classical APC cell populations, they are referred to as non-professional APCs. Non-professional APCs are often in contact with antigens from the intestine, the respiratory system or the blood stream, and it has indeed been shown, that in homeostasis non-professional APCs can induce tolerance (Pinchuk et al., 2008, Pinchuk et al., 2011, Hutton et al., 2017), which can generally be explained by the balance between co-stimulatory and co-inhibitory signals, that are transduced by the non-professional APC to T cells (Pinchuk et al., 2008, Diehl et al., 2008). However, similar to DCs, the expression of co-stimulatory molecules can be upregulated in non-professional APCs under inflammatory conditions (François et al., 2009, Harryvan et al., 2021). Moreover, the presence of a proinflammatory microenvironment can potentially override existing inhibitory signals, leading to a net stimulation of T cells (Schurich et al., 2010). A well-studied population of non-professional APCs are the liver sinusoidal endothelial cells (LSECs). LSECs are potent inducers of tolerance and, interestingly, the expression of the co-stimulatory molecules CD80 and CD86 is not upregulated in LSECs, even under inflammatory conditions. However, certain inflammatory stimuli can induce LSEC maturation and lead to the induction of immunity in T cells by LSECs, although not by co-stimulation via CD80 and CD86, but by secretion of stimulating cytokines (Kern et al., 2010, Schurich et al., 2010, Liu et al., 2013, Huang et al., 2018). As potent inducers of tolerance, the LSECs present exogenous antigen on MHC-II to $CD4^+$ T cells or via cross-presentation on MHC-I to $CD8^+$ T cells and contribute to what is known as the “liver tolerance effect”, which describes effects such as tolerance towards transplants and oral antigens as well as weaker immune activity against liver infections and metastasis and can be explained by an interplay of LSECs, Kupffer cells, hepatic stellate cells, hepatocytes and hepatic DCs acting as tolerance inducing (non)-professional APCs. (Knolle et al., 1999, Limmer et al., 2000, Diehl et al., 2008, Kruse et al., 2009, Tiegs and Lohse, 2010, Shetty et al., 2018). In autoimmune diseases, it could be shown, that non-professional

APCs can induce a proinflammatory phenotype in T cells and propel disease progression (Boots et al., 1994, Savinov et al., 2003).

2.3.1 Proximal tubular epithelial cells

The proximal tubular epithelial cells (PTECs) in the kidney form the epithelia of the first segment of the nephron, which begins at the bowman's capsule and ends at the proximal descending part of the loop of Henle. Equipped with the brush border, that enlarges their surface area, the PTECs have the highest absorptive capacity amongst the renal tubular cells. The reabsorption of approximately two thirds of the sodium and water as well as all amino acids and all of the glucose takes place in the proximal tubule (Nakhoul and Batuman, 2011).

In the context of immunity, PTECs drew the attention of researchers at least as early as 40 years ago, when it was reported, that MHC-II molecules in the kidney cannot only be found on the surface of renal DCs but also on PTECs (Mayrhofer and Schon-Hegrad, 1983). Furthermore, similar to the observations with professional APCs, it was shown, that PTECs upregulate the expression of MHC-II under inflammatory conditions (Sinclair et al., 1984, Benson et al., 1985, Gastl et al., 1996). Additionally, also analogous to professional APCs, the PTECs upregulated the expression of the co-stimulatory molecules CD80 and CD86 under inflammatory conditions, whereas the expression correlated with the severity of inflammation and could be reproduced in vitro by simulating inflammatory stimuli (Niemann-Masanek et al., 2002, Wu et al., 2004). Recently, the PTECs were studied in 2019 by Breda et al. Using a fluorescence activated cell sorting (FACS) based protocol, the authors were able to show, that PTECs express MHC-II and co-stimulatory molecules such as CD80 and CD86 under steady state conditions. Interestingly, although the expression levels were generally lower compared to DCs, a higher proportion of PTECs expressed CD86 in comparison to DCs. Furthermore, in coculture experiments with naïve OVA-specific $CD4^+$ T cells in the presence of OVA peptide, it could be shown, that PTECs can induce activation of $CD4^+$ T cells with the production of the proinflammatory cytokines IFN-γ, IL-2 and tumor necrosis factor (TNF)-α and proliferation in vitro. However, as the cytokine production and the expression of activation markers was generally lower in PTEC-activated $CD4^+$ T cells in comparison to DC-activated ones, the PTECs were found to be a less potent APC population to induce immunity. Additionally, immunohistochemical staining of kidney biopsies from patients with ANCA-associated

vasculitis could show, that the co-stimulatory molecule CD86 is expressed by PTECs under inflammatory conditions. Thus, the PTECs were recently identified as non-professional APCs towards $CD4^+$ T cells and it was speculated that PTEC-mediated activation of $CD4^+$ T cells might contribute to the disease progression of glomerulonephritis (Breda et al., 2019).

3 Materials and Methods

3.1 Materials and equipment

3.1.1 Technical equipment

Table 1: Technical equipment

Technical equipment	Supplier
BZ-9000 Fluorescence Microscope	Keyence, Osaka, Japan
Canto II	BD Bioscience, Franklin Lakes, USA
Centrifuge 5427 R	Eppendorf, Hamburg, Germany
Centrifuge 5810 R	Eppendorf, Hamburg, Germany
CK40 Inverted Microscope	Olympus, Shinjuku, Japan
Eppendorf Research Plus pipettes (2.5, 10, 20, 100, 200 and 1000 µl)	Eppendorf, Hamburg, Germany
Galaxy 48 R CO_2 Incubator	Eppendorf, Hamburg, Germany
HandyStep touch	Brand, Wertheim, Germany
Heating block	Cole-Parmer, Wertheim, Germany
Infinite M200 Plate Reader	Tecan Group, Männerdorf, Switzerland
Mini Trans Blot Cell	Bio-Rad Laboratories, Hercules, USA
MSC-Advantage 1.8, clean bench	Fisher Scientific, Schwerte, Germany
MyCycler thermal cycler	BioRad, München, Germany
NanoDrop photometer ND-1000	PEQLAB Biotechnologie GmbH, Erlangen, Germany
Neubauer Improved Chamber	Roth, Karlsruhe, Germany
Pipetboy	Integra Bioscience, Hudson, USA
QuantStudio 7 Flex	Applied Biosystems, Waltham, USA
Sonorex Super RK100H, ultrasonic bath	Bandelin, Berlin, Germany
VersaDoc MP 4000	Bio-Rad Laboratories, Hercules, USA
Vortexer	Heidolph, Schwabach, Germany
High-speed centrifuge	Herolab, Wiesloch, Germany

Xcell SureLock Mini-Cell Electrophoresis System	Thermo Fisher, Waltham, USA

3.1.2 Consumables

Table 2: Consumables

Consumable	Supplier
24-well plate	Thermo Fisher Scientific, Waltham, USA
384-well plate	Sigma-Aldrich, St. Louis, USA
Centrifuge tubes (15 and 50 ml)	Thermo Fisher Scientific, Waltham, USA
Nitrocellulose	Thermo Fisher Scientific, Waltham, USA
NuPAGE 4 to 12%, Bis-Tris	Invitrogen, Carlsbad, USA
Polystyrene FACS tubes (5 ml)	BD Bioscience, Franklin Lakes, USA
Reaction tubes (0.2, 1.5 and 5 ml)	Eppendorf, Hamburg, Germany

3.1.3 Reagents and kits

Table 3: Reagents and kits

Reagents and kits	Supplier
2-mercaptoethanol (2-ME)	Sigma-Aldrich, St. Louis, USA
Antibody Diluent with background reducing components	Dako, Santa Clara, USA
Bloxall Blocking Solution SP-6000	Vector Laboratories, Burlingame, USA
Bovine serum albumin (BSA)	PAA Laboratories, Pasching, Austria
Bradford reagent	Thermo Fisher Scientific, Waltham, USA
CD11c microbeads, mouse	Miltenyi Biotec, Bergisch Gladbach, Germany
CD146 (LSEC) microbeads, mouse	Miltenyi Biotec, Bergisch Gladbach, Germany
Chloroform	Thermo Fisher Scientific, Waltham, USA
Collagenase V from Clostridium histolyticum	Sigma Aldrich, St. Louis, USA
Crystal mount	Sigma Aldrich, St. Louis, USA

DNA-free kit	Invitrogen, Carlsbad, USA
Dulbecco's Modified Eagle Medium: Nutrient Mixture F12 (DMEM/F12)	Gibco, Carlsbad, USA
DMEM, high glucose	Gibco, Carlsbad, USA
Entellan	Merck, Darmstadt, Germany
Ethanol (EtOH)	Sigma Aldrich, St. Louis, USA
Fetal bovine serum (FBS)	Sigma Aldrich, St. Louis, USA
Granulocyte-macrophage colony-stimulating factor (GM-CSF)	Sigma Aldrich, St. Louis, USA
Isopropanol	Sigma Aldrich, St. Louis, USA
L-Glutamin	Thermo Fisher, Waltham, USA
Luminol	Sigma Aldrich, St. Louis, USA
Mayer's hemalum solution	Sigma Aldrich, St. Louis, USA
New Fuchsin	Sigma Aldrich, St. Louis, USA
NuPAGE antioxidants	Invitrogen, Carlsbad, USA
NuPAGE LDS sample buffer	Invitrogen, Carlsbad, USA
NuPAGE reducing agent	Invitrogen, Carlsbad, USA
NuPAGE Running Buffer	Invitrogen, Carlsbad, USA
Nycodenz	Progen Biotechnik, Heidelberg, Germany
Para hydroxy coumarin acid	Sigma Aldrich, St. Louis, USA
Penicillin (10000 U/mL)/ streptomycin (10000 µg/mL)	Invitrogen, Carlsbad, USA
Percoll	GE Healthcare, Uppsala, Sweden
Ponceau S Staining Solution	Thermo Fisher, Waltham, USA
Precision Plus Protein Western Blotting Standards	Bio-Rad, Hercules, USA
Reducing agent, 10x	Thermo Fisher, Waltham, USA

Restore PLUS Western Blot Stripping-Puffer	Thermo Fisher Scientific, Waltham, USA
Roswell Park Memorial Institute (RPMI) 1640 medium	Gibco, Carlsbad, USA
Strep-Tactin-HRP conjugate	Bio-Rad, Hercules, USA
SYBR Green PCR Master Mix	Thermo Fisher Scientific, Waltham, USA
Target Retrieval Solution pH 6	Dako, Santa Clara, USA
Target Retrieval Solution pH 9	Dako, Santa Clara, USA
TRIzol	Thermo Fisher, Waltham, USA
Ketamine/xylazine	Sigma Aldrich, St. Louis, USA
Trypsin/EDTA	Sigma Aldrich, St. Louis, USA
Verso cDNA Synthesis Kit	Thermo Fisher Scientific, Waltham, USA
ZytoChem Plus (AP) Polymer Kit	Zytomed Systems, Berlin, Germany
2,6,10,14-tetramethylpentadecane (pristane)	Sigma-Aldrich, St. Louis, USA

3.1.4 Solutions

Table 4: Solutions

Solution	**Composition**
Ammonium chloride buffer	19 mM Tris/HCl 140 mM NH_4Cl pH 7.2
Chemiluminescence solution A	250 µg/ml Luminol solved in 0.1 M Tris/HCl
Chemiluminescence solution B	1.1 mg/ml Para hydroxy coumarin acid solved in DMSO
PTEC medium	500 ml DMEM/F12 1% FCS 1X I/T/S (insulin, transferrin, sodium selenite) 1% PenStrep 50 nM Hydrocortison 5 nM T_3 5 nM EGF
FACS buffer	PBS (5x) 1% BSA 15.4 mM NaN_3 (0.1%)

	pH 7.1
Hank's balanced salt solution (HBSS)	5.4 mM KCl 0.3 mM Na_2HPO_4 x 7 H_2O 4.2 mM $NaHCO_3$ 1.3 $CaCl_2$ 0.5 mM $MgCl_2$ x 6 H_2O 0.6 mM $MgSO_4$ x 7 H_2O 137 mM NaCl 5.6 mM D-Glucose pH 7.4
Gey's balanced salt solution (GBSS)	2.225 g/l $CaCl_2$ 0.21 g/l $MgCl_2$ x 6 H_2O 0.0342 g/l $MgSO_4$ 0.37 g/l KCl 0.03 g/l KH_2PO_4 2.27 g/l $NaHCO_3$ 7.0 g/l NaCl 0.12 g/l Na_2HPO_4 1.0 g/l D-glucose 2.27 g/l $NaHCO_3$
KLB buffer	25 mM Tris 150 mM NaCl 5 mM EDTA 10% Glycerol 1% Triton X-100 10 mM Na-pyrophosphate 1 mM Na-orthovanadate 10 mM Glycerol phosphate
MACS buffer	PBS (5x) 0.5% BSA 2 mM EDTA
Phosphate-buffered saline (PBS)	137 mM NaCl 10 mM Na_2HPO_4 x 2 H_2O 2 mM KH_2PO_4 2.7 mM KCl pH 7.4
Tris-buffered saline (TBS)	10 mM Tris (Trizma base) 150 mM NaCl pH 7.4
TBS-T	TBS (1x) 2% Tween
Western Blot transfer buffer	25 mM Tris 200 mM Glycin 20% Methanol
Tris NaCl Tween (TNT) buffer	50 mM Tris 150 mM NaCl 1% Tween pH 8,2 – 8,4
New Fuchsin working solution	150 ml TNT buffer 7.5 ml 4% Na-NO_2

	300 µl New Fuchsin stock solution (solved in 2N HCl, 0.05 g/ml) 800 µl Naphtol-AS-BI-phosphate (solved in NN-dimethylformamide, 2.5%)

For all buffers and solutions bi-distilled water (ddH_2O) was used, if not otherwise declared.

3.1.5 Primers for polymerase chain reaction

Table 5: Primers for polymerase chain reaction

Target	Forward primer (fw) Reverse primer (rv)	Amplicon length	Annealing temperature
Actb	(fw) TATTGGCAACGAGCGGTTCC (rv) GGCATAGAGGTCTTTACGGATGTC	180 bp	60°C
Mrc1	(fw) GGAGGCTGATTACGAGCAGT (rv) TCCAGGTGAACCCCTCTGAA	87 bp	60°C
Sec61a1	(fw) TTCTGTGTCATCTTGCCGGA (rv) TGCCAAACAGGGGGATCTGA	124 bp	60°C
Sec61b	(fw) TGAGTGCTCGGCAACTTCAC (rv) GGGACAGGGCCCACTTTGA	282 bp	60°C
Sec61g	(fw) GCTCTCAATCCGCCATCCAA (rv) AGGACTCAGCCACCCACAAT	237 bp	60°C
Vcp	(fw) TGACCCTCATGGATGGCCTA (rv) TGTCAAAGCGACCAAATCGC	108 bp	60°C
Tap1	(fw) GGCTTACGTGGCTGAAGTCT (rv) AATGAGACAAGGTTGCCGCT	123 bp	60°C
Tap2	(fw) TGTGCAGACGACTTCATAGGG (rv) ATCTCCAGTTCTGTAGGGCCTG	199 bp	60°C
Lnpep	fw) TTCGGCATGCTGTCATTCTT (rv) GAGTTTTGTCTGTGACCTCATTG	99 bp	60°C
Cybb	(fw) GCCAGTGTGTCGAAATCTG (rv) AATTGTGTGGATGGCGGTGT	145 bp	60°C
Psmb8	(fw) GCCAAGGAGTGCAGGTTGTAT (rv) GCCGAGTCCCATTGTCATCT	184 bp	60°C
H2-D1	(fw) GAAGGAGACTGTCTGGATGCT (rv) TGTTTTGCAGTCCACCTTGG	74 bp	60°C

2.1.6 Primary antibodies for western blot and immunohistochemistry

Table 6: Primary antibodies for western blot and immunohistochemistry

Name	Host	Clonality	Reactivity	Dilution	Supplier
Anti-CD3	rabbit	polyclonal	mouse, rat, human, pig	1:100	Agilent, Santa Clara, USA
Anti-CD8α	rabbit	monoclonal	mouse	1:200	Cell Signaling Technology, Cambridge, UK
Anti-GAPDH	mouse		mouse, rat, rabbit	1:1000	HyTest, Turku, Finland

Anti-LNPEP	rabbit	polyclonal	human, mouse, rat	1:1000	Thermo Fisher Scientific, Waltham, USA
Anti-MMR/CD206	goat	polyclonal	mouse	1:200	Thermo Fisher Scientific, Waltham, USA
Anti-NOX2	rabbit	polyclonal	human, mouse, rat	1:1000	Thermo Fisher Scientific, Waltham, USA
Anti-SEC61A1	rabbit	polyclonal	human, mouse, rat, primate	1:500	Thermo Fisher Scientific, Waltham, USA
Anti-TAP1	rabbit	polyclonal	human, mouse, primate	1:500	Thermo Fisher Scientific, Waltham, USA
Anti-VCP	rabbit	polyclonal	human, mouse, rat	1:1000	R&D Systems, Minneapolis, USA

3.1.7 Secondary antibodies for western blot and immunohistochemistry

Table 7: Secondary antibodies for western blot and immunohistochemistry

Name	Host	Conjugation	Reactivity	Dilution	Supplier
Anti-goat IgG (H+L)	rabbit	HRP	goat	1:5000	Jackson ImmunoResearch, Philadelphia, USA
Anti-mouse IgG (H+L)	goat	HRP	mouse	1:3000	Bio-Rad, Hercules, USA
Anti-rabbit IgG (H+L)	goat	HRP	rabbit	1:5000	Jackson ImmunoResearch, Philadelphia, USA

3.1.8 Fluorescence-labelled antibodies and substances for flow cytometry

Table 8: Fluorescence-labelled antibodies and substances for flow cytometry

Name	Clone	Host	Fluorescence	Dilution	Supplier
Anti-CD11c	N418	hamster	PE-Cy7	1:100	Biolegend, San Diego, USA
Fc-block (CD16/32)	93	rat		1:100	Biolegend, San Diego, USA
Ovalbumin, fluorescent			Alexa Fluor 647	see table 10	Thermo Fisher, Waltham, USA
Zombie NIR (viability stain)			APC/Cy7	1:1000	Biolegend, San Dieg USA

3.1.9 Software

Table 9: Software

Name	Supplier
FlowJo	FlowJo LLC, Ashland, USA
GraphPad Prism 9	GraphPad Software Inc., San Diego, USA
Microsoft Office Professional 2022	Microsoft, Washington, USA
Zen lite	Carl Zeiss AG, Oberkochen, Germany

3.2 Methods

3.2.1 Animals

C57BL/6 wild-type (WT) mice were bred in the animal facility of the University Medical Center Hamburg-Eppendorf (UKE; Hamburg, Germany). The MRL/MpJ (MRL) and the MRL/MpJ-*Fas*^{lpr}/J (MRL-lpr) mice were acquired from the Jackson Laboratory (Bar Harbor, USA). Mice breeding was conducted according to the Federation of European Laboratory Animal Science Association guidelines, and specific-pathogen-free conditions were maintained. All mouse experiments were approved by the Behörde für Justiz und Verbraucherschutz (Hamburg, Germany; approval codes: N057/19, ORG 960, ORG 1032), and they were carried out according to the current existing guidelines on mouse experimentation. All efforts were made to minimize suffering.

MRL/MpJ-*Fas*^{lpr}/J (MRL-lpr) and MRL/MpJ (MRL) mice

In 1976, Murphy and Roths developed the MRL strain, which derives from LG/J, AKR, C3H and C57BL/6 mice (MURPHY, 1976, Theofilopoulos and Dixon, 1981). Inbreeding of the MRL strain led to the development of a MRL substrains, which showed an abnormal accumulation of T-lymphocytes, that could be related to a mutation, which was then termed lymphoproliferative (lpr) (McGaha and Madaio, 2014). Later, Adachi et al. were able to show, that this was a loss-of-function mutation caused by an insertion in intron 2 of the apoptosis mediating Fas gene (Adachi et al., 1993). MRL-lpr mice develop a lupus-like disease with circulating immune complexes, complement consumption, polyarteritis, arthritis and severe glomerulonephritis (Andrews et al., 1978, Dixon et al., 1978). This severe lupus-like glomerulonephritis is the leading cause of death in MRL-lpr mice with reports of 50% mortality within 20 weeks (Andrews et al., 1978, Dixon et al., 1978). Although the glomerulonephritis in MRL-lpr mice is

severe, crescents are only found occasionally in histological sections (Andrews et al., 1978).

3.2.2 Animal treatment

Induction of acute glomerulonephritis with nephrotoxic serum

Nephrotoxic serum (NTS) is generated by injecting a fraction of the GBM from mice into a sheep, which leads to the development of sheep anti-mouse GBM antibodies. Injected into mice, in the first heterologous phase the antibodies bind to mouse GBM and cause complement activation, (predominantly neutrophilic) leucocyte infiltration and proteinuria. In the second, homologous phase, the sheep antibodies, that act as planted antigens, cause the deposition of specific anti-sheep antibodies, leading to progression of renal damage with infiltration of T cells. This homologous phase has a similar pathomechanism to the human Goodpasture's disease. (Tipping et al., 1985, Huang et al., 1994, Sheerin et al., 2001).

C57BL/6 mice were injected intraperitoneally (i.p.) with 150 µl NTS and sacrificed at day 8 after disease induction.

Induction of chronic lupus nephritis with pristane

Mice injected with 2,6,10,14-tetramethylpentadecane (pristane) develop a moderate level of anti-nuclear antibodies such as anti-ribonucleoprotein and anti-DNA antibodies, which are typical for SLE (Satoh and Reeves, 1994, Satoh et al., 1995). Accordingly, pristane-treated mice show lupus symptoms such as hemorrhage in the lung, arthritis and lupus nephritis, the latter of which can be observed 6 months after injection (Satoh et al., 1995). The lupus nephritis, that is induced by pristane, is mild and is not the decisive factor for mortality in experiments with pristane-treated mice (McGaha and Madaio, 2014).

C57BL/6 mice were injected i.p. with 500 µl pristane (Sigma-Aldrich, St. Louis, USA) and sacrificed 9 months after injection.

3.2.3 Isolation and cultivation of cell populations

To conduct comparative analyses of the mRNA and protein expression levels of target genes/proteins associated with cross-presentation, PTECs, progenitor cells of bone marrow-derived DCs and LSECs were isolated from naïve C57BL/6 mice and

cultivated. The cell cultures were performed according to standardized protocols described previously (Masters and Stacey, 2007).

Mice were anesthetized by an intravenous injection of 150 µl ketamine (80 mg/ml)/xylazine (12 mg/ml) (Sigma Aldrich, St. Louis, USA) in one of the tail veins. Sufficient anesthesia was ensured by loss of pedal reflexes and the mice were killed by cervical dislocation.

Isolation of PTECs

To isolate PTECs from C57BL/6 mice, both kidneys were removed, and the capsules were dissected of. The kidneys were placed on a petri dish and finely minced using a razor blade. The two kidneys of one mouse were digested in 10 ml of collagenase digestion solution, which consisted of 50% HBSS + 50% DMEM/F-12 (V/V), containing 2.5 mg/ml BSA and 1 mg/ml collagenase V from *clostridium histolyticum*, for 17 minutes in a 37°C water bath under constant stirring. After digestion, the solution was passed through a 250 µm sieve and collected in a centrifuge tube, which was centrifuged at 600 g for 3 minutes at 4° C. Cell separation was achieved by a Percoll density gradient. The pellet was resuspended in 24 ml of Percoll gradient (45% Percoll + 55 % 2x PBS (solution as described above with doubled salt concentration) + 5 mM D-glucose (V/V)) and centrifuged at 17500 rpm for 30 minutes at 4° C. From the lowest interphase, containing the PTECs (Vinay et al., 1981), about 5-7 ml was transferred to a new centrifuge tube, which was filled with 20 ml 2x PBS + 5 mM D-glucose. The cells were then washed four times by centrifugation at 1000 g for 4 minutes at 4° C and resuspended in 20 ml 2x PBS + 5 mM D-glucose. After the fourth centrifugation, the cells were resuspended in 12 ml PTEC medium (see table 4) and plated in the wells of a 24-well plate, 2 ml of the cell suspension in each well. The PTECs were incubated at 37° C using in the Galaxy 48 R CO2 Incubator. After 3 days, half of the medium was replaced with 1 ml fresh PTEC medium. The day after, the medium was completely renewed after washing the cells with 1 ml sterile PBS. On the fifth day, the cells had formed a dense monolayer and were ready for harvest or further cultivation for other experiments.

Cultivation of PTECs with fluorescently labelled OVA

For functional analyses of the antigen internalization by the PTECs, the PTECs were incubated with fluorescent OVA-Alexa Fluor 647 for a fixed time span in different

concentrations and for different time spans with a fixed concentration. To rule out unspecific internalization or binding of the fluorescent OVA on the cell surface, a group of PTECs was cooled down with ice (4° C) before and during incubation with the fluorescent OVA.

Medium of PTECs, that were cultivated for 5 days as described above, was pipetted off and the PTECs were washed 2 times with sterile PBS. 500 µl of RPMI 1640 medium with the following additives was added to each well: heat inactivated FCS [10% (V/V)], penicillin [100 U/mL] & streptomycin [100 µg/mL], L-glutamin [2 mM] and 2-ME [50 µM]. The PTECs were put back into the Galaxy 48 R CO2 Incubator for 30 minutes at 37° C or put on ice for 4 hours (4° C) to stop energy dependent processes within the cells. After these time periods, the medium was discarded and 200 µl of RPMI 1640 with the additives just listed above was added without or with fluorescent OVA according to the following table.

Table 9: Systematic of the OVA-Alexa Fluor 647 incubation cultures

Variant	c[OVA-Alexa Fluor 647]	Incubation time	Temperature
1	w/o	1 hour	37° C
2	100 µg/ml	1 hour	37° C
3	10 µg/ml	1 hour	37° C
4	1 µg/ml	1 hour	37° C
5	0.1 µg/ml	1 hour	37° C
6	0.01 µg/ml	1 hour	37° C
7	10 µg/ml	1 hour	37° C
8	w/o	1 hour	37° C
9	10 µg/ml	2 hours	37° C
10	w/o	2 hours	37° C
11	10 µg/ml	4 hours	37° C
12	w/o	4 hours	37° C
13	10 µg/ml	1 hour	4 °C
14	w/o	1 hour	4° C

After the listed incubation times, detaching of the PTECs from the culture plate was achieved using trypsin/EDTA (Sigma Aldrich, St. Louis, USA) using 200 µl of trypsin/EDTA for each well and incubation for 5 minutes at 37° C. After incubation time, the culture plates were gently tapped, and the wells were scraped. The cells were transferred to 50 ml centrifuge tubes, containing 10 ml of cold RPMI medium to stop the trypsin/EDTA reaction. The wells were rinsed with 1 ml PBS and the content was given again into the centrifuge tubes, after which the tubes were centrifuged at 500 g

for 5 minutes at 4° C. The cell suspensions were then analyzed using flow cytometry (see chapter 2.2.7).

Generation of bone marrow-derived DCs

To generate bone marrow-derived DCs, progenitor cells were isolated from the femurs of C57BL/6 mice. After removal, the femurs were carefully cleaned of residual tissue and temporarily placed in 15 ml ice-cold HBSS. The removed femurs were cut open at one end and each placed in one 0.2 ml reaction tube, of which the bottom had been pierced and which were placed in 1.5 ml reaction tubes. These nested reaction tubes with a femur inside were centrifuged for 15 seconds at 8000 rpm, until the bone marrow was centrifuged out of the bone into the 1.5 ml tube. Next, the erythrocytes were lysed using 1 ml of ammonium chloride buffer for 90 seconds at room temperature. The lysis reaction was stopped by resuspending the cells in RPMI 1640, after which the suspension was centrifuged at 500 g for 8 minutes at 4° C. After the centrifugation, the supernatant was discarded, and the cell pellet was resuspended in 20 ml RPMI 1640 medium. A sample was taken for cell counting using a Neubauer Improved Chamber, and the cell suspension was centrifuged again at 300 g for 10 minutes at 4 °C. A maximum of 10^6 cells were plated per 10 cm petri dish in 10 ml of RPMI 1640 with the following additives: 10% (V/V) heat inactivated FCS + 100 U/ml penicillin & 100 µg/ml streptomycin + L-glutamin [2 mM] + 2-ME [50 µM] + GM-CSF [10 ng/mL]. The presence of GM-CSF induces the differentiation of DCs, macrophages and granulocytes from progenitor cells (Inaba et al., 1992). The cells were incubated in the Galaxy 48 R CO2 Incubator and the medium was changed 2-3 times before harvest. To minimize the loss of cells that were not yet adherent at the first medium change, the supernatant was collected, centrifuged and added again during the first medium change. Cell growth was assessed visually by microscopy and after 7 to 10 days the cells were ready for harvest.

On harvest day, the medium was discarded from each petri dish and the cells were washed with 3 ml sterile PBS. To detach the cells from the Petri dishes, 3 ml of trypsin/EDTA was added and the cells were placed in the incubator for 5 minutes. Afterwards, the dishes were gently tapped to detach the cells and each cell suspension was placed in a centrifuge tube containing PBS to stop the trypsin reaction. To collect the remaining cells from the Petri dish, PBS was added to the dishes, the dishes were

scraped and the suspensions were added to the centrifuge tubes again. The cells of each sample were counted and the tubes were centrifuged. To collect the DCs from the cultures and thereby enhance the portion of the DCs in the sample, the cells were sorted using magnetic-activated cell sorting (MACS) (see chapter 2.2.2.1).

Isolation of LSECs

Livers from C57BL/6 mice were perfused through the portal vein with 0.05% (m/V) collagenase V from *clostridium histolyticum* solved in GBSS for 20-60 seconds under a flow of 10 ml/min until the livers were drained of all blood. The gall bladders were dissected off and residual connective tissue was removed from the livers. The livers were finely minced and digested in 5 ml collagenase/GBSS solution for 20 minutes at 37° C. Afterwards, the cell suspensions were passed through a 100 µm steel mesh into a centrifugation tube. The cells were washed twice by filling the tube up (40 ml) with GBSS and a subsequent centrifugation at 40 g for 4 minutes at room temperature. After washing, the cells were centrifuged in 30% (V/V) Nycodens density gradient solved in GBSS at 500 g for 20 minutes at room temperature without breaking. The nonparenchymal cells were collected from the interphase and resuspended with GBSS. LSECs were isolated using MACS with CD146 microbeads (see chapter 3.2.2.1). After MACS, 10^6 LSECs were plated on collagen-coated 24-well plates and the medium was changed after 1 day. After 2 days, the LSECs had formed a monolayer and were ready for harvest.

3.2.2.1 Magnetic-activated cell sorting (MACS)

Heterogenous cell populations can be separated based on the expression of surface molecules using magnetic-activated cell sorting (MACS). Antibodies coupled to magnetic beads are used to bind to specific surface molecules. If the cell suspension is subsequently passed through a column, which is in a magnetic field, the cells, that are labeled with the antibodies, are attracted and stay in the column (positive selection), while the unlabeled cells pass through (negative selection) (Zeb et al., 2019).tin

Isolation of $CD11c^+$ bone marrow-derived DCs by MACS

Cells from the DC cultures were centrifuged at 500 g for 5 minutes at 4° C after which they were incubated with fragment crystallizable (Fc) blocking antibodies solved in

PBS in the concentration listed in table 2.1.8. The cells were incubated at a concentration of 2 x 10^6 cells/100 µl Fc blocking solution for 10 minutes at 4° C in centrifugation tubes. Afterwards, 20 ml MACS buffer was added to the tubes and the tubes were centrifuged at 500 g for 5 minutes at 4° C, after which the cells were resuspended in MACS buffer in a concentration of 2.5 x 10^6 cells/ml. 2 x 10^4 were taken as a pre-sort sample and to the remaining cells 100 µl/1 x 10^8 cells anti-CD11c microbeads (Miltenyi Biotec, Bergisch Gladbach, Germany) were given and the suspension was incubated for 15 minutes at 4° C. CD11c is a surface protein, that is constitutively expressed by all DCs and thus was used to isolate the $CD11c^+$ DCs (Merad et al., 2013). Afterwards, 500 µl of MACS buffer was added to the suspension, before it was centrifuged at 500 g for 5 minutes at 4° C, after which the cells were resuspended in MACS buffer in a concentration of 2 x 10^8 cells/ml. The MACS columns were rinsed with 3 ml MACS buffer and a maximum of 1 x 10^8 cells at once was given into the columns through a 30 µm filter. The cells retained by the magnetic field were solved with a piston and collected in a tube. 2 x 10^4 cells were taken as a sample to check the purity of the sort using flow cytometry (see chapter 2.2.7). As shown in Figure 3, the high portion of $CD11c^+$ cells, that was already present before the sort, could be increased by the MACS.

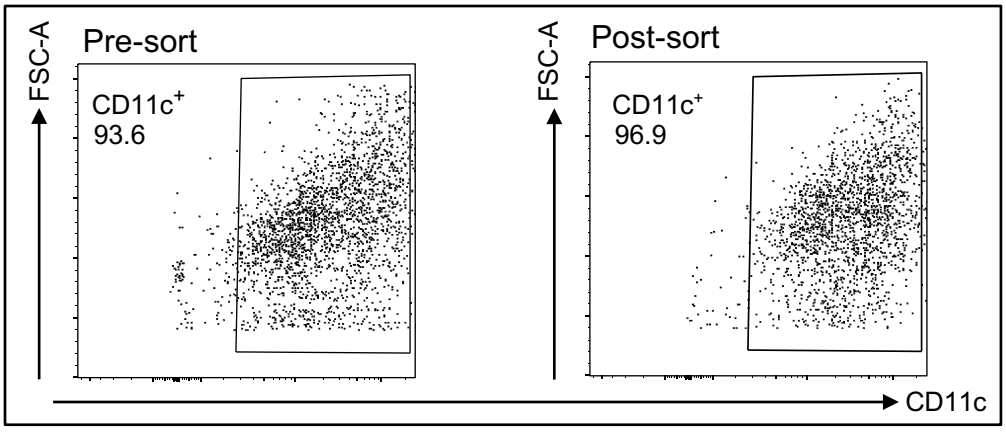

Figure 2: Purity of in vitro differentiated bone marrow-derived DCs
Bone marrow progenitor cells, that had been cultured for 7 to 10 days in the presence of GM-CSF and differentiated into dendritic cells, were separated from the culture using MACS. After gating (see chapter 2.2.7), the cells were plotted for FSC and the dendritic cell surface marker CD11c. The Frequency of $CD11c^+$ cells is shown in the top left corner of the plots.

Isolation of $CD146^+$ LSECs by MACS

Nonparenchymal cells were centrifuged at 1500 rpm for 5 minutes, after which the pellet was resuspended in MACS buffer (90 µl/10^7 cells) and 1 µl Fc block was added. The cells were incubated for 5 minutes at 4° C, after which CD146 microbeads (Miltenyi Biotec, Bergisch Gladbach, Germany) were added (10 µl/10^7 cells) and the suspensions were incubated for 10-15 minutes at 4° C in centrifugation tubes. 20 times of the volume present in the centrifugation tubes were added in MACS buffer to the suspensions and the cells were centrifuged for 10 minutes at 1500 rpm, after which the pellets were resuspended in 500 µl MACS buffer and passed through a 30 µm filter into MACS columns. The cells retained by the magnetic field were pressed out of the MACS columns into centrifugation tubes using a piston and were subsequently centrifugated at 1600 rpm for 7 minutes. The pellet was then resuspended in DMEM (high glucose) with the following additives: 8% FCS, 2% L-glutamine and 1% penicillin/streptomycin (all V/V).

3.2.4 Flow cytometry

Flow cytometry is a method to analyze cells on a single-cell level using their interaction with light. A cell suspension is passed through a nozzle, which creates droplets, containing single cells. After these droplets leave the nozzle, they pass a laser, the light of which is scattered by the cells within the droplets. This scattering can occur in the direction of the axis of the incident light (forward scatter (FSC)) or the light can be scattered in a 90° angle by the cells (side scatter (SSC)). The amount of forward scattering depends on the size of the cells, whereas the side scatter measures the internal complexity of cells like its granularity. Besides these physical characteristics, flow cytometry can be used to analyze the viability of cells by adding fluorescent substances, that fluorescently stains dead cells, or the expression of certain proteins with the use of fluorescently labelled antibodies. The scattering and the fluorescence signals are measured by the flow cytometry device with diodes, translated into electrical signals and amplified for further computational analyses (Gross et al., 2015).

Staining for surface markers and viability stain

For flow cytometry analyses the sample pellets were resuspended in 1 ml PBS and passed through a cell sieve into flow cytometry tubes, which were then centrifuged at 500 g for 5 minutes at 4° C. The staining solution was prepared in PBS containing the viability stain Zombie NIR for all sample and optionally surface staining in the

concentrations listed in table 8. After centrifugation the supernatant was discarded and the cells were resuspended in 50 µl of the staining solution for 30 minutes at 4° C. Afterwards, the cells were washed using 1 ml PBS and centrifuged at 500 g for 5 minutes at 4° C. The supernatant was discarded and the cells were resuspended in 350 µl FACS buffer.

Gating strategy

All samples were gated using the strategy shown below (Figure 3). To only include cells and exclude debris, the samples were plotted for FSC and SSC and all events showing too low FSC or SSC signals were excluded (Figure 4A). Present cell conglomerates were excluded using FSC height and area (FSC-H, FSC-A), based on their cytometric behavior not to show a proportional relation between FSC-H and FSC-A (Figure 4B). Finally, to gate for living cells, all cells showing a signal for the viability stain were excluded as only dead cells take up Zombi NIR (Figure 4C).

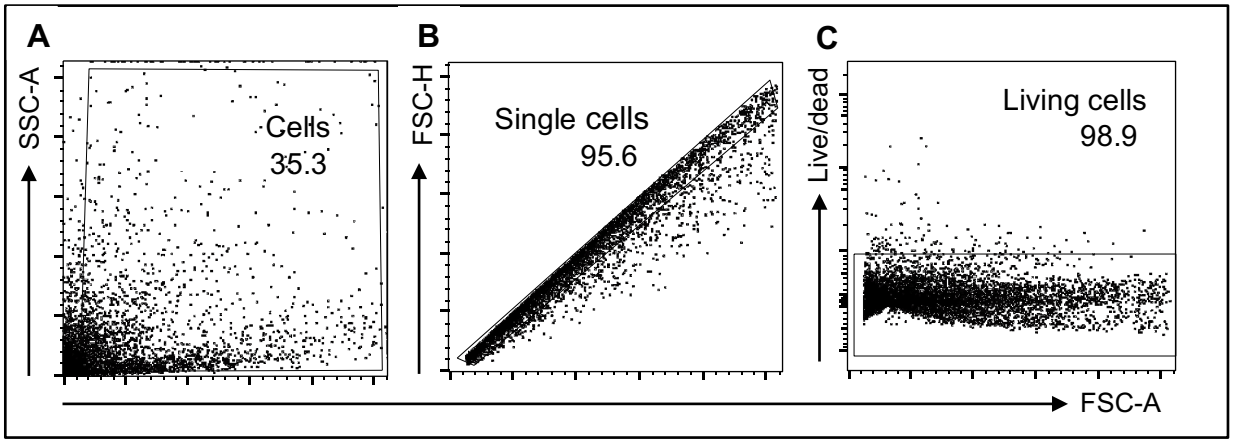

Figure 3: Gating strategy
Gating strategy using the example of a PTEC sample. To gate out debris, all the samples were plotted for FSC and SSC (A). To gate for single cells, the cells were plotted for FSC-H and FSC-A (B). To gate for living cells, all the cells that take up the viability stain (Zombi NIR, APC/Cy7) were gated out (C).

3.2.5 RNA isolation and synthesis of complementary DNA (cDNA)

For the RNA isolation a TRIzol-based protocol was used. TRIzol is a reagent that disrupts cells and proteins, while maintaining the integrity of the RNA. After the TRIzol reaction, chloroform can be added to separate the solution in three phases, the upper, aqueous phase of which contains the RNA. Subsequently, the RNA is precipitated with

isopropanol and can be washed with ethanol, which further purifies the sample from DNA and proteins (Rio et al., 2010).

RNA isolation

To compare the expression levels of mRNA of target-genes, associated with cross-presentation, RNA was isolated from PTECs, bone marrow-derived DCs and LSECs, that were cultured as described above (see chapter 2.2.2). Cells of one sample were suspended in 1 ml TRIzol reagent and homogenized by pipetting up and down. 200 µl chloroform was added and the solution was shaken vigorously by hand for 15 seconds. The solution was centrifuged at 12000 g for 15 minutes at 4° C, until 3 phases had formed. The uppermost aqueous phase containing the RNA was carefully transferred to a new tube filled with 500 µl isopropanol. For precipitation the solution was incubated at -20° C for 20-30 minutes, before being centrifuged at 12000 g for 10 minutes at 4° C. The supernatant was discarded and 500 µl of 75% ethanol (EtOH) were added, followed by another centrifugation at 7500 g for 5 minutes at 4° C. The supernatant was discarded and after another centrifugation at 7500 g at 4° C for 1 minute, followed by carefully pipetting off remaining EtOH, the then still remaining EtOH was removed by letting it evaporate in the heating block for 10 minutes at 55° C. The resulting RNA pellet was resuspended in RNase free water and solution was achieved by heating the sample for 10 minutes at 55° C. RNA concentrations of the generated RNA samples were determined photometrically by measuring the extinction at 260 nm using the NanoDrop photometer ND-1000 (PEQLAB Biotechnologie GmbH, Erlangen, Germany).

Digestion of contaminating DNA

As residual genomic DNA, that may be present in the samples, could lead to false positive signals in subsequent polymerase chain reaction (PCR) analyses, the potentially contaminating DNA was digested after the RNA isolation using the DNA free kit. Firstly, a DNase buffer was added in 0.1 times the volume of the initial solution. Then, depending on the RNA concentration (≤200 µg/ml vs. >200 µg/ml) of the sample 0.5 or 1 µl recombinant DNase I were added and the solution was incubated for 30 minutes at 37° C. This process was repeated one more time, before the DNase inactivation reagent was applied at 0.1 or 0.2 times the samples volume (depending on the initial RNA concentration) and the samples were incubated at room temperature

for 2 minutes, whilst being vortexed every 30 seconds. Afterwards the solution was centrifuged at 10000 g for 1.5 minutes and the supernatant, containing the RNA, was transferred to a fresh tube. The RNA concentration was measured photometrically as described above and the samples were stored at -80° C.

Synthesis of complementary DNA (cDNA)

For the subsequent PCR analyses, the mRNA in the isolated RNA was written into complementary DNA (cDNA) using the Verso cDNA synthesis kit. 1 µg RNA was used from each sample and pipetted into a 0.2 ml reaction tube, which was filled to 11 µl volume with RNase free water. As primers OligodTs and Random hexamer primers from the cDNA synthesis kit were mixed in the ratio of 1:2 (V/V) and 1 µl of this mix was added to each sample. The samples were placed in the MyCycler thermal cycler and heated to 70° C for 10 minutes. After this first step, 4 µl 5x cDNA synthesis buffer, 2 µl of deoxynucleotide triphosphates (dNTPs), 1 µl reverse transcription (RT)-Enhancer and 1 µl of the reverse transcriptase from the cDNA synthesis kit were added to the samples. The reverse transcriptase is an RNA-dependent DNA polymerase, that uses the dNTPs as building blocks to synthesize a strand of cDNA corresponding to the mRNA in the sample. The RT-Enhancer degrades double stranded DNA and thus removes possibly contaminating genomic DNA. After the addition of these reagents, the cDNA synthesis program was continued by heating the samples to 42° C for 60 minutes, after which the temperature was risen to 95° C for 3 minutes. After completion of the synthesis program, the cDNA samples were stored at -20° C.

3.2.6 Quantitative real-time polymerase chain reaction (qRT-PCR)

The PCR is a method to amplify DNA and is conducted in three steps. In the first step, called denaturation, the double stranded DNA of a sample is broken apart into two separate strands using high temperatures. In the second step, the temperature is cooled down and the primers, that were given to the sample before, anneal to the DNA at their specific regions. In the last step, the temperature is risen again and new DNA strands are synthesized using the existing single stranded DNA as a template, which is carried out by a DNA polymerase, that has to be heat-stable in order to survive the high temperatures of the denaturation phase and uses dNTPs, that have to be given to the sample beforehand. These three steps make up one cycle and are constantly

repeated (Canene-Adams, 2013). Under optimal conditions the number of DNA copies doubles with every cycle.

In quantitative real-time PCR, the amount of DNA is measured after each cycle, allowing a constant monitoring of the reaction. To measure the DNA quantity a fluorescent dye can be added, that binds to double stranded DNA and thus generates a light signal proportional to the quantity of double stranded DNA. In the first cycles of a real-time PCR, where there are only a few copies of DNA, the fluorescent signal of the copies barely exceeds background noise signals, which is known as the stationary baseline phase. As the reaction proceeds, more DNA copies are generated, resulting in a fluorescent signal, that significantly exceeds the background noises. This phase is called the exponential phase and is represented as a straight line on a graph, that plots the number of cycles on the x and the fluorescence signal on a logarithmic y axis. The fluorescence signal, at which the reaction transitions from the stationary baseline to the exponential phase, is usually chosen as the threshold and the cycle at which this happens is recorded as the cycle of threshold (ct). When performing comparative analyses this threshold can technically be chosen arbitrarily as long as it is in the exponential phase and the same for all samples tested (Arya et al., 2005). Also, it should be noted, that the ct-value alone does not allow any real conclusion about the absolute amount of DNA, when using dye, that binds to DNA unspecifically, because the amount of fluorescence signal per DNA is proportional to the length of the copies, resulting in lower ct-values for larger genes.

Because DNA yields can vary for different cell populations, samples are normalized to a reference gene to better assess the functional meaning of a certain DNA expression level for the cell (see calculation below). A reference gene is a gene that is assumed to be expressed on the same proportional level by all (analyzed) cell populations, and thus correlates with the total amount of DNA present in samples. Examples for reference genes are the genes of the cytoskeletal protein beta-actin or the metabolic protein glyceraldehyde 3-phosphate dehydrogenase (GAPDH) (Vandesompele et al., 2002).

Calculation of comparative expression levels

To compare the gene expression levels of samples, that were normalized to a certain reference gene, the $2^{-\Delta\Delta ct}$ method can be used. In this method, the goal is to calculate the ratio of the normalized expression levels (X_{N1}/X_{N2}) between two compared

samples. Exponential growth ($X_n = X_0 \times 2^n$) of the number of copies with every cycle is assumed (Livak and Schmittgen, 2001) and the ratio of the normalized expression levels between two samples can be calculated using the ct-values for the target gene and reference gene of each sample with the following derivation:

$$X_T = X_0 \times 2^{ct_x} \quad (1)$$

$$\frac{X_T}{H_T} = \frac{X_0}{H_0} \times \frac{2^{ct_x}}{2^{ct_H}}$$

$$\frac{X_T}{H_T} = \frac{X_0}{H_0} \times 2^{ct_x - ct_H} = X_N \times 2^{\Delta ct} \quad (2)$$

$$<=> X_N = \frac{X_T}{H_T} \times 2^{-\Delta ct}$$

$$\frac{X_{N,1}}{X_{N,2}} = \frac{\frac{X_T}{H_T}}{\frac{X_T}{H_T}} \times \frac{2^{-\Delta ct1}}{2^{-\Delta ct2}} \quad (3)$$

$$\frac{X_{N,1}}{X_{N,2}} = 2^{-\Delta ct1 + \Delta ct2} = 2^{-(\Delta ct1 - \Delta ct2)} = 2^{-\Delta\Delta ct}$$

Figure 4: The mathematics of the $2^{-\Delta\Delta ct}$ method

(1) Equation for the exponential growth of a PCR reaction, X_T: Fluorescence signal/number of copies at threshold, X_0: number of copies at the start of the reaction, ct_x: threshold cycle.
(2) Division of target gene equation by the housekeeper equation. The division is rearranged for the normalized expression level X_N, H: housekeeper.
(3) Division of the equation for the normalized expression levels of one sample ($X_{N,1}$) by another ($X_{N,2}$) ($\frac{X_{N,1}}{X_{N,2}}$: gene expression in sample 1 relative to sample 2). Note, that the thresholds cancel out.

In comparative analyses it is also permissive to calculate the $2^{-\Delta ct}$ values and plot them against each other. This is especially useful when comparing more than two populations, because otherwise more than one ratio of normalized expression levels would need to be calculated.

Comparative expression analyses using qRT-PCR

For the comparative PCR analyses, the cDNA samples from PTECs, bone marrow-derived DCs and LSECs were tested using the exon spanning primers listed in table

5. Exon spanning primers have the advantage, that they do not anneal to potentially contaminating genomic DNA, which contains introns, and thus exclude false positive results. In the wells of a 384-well plate 0.7 µl of each 5´ and 3´ primer was given as well as 2.6 µl double distilled water and 5 µl of SYBR Green PCR Master Mix. The Master mix contains the heat-stable DNA polymerase AmpliTaq Gold and dNTPs as well as the fluorescent dye SYBR Green I. SYBR Green I binds to double stranded DNA and emits light in the wavelength of 497 nm when decaying from its excited state, which can be measured by the PCR device. In every well 1 µl cDNA was given and the samples were measured in triplets. After preparation, the 384-well plate was centrifuged at 1000 g for 1 minute at room temperature and for the PCR reaction the QuantStudio 7 Flex was used. Denaturation was achieved at 95 °C for 15 seconds, after which annealing was performed at 60° C for 20 seconds. Finally, the elongation phase was conducted at 72° C for 12 seconds at the end of which the fluorescence signal was measured. 45 of these cycles were performed. After the 45 cycles melting curves were obtained to ensure the purity of the amplified DNA.
The average ct-values of the triples were determined, and the normalized expression levels of the samples were calculated. For normalization the cytoskeletal protein beta-actin was used.

3.2.7 Protein isolation

For comparative analyses of the expression of proteins associated with cross-presentation, protein lysates were generated from PTECs, bone marrow-derived DCs and LSECs, that were cultured as described above (see chapter 2.2.2).
For protein isolation, a lysis buffer was used, based on the KLB buffer described above (see table 4). Protection from proteases was ensured by the presence of EDTA, Na-pyrophosphate, Na-orthovanadate and glycerol phosphate. Additional protection was assured by addition of 1 mM PMSF, 10 mM NaF, 0.1 mM Na-pervanadate solution and Aprotinin solution (1:100 dilution). For cell lysis, the detergent Triton X-100 was present.
The samples were suspended in the lysis buffer and cold storage was ensured during cell suspension. Sufficient cell crushing was performed by 3 minutes in an ultra-sonic bath, after which the solutions were put on ice for 30 minutes and vortexed every 10 minutes. The solutions were centrifuged at the maximal possible speed (25000 g) for 10 minutes at 4° C and the supernatant was collected in a new tube. The total protein

concentrations were determined using the Bradford assay, which is a Coomassie G-250 dye-based assay. The dye binds to proteins and the protein concentration can be determined by photometric measurement of the extinction at 595 nm wavelength (Bradford, 1976). For photometrical measurement the Tecan reader was used. Protein samples were stored at -80° C.

3.2.8 Western Blot

Western blot is a semiquantitative method for protein detection and was first described in the late 1970s by Tobwin et al. (Towbin et al., 1979). It is based on the electrophoretical separation of proteins with subsequent transfer (blotting) to a carrier membrane. After the proteins are transferred to the membrane, the proteins of interest can be detected using an immunoassay, i.e., antibodies, that bind to the proteins and that are equipped with a reporting system. To ensure that protein migration correlates with protein mass during electrophoresis, firstly the proteins in the sample need to be denaturized and protein charging proportional to the proteins' length needs to be ensured. Additionally, the proteins' structure needs to be straightened out to form a line, called linearization. Denaturation, linearization and adequate charging can be achieved by heat and addition of a charged detergent, that binds to the protein proportional to its mass (Jensen, 2012).

Protein electrophoresis

The protein concentrations of lysates from the PTECs, bone marrow-derived DCs and LSECs were measured using a Bradford Assay as described above and equal quantities of protein were used to compare the samples. To the protein solutions, the NuPAGE LDS sample buffer was added. The sample buffer contains the negatively charged dodecyl sulfate, which denatures the proteins and binds to them proportional to their mass, with a binding of 1.4 g dodecyl sulfate per gram protein (Reynolds and Tanford, 1970). Through the repelling forces between the negatively charged dodecyl sulfate, it also ensures protein linearization. Additional denaturation of the protein samples was assured by addition of the NuPAGE Reducing agent, which contains dithiothreitol, that can solve disulfide bounds of proteins, and application of heat (70° C) for 10 minutes. After heating the samples, they were centrifuged at 7500 g for 5 minutes. For the protein electrophoresis the XCell SureLock Mini-Cell was used and filled with the NuPAGE MES (2-(N-morpholino)ethanesulfonic acid) running buffer. To

the inner chamber, the NuPAGE antioxidants was added. The Mini-Cell was loaded with NuPAGE 4 to 12% Bis-Tris polyacrylamide gels with a gradient polyacrylamide concentration of 4 to 12%, which functions as an increasingly fine sieve and thus separates the proteins according to their size. The prepared protein samples were loaded onto the gels and as a marker Precision Plus Protein Western Blotting Standards was used. A constant voltage of 200 V was applied to the chamber for 35 minutes, until protein separation was achieved.
This electrophoresis method is known as SDS-PAGE (sodium dodecyl sulfate polyacrylamide gel electrophoresis) since 1970 (Laemmli, 1970).

Protein transfer

After electrophoresis, the proteins were transferred onto a nitrocellulose carrier membrane using the Mini Blot Cell, which was filled with western blot transfer buffer (for composition see table 4). A constant current of 350 A was applied for 70 minutes and cooling was ensured by ice in and around the device. Sufficient protein transfer was checked with ponceau red dye after protein transfer.

Protein detection

For protein detection, firstly unspecific antibody binding was inhibited by incubation with 5% non-fat dry milk solved in TBS-T for 30 minutes. The marker bands were separated from the samples on the membrane and the samples were incubated with anti-TAP1, anti-SEC61A1, anti-NOX2, anti-LNPEP, and anti-VCP or anti-MMR/CD206 antibodies solved in the TBS-T/dry milk solution in the concentrations listed in the table 6 over night at 4° C in tubes on a rotary shaker. The next day, the membranes were washed, and the horseradish peroxidase (HRP)-conjugated secondary antibodies anti-rabbit or anti-goat were applied, solved in TBS-T in the concentrations listed in table 7, for 1 hour at room temperature. To the marker bands the Strep-Tactin-HRP conjugate was added, also solved in TBS-T in a concentration of 1:10000 for 1 hour.
All washing steps in between were conducted using TBS-T.
Protein visualization was achieved using chemiluminescence. 3 ml of the chemiluminescence solution A and 30 µl of the solution B (see table 4) were combined, together with 1 µl H_2O_2. In the presence of HRP the oxidation of luminol to 3-aminophthalate by H_2O_2 is catalyzed, which emits light in the wavelength of 425 nm when decaying.

Normalization with GAPDH

To confirm equal protein loading within the samples, the membranes were analyzed for the metabolic protein GAPDH (see chapter 2.2.6, paragraph 3 for more information on reference genes). The blots, that had previously been stained for the proteins mentioned above were firstly washed with TBS-T. After washing, the blots were stripped using Restore PLUS Western Blot Stripping-Puffer for 12 minutes at room temperature. This used stripping buffer is highly acidic and removes existing antibody-antigen bonds by decreasing the binding capabilities of antibodies by conformity change. After stripping, the blots were again washed with TBS-T and the blots were stained and protein was visualized as described in the section above (protein detection). After blocking, the blots were stained with anti-GAPDH, solved in 5% non-fat dry milk solved in TBS-T in the concentration listed in table 6. As secondary antibody anti-mouse IgG was used, solved in TBS-T in the concentration listed in table 7.

3.2.9 Immunohistochemistry

Immunohistochemistry is a method to visualize a certain antigen in tissue sections, using the principles of antibody to antigen binding, which are the same used for protein detection in western blot discussed above (chapter 2.2.8). Generally, two antibodies are used: a primary and a secondary one. A primary antibody with sufficient sensitivity and specificity for the antigen of interest binds this antigen. A secondary antibody is applied, which has an affinity to the Fc region of the primary antibody and binds to this. This secondary antibody contains an enzyme, called the reporter, that can react with color signal generating substrates, that are called chromogen. Two commonly used reporter enzymes are horseradish peroxidase (HRP) or alkaline phosphatase (AP). Examples for chromogens are DAB, New Fuchsin, TMB or Stay Yellow.

If tissue sections are paraffin-embedded, they firstly need to be deparaffinated and rehydrated. This can be achieved by xylene or a substitute medium and a following decreasing ethanol series.

Before embedding, the tissue sections are fixated, which can change the molecular structure of the analyzed tissue, mainly due to cross-links in amino acid residues of proteins. Thereby, the binding of antibodies to their target proteins can be impaired, which leads to a decreased sensitivity. This impaired antigenicity can be restored

(retrieved) by physical and chemical procedures such as the appliance of heat (heat induced epitope retrieval (HIER)) and acidic or basic buffers (D'Amico et al., 2009).
After antigen retrieval unspecific binding of the primary antibody is usually blocked using a blocking solution.
After primary and secondary antibody application and the development of the color signal by the chromogen, the tissue sections can be counterstained, i.e., stained with an additional dye, which stains the tissue generally and thus makes it significantly easier to evaluate the immunostaining in the context of the histology of the tissue. Counterstaining can be conducted by hemalum. As a basic dye, it stains all basophilic structures, such as DNA and the rough endoplasmic reticulum, in blue.
After the counterstaining, the tissue sections are mounted and available for further evaluation (Magaki et al., 2019).

Staining for CD3 and CD8 in serial kidney sections

To analyze localization and number of renal $CD8^+$ T cells, paraffin-embedded, serial kidney sections of 2 µm width from NTS-treated and naïve mice, MRL-lpr and MRL mice as well as pristane-treated and age-matched, 9-month-old naïve mice were stained with anti-CD8 (D4W2Z, Cell Signaling, Danvers, USA) and anti-CD3 (Agilent, Santa Clara, USA) antibodies.

For the CD3 staining, a deparaffination procedure was performed using a xylene substitute, based on natural citrus oil extracts (DiaTec, Bamberg, Germany), two times for 10 minutes. Subsequently, the sections underwent a decreasing ethanol series consisting of a 100%, 90%, 70% and 50% ethanol solution, each applied for 4 minutes. After the deparaffination procedure, the sections were washed using ddH_2O until no more ethanol odor was perceptible. HIER was achieved in a microwave oven at sub boiling temperatures for 20 minutes, whilst the sections were submerged in Dako Target Retrieval Solution with a pH of 9. Blocking was performed with the blocking solution from the ZytoChem-Plus AP Polymer-Kit, that was applied for 5 minutes at room temperature. After blocking, the sections were washed and 50 µl of antibody solution with the primary antibody anti-CD3, that was solved in the buffer from the kit in the concentration listed in table 6 was given to each section and the sections were incubated overnight at 4°C. The next day, the sections were washed and the secondary antibody anti-rabbit AP-Polymer - also from the ZytoChem-Plus AP

Polymer-Kit – was applied for 30 minutes at room temperature. After incubation with the secondary antibody, New Fuchsin was used as chromogen. Sufficient incubation time was determined by visual assessment of the red color signal, which was usually achieved after 10 minutes. After the development of the color signal, floating tap water was applied for 5 minutes. Afterwards, counterstaining was performed using Mayer's hemalum solution in a dilution of 1/1 (V/V) in ddH_2O for 5 seconds, after which again floating tap water was applied for 5 minutes. Finally, the tissue sections were mounted using Crystal mount and dried for 1h, before being embedded using Entellan.
All washing steps in between were conducted with TBS, if not otherwise declared.

For the CD8 staining, deparaffination and rehydration was performed as described above for the CD3 staining. HIER was again achieved in a microwave oven at sub boiling temperatures, but for 10 minutes and with the Dako Target Retrieval Solution with a pH of 6. After washing, blocking was performed by the Bloxall Blocking solution, which was applied for 10 minutes at room temperature. The blocking solution was washed off and 50 µl of the antibody solution, in which the primary antibody anti-CD8α was solved in Dako Antibody Diluent in the concentration listed in table 6, was applied over night at 4°C. The next day, the sections were washed and the secondary antibody goat anti-rabbit IgG H&L, that was solved in Dako Antibody Diluent as listed in table 7, was applied for 1 hour at room temperature. After washing, DAB chromogen was used, which led to the development of a color signal 5 minutes after application. Following this, the tissue sections were washed with ddH_2O two times for 5 minutes and counterstained by using Meyer's hemalum solution as described above. Again, floating tap water was applied for 5 minutes, before the sections were mounted with Crystal Mount and embedded with Entellan.
All washing steps in between were conducted with TBS, if not otherwise declared.

Digital evaluation

For evaluation, the whole tissue sections were scanned using the Zeiss Axioscan 7 and digitally viewed using the Zeiss Zen lite software. Two corresponding, serial tissue sections of the CD3 and CD8 stain were aligned digitally using the rotation tool of the software. After alignment five corresponding high power fields (HPFs) were marked randomly in the cortices of the tissue sections. Cells showing a signal for CD3 and CD8

were interpreted as $CD8^+$ T cells and were counted as intraglomerular or tubulointerstitial. Pictures were taken using the Keyence BZ-9000.

3.2.10 Statistical analyses

Statistical significance was assessed with the non-parametric Mann-Whitney-U-Test (Mann and Whitney, 1947) for comparisons between two groups or a one-way Analysis of variance (ANOVA) with post analysis by Tukey-Kramer test (Driscoll, 1996) when comparing multiple groups using GraphPad Prism 9 (GraphPad Software Inc., San Diego, USA). Data are shown as means ± standard error mean (SEM). A p-value of ≥ 0.05 was considered non-significant (ns), while $p<0.05$ was regarded significant (*$p<0.05$, **$p<0.01$, ***$p<0.001$, ****$p<0.0001$).

4 Results

4.1 PTECs express RNA and proteins, that are associated with cross-presentation

4.1.1 PTECs express RNA of target genes associated with cross-presentation

PTECs have been previously shown to act as non-professional APCs towards $CD4^+$ T cells, which can be explained by the expression of the co-stimulatory molecules CD80 and CD86 as well as MHC-II on the surface of PTECs (Breda et al., 2019). In this study, it was postulated, that PTECs also exert non-professional APC functions towards $CD8^+$ T cells. A distinguishing feature of APCs is the ability to present exogenous antigen on MHC-I, on which non-APC cell populations can only present endogenous antigens. For this presentation of exogenous antigen on MHC-I APCs have an additional cellular mechanism, which is called cross-presentation (Sigal et al., 1999, den Haan and Bevan, 2001).

In order to assess the capability of PTECs to conduct cross-presentation, in a first series of experiments PTECs were compared to bone marrow-derived DCs and LSECs, both of which are a well-described cross-presenting cell population, either as professional or non-professional APCs. All these cell populations were obtained from kidneys, livers or bone marrow from C57BL/6 WT mice and RNA from each population was isolated using a TRIzol based protocol and reverse transcribed into cDNA. Afterwards the expression levels of target genes associated with the endosome-to-cytosol pathway of cross-presentation were determined by qRT-PCR. After normalization to the reference gene *Actb*, the gene expression levels in PTECs, DCs and LSECs were compared. Figure 6 shows the comparative data for all investigated target genes.

These analyses showed that mRNA of every target gene was detectable in PTECs.

Comparison of PTECs to DCs

mRNA expression levels of the histocompatibility 2, D region locus 1 (*H2-D*) gene, which encodes for MHC-I had similarly high expression levels in PTECs and DCs (10.8 ± 3.5 vs. 8.4 ± 2.8). Also similarly high were the mRNA expression levels of *Sec61a1* (28.2 ± 7.3 vs. 4.7 ± 0.8), *Sec61b* (8.0 ± 2.3 vs. 3.4 ± 0.8) and *Sec61g* (10.0 ± 2.2 vs.

3.2 ± 0.6), which encode for the three subunits of the Sec61 translocon. Similar mRNA expression levels could also be observed for the leucyl and cystinyl aminopeptidase (*Lnpep*) gene (4.2 ± 0.63 vs. 4.4 ± 1.8), that encodes for IRAP, the proteasome 20S subunit beta 8 (*Psmb8*) (14.84 ± 4.9 vs. 27.1 ± 5.3), that encodes for LMP7, a subunit of the immunoproteasome and the valosin-containing protein (*Vcp*) (15.3 ± 4.1 vs. 3.8 ± 0.8), which is the gene encoding for the AAA+ ATPase p97. Whilst the mRNA expression levels for *Tap2* (14.5 ± 6.6 vs. 9.7 ± 3.0), a subunit of TAP, were similarly high, DCs expressed higher mRNA levels for the other subunit of TAP, *Tap1* (3.8 ± 1.1 vs. 10.1 ± 1.0). Significantly lower were the mRNA expression levels in PTECs in comparison to DCs for cytochrome b-245 beta chain (*Cybb*) (85.3 ± 30.2 vs. 20946 ± 5504), which encodes for NOX2, and the mannose receptor (*Mrc1*) (71.4 ± 20.9 vs. 19710 ± 4515).

In conclusion, the PTECs showed similar expression levels to DCs of mRNA, which encodes for proteins, that mediate antigen translocation into the cytosol after internalization, cytosolic antigen degradation, peptide trimming prior to loading onto MHC-I, presentation of antigen and partially peptide translocation into endosomes after antigen degradation (*Tap1*). mRNA for the other subunit (*Tap2*) was expressed on lower levels in PTECs in comparison to DCs and the DCs had significantly higher expression levels of mRNA for proteins, that mediate endosomal antigen stability and antigen internalization.

Comparison of PTECs to LSECs

As the LSECs are a well-described population of non-professional APCs (Knolle et al., 1999, Limmer et al., 2000, Diehl et al., 2008, Schurich et al., 2009, Tiegs and Lohse, 2010), the mRNA expression in PTECs was also compared to LSECs. Similar to the comparison of PTECs to DCs, there were similarly high expression levels of *H2-D* (10.8 ± 3.5 vs. 12.4 ± 0.4), *Sec61b* (8.0 ± 2.3 vs. 3.6 ± 0.5), *Sec61g* (10.0 ± 2.2 vs. 6.6 ± 1.2), *Tap2* (14.5 ± 6.6 vs. 30.0 ± 4.9), *Lnpep* (4.2 ± 0.63 vs. 4.1 ± 0.5), *Psmb8* (14.84 ± 4.9 vs. 10.2 ± 1.6) and *Vcp* (15.3 ± 4.1 vs. 25.2 ± 3.6). Additionally, *Cybb* (85.3 ± 30.2 vs. 143.0 ± 24.0) had no significantly differing expression level in PTECs compared to LSECs.

Also similarly to DCs, the LSECs expressed higher levels of *Mrc1* (71.4 ± 20.9 vs. 44853 ± 3752) and *Tap1* (3.8 ± 1.1 vs. 17.5 ± 2.9) in comparison to PTECs.

Additionally, LSECs had higher mRNA expression levels of *Sec61a1* (28.2 ± 7.3 vs. 466.5 ± 82.6).
Conclusively, the PTECs expressed mRNA of all target genes on equal or lower levels in comparison to LSECs.

Comparison of LSECs and DCs

Another interesting question is the comparison of the DCs as professional and the LSECs as non-professional APCs. Here, the LSECs had similar mRNA expression levels of *H2-D* (12.4 ± 0.4 vs. 8.4 ± 2.8), *Sec61b* (3.4 ± 0.8 vs. 3.6 ± 0.5), *Sec61g* (6.6 ± 1.2 vs. 3.2 ± 0.6), *Tap2* (30.0 ± 4.9 vs. 9.7 ± 3.0), *Lnpep* (4.1 ± 0.5 vs. 4.4 ± 1.8), *Psmb8* (10.2 ± 1.6 vs. 27.1 ± 5.3) and *Vcp* (25.2 ± 3.6 vs. 3.8 ± 0.8). Higher mRNA expression levels were found in LSECs compared to DCs of *Mrc1* (44853 ± 3752 vs. 19710 ± 4515), *Sec61a1* (466.5 ± 82.6 vs. 4.7 ± 0.8) and *Tap1* (17.5 ± 2.9 vs. 10.1 ± 1.0). Only the mRNA expression of *Cybb* was higher in DCs compared to LSECs (143.0 ± 24.0 vs. 20946 ± 5504).
Conclusively, LSECs expressed mRNA of all target genes on an equal or higher level in comparison to DCs, with the only exception of *Cybb*.

In conclusion, the PTECs showed mostly similar mRNA expression levels in comparison to DCs and LSECs for all analyzed target genes with the exception of *Mrc1* and *Cybb*, which mediate antigen internalization and stabilization, respectively. Notably, mRNA of every analyzed target gene was detectable in PTECs.

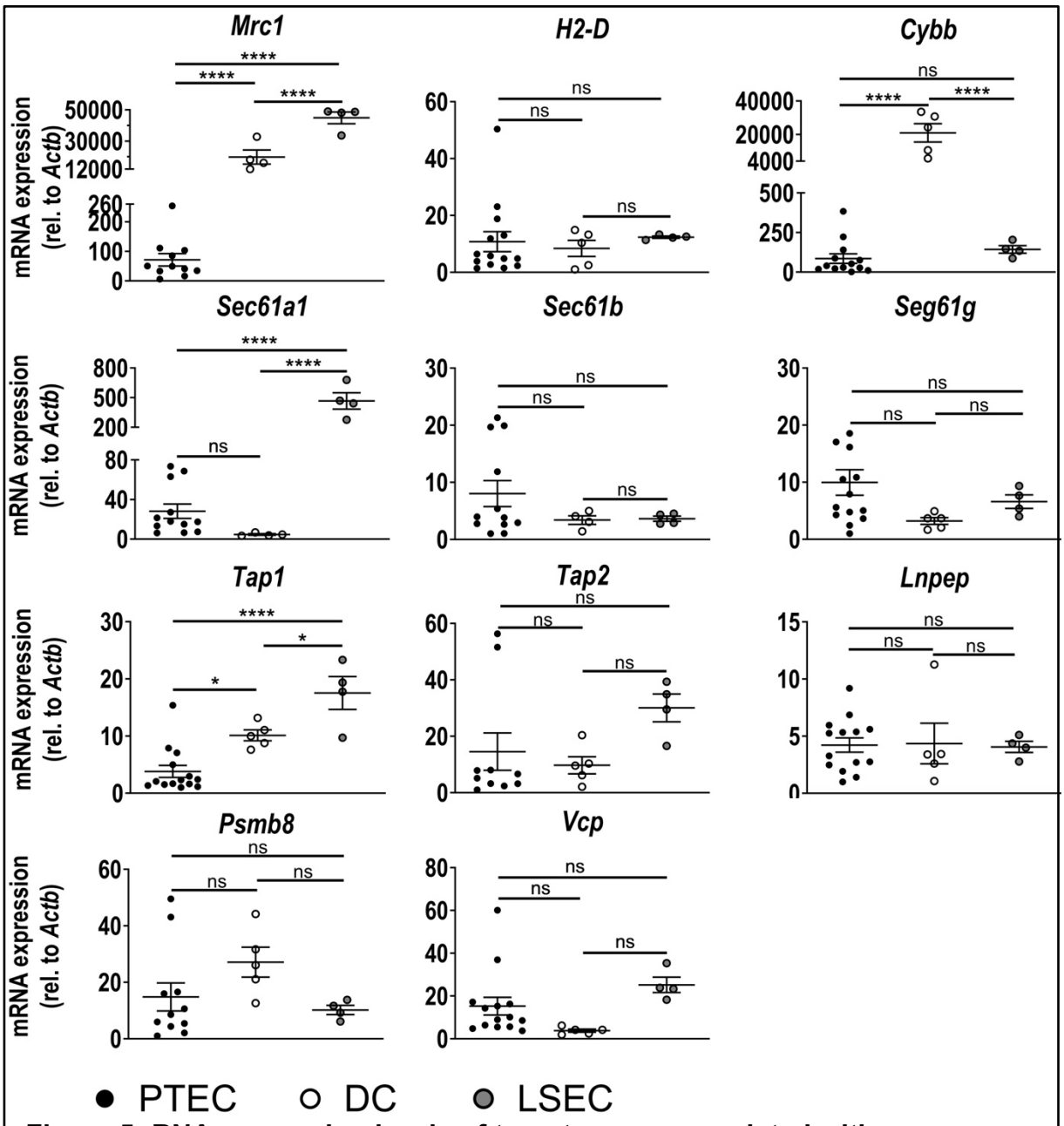

Figure 5: RNA expression levels of target genes associated with cross-presentation in PTECs, DCs and LSECs

RNA from PTECs, DCs and LSECs was transcribed into cDNA and analyzed using quantitative real-time PCR. Expression levels were normalized to *Actb*. Means ± SEM of 4-14 independent experiments are shown. ****p<0.0001; *p<0.05; ns=non-significant.

4.1.2 PTECs express proteins associated with cross-presentation on an equal or higher level compared to DCs, except for the mannose receptor

Having shown, that RNA of all target genes, that are associated with the endosome-to-cytosol pathway of antigen cross-presentation, can be found in PTECs, the next aim was to determine whether and to what extent the abundant RNA was translated into proteins. Again, the PTECs were compared with DCs, which are a well-described population of professional APCs. Protein lysates from PTECs and bone marrow-derived DCs were generated and the proteins were detected using western blot. Equal loading was ensured by equal sizes of the bands for the reference protein GAPDH. Two experiments were conducted for every target protein.

Figure 7 shows snippets of each target from one of two experiments. As it is shown, every analyzed protein was detectable in PTECs. Expression levels of LNPEP and VCP were on approximately equal levels in PTECs and DCs. Surprisingly, the PTECs expressed higher protein levels of NOX2, TAP1 and the SEC61a1 subunit of Sec61, that was analyzed representatively for all three subunits. Expression of the mannose receptor (MR) was considerably higher in DCs compared to PTECs.

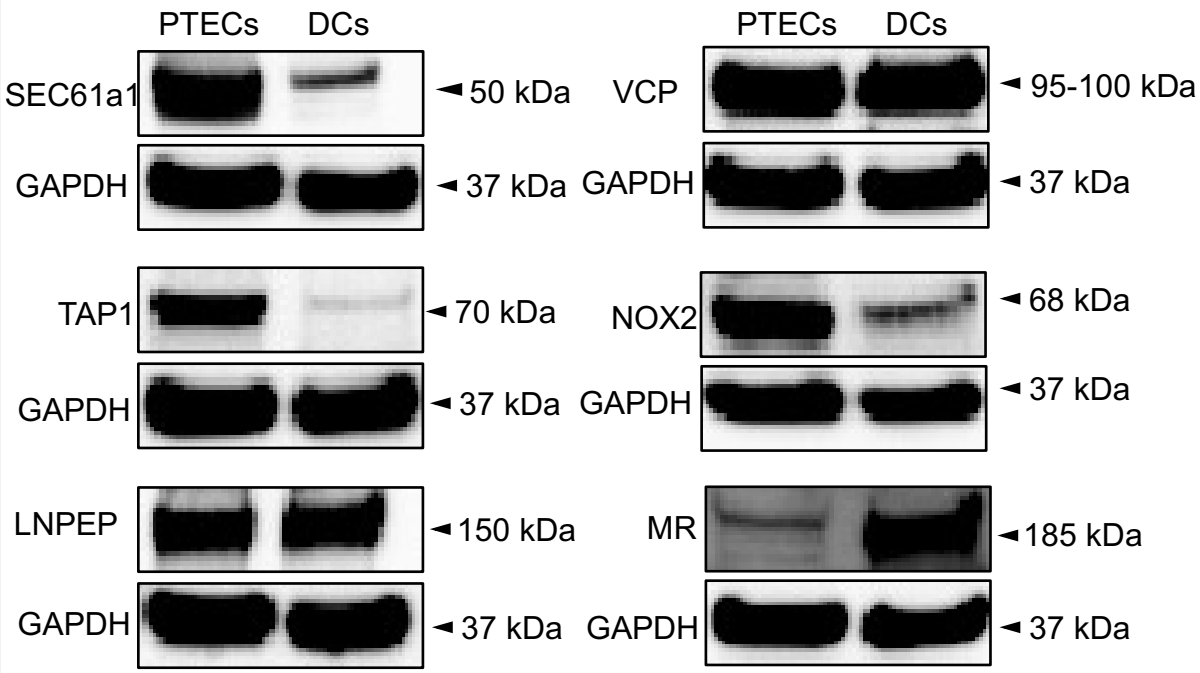

Figure 6: Expression of proteins associated with cross presentation in PTECs and DCs

Protein lysates from PTECs and DCs were analyzed using western blot. The images show snippets of blots from one of two experiments. The molecular weight of the detected proteins is shown on the right side. Equal loading was controlled with GAPDH. kDa= kilodalton.

4.1.3 PTECs express proteins associated with cross-presentation on a similar level compared to LSECs, except for the mannose receptor

After comparing the protein expression levels of PTECs with the ones of the DCs as a population of professional APCs, the PTECs were also compared to LSECs as they are a well described population of non-professional antigen-presenting cells (Knolle et al., 1999, Limmer et al., 2000, Diehl et al., 2008, Schurich et al., 2009, Tiegs and Lohse, 2010). Again, each target protein was analyzed in two independent experiments. Equal protein amounts were again confirmed by equal band sizes of the reference protein GAPDH.

Figure 8 shows snippets from one of the two experiments. Interestingly, the PTECs and LSECs showed approximately equal protein amounts of almost all proteins analyzed (SEC61a1, VCP, TAP1, NOX2, LNPEP). The only exception was the mannose receptor, of which significantly less was detectable in the PTECs compared to LSECs.

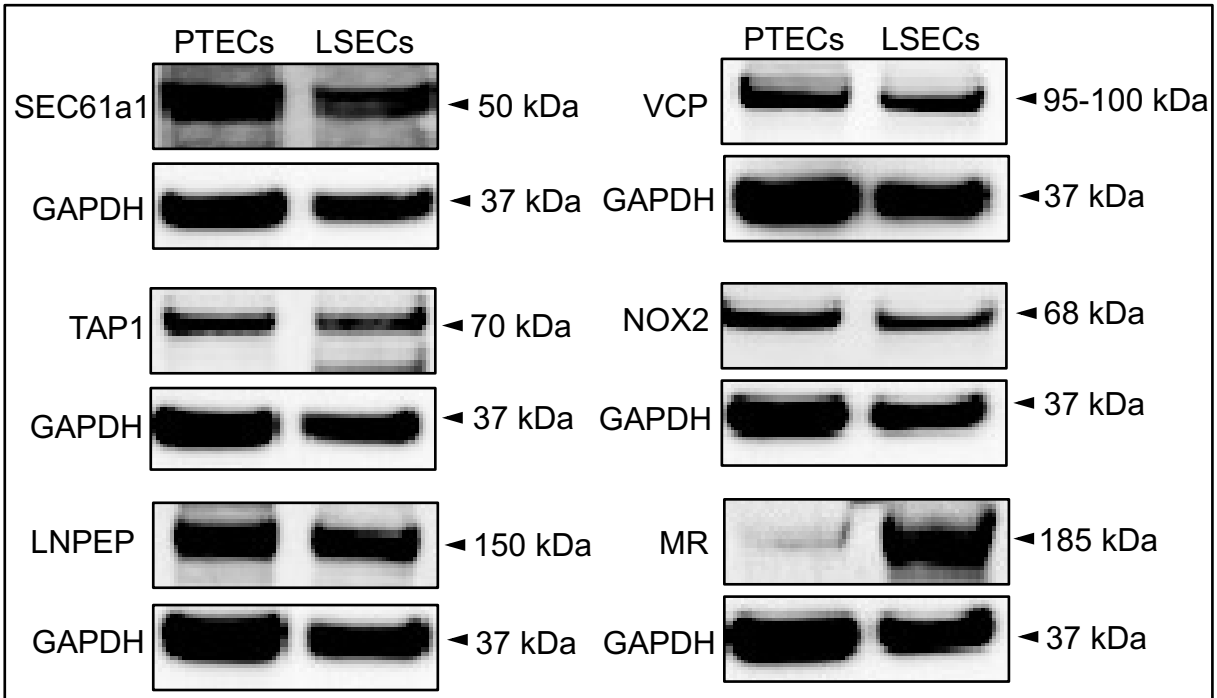

Figure 7: Expression of proteins associated with cross-presentation in PTECs and LSECs

Protein lysates from PTECs and LSECs were analyzed using western blot. The images show snippets of blots from one of two experiments. The molecular weight of the detected proteins is shown on the right side. Equal loading was controlled with GAPDH. kDa= kilodalton.

4.2 OVA internalization by PTECs is concentration, time and energy dependent

After showing, that RNA for proteins associated with cross-presentation is expressed in PTECs, the western blot analyses revealed, that PTECs express the proteins associated with cross-presentation on a higher level or equal level in comparison to DCs and on similar levels in comparison to LSECs, with the exception of the mannose receptor, of which only low levels were present in the PTECs.
The mannose receptor belongs to the group of C-type lectin receptors and plays an important role in antigen cross-presentation, not only because receptor-mediated endocytosis is the first step of cross-presentation, but also because the mannose receptor is known to target endosomal compartments with low lysosomal activity during cross-presentation, leading to prolonged antigen stability after internalization, which is a mandatory requirement for sufficient cross-presentation (Burgdorf et al., 2007).

As the PTECs showed low gene and protein levels for the mannose receptor, this study aimed to investigate the capability of PTECs for endocytosis of soluble exogenous antigens. PTECs, that were cultured for 5 days as described above, were incubated with fluorescently labelled OVA (Alexa Fluor 647) at 37° C for 1 hour with different concentrations of OVA or without OVA and subsequently analyzed using flow cytometry. Using the flow cytometry data of the PTECs, that were incubated without OVA, a gate was set to identify OVA^+ PTECs. It could be shown that the percentage of OVA^+ PTECs was depended on the concentration of OVA (Figure 9B). In two following experiments, the PTECs were incubated with a fixed concentration of OVA (10 µg/ml) or without OVA for 1, 2 or 4 hours and again measured using flow cytometry. These experiments revealed that the percentage of PTECs, that have internalized OVA, depended on the time the PTECs were incubated with OVA (Figure 9A). To rule out unspecific binding of OVA on the cell surface or any kind of unspecific, non-energy dependent internalization of OVA into the PTECs, PTECs were also preincubated for 4 hours on ice (4° C) in order to stop energy-dependent processes within the cells, before being incubated with the fluorescent OVA for 1 hour on ice. This group of PTECs showed almost no OVA^+ PTECs and thus had significantly reduced OVA internalization in comparison to the reference group of PTECs, that were also incubated for 1 hour with the fluorescent OVA, but at 37° C and without preincubation on ice (13.7% ± 1.6%

vs. 0.8% ± 0.4%) (Figure 9A). Thus, unspecific binding of OVA on the cell surface could be ruled out.

In summary, these experiments showed that although the PTECs expressed low levels of the mannose receptor, they were able to internalize soluble exogenous antigen, and that this internalization was active and energy dependent as well as concentration and time dependent.

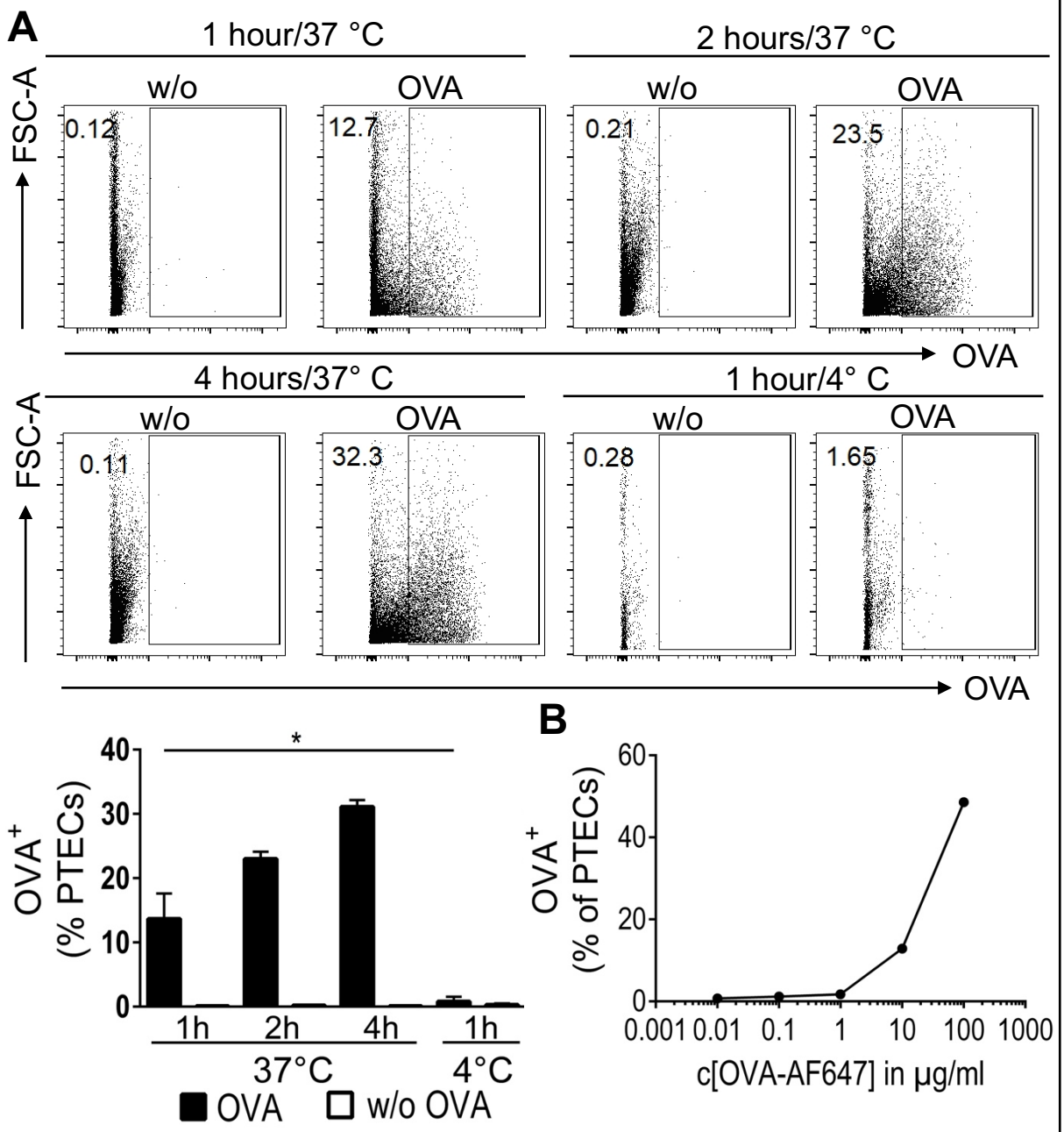

Figure 8: Kinetic of OVA internalization by PTECs

PTECs, that had been cultured for 5 days, were incubated with fluorescently labeled OVA in different concentrations, for different time spans and at different temperatures, followed by analyses using flow cytometry. (A) Representative dot plots of PTECs, that have been cultured with or without fluorescent OVA (10 µg/ml) at 37°C for three different time spans or at 4°C for 1 hour after preincubation at 4°C for 4 hours. Mean ± SEM of two independent experiments are shown. (B) PTECs were cultured for 1 hour at 37° C with different concentrations of fluorescent OVA and analyzed using flow cytometry. *p<0.05; OVA: ovalbumin; w/o: without.

4.3 Significant infiltration by $CD8^+$ T cells in murine models with severe, but not mild glomerulonephritis

4.3.1 Establishment of a staining and analysis method for $CD8^+$ $CD3^+$ T cells in murine kidney sections

In this study, it could be shown, that PTECs express proteins, that are associated with cross-presentation, and that PTECs are capable of antigen internalization.

If the PTECs are able to conduct cross-presentation and therefore activate $CD8^+$ T cells, the question arises, how plausible an activation of $CD8^+$ T cells by PTECs is in vivo, which in turn could suggest a contribution of PTEC-mediated modulation of T cell activity during glomerulonephritis. In order to activate T cells, an APC has to come in close contact with them and form a structure, which is referred to as an immunological synapse, consisting of the TCR, co-stimulatory molecules and adhesion molecules (Dustin, 2014). To answer the question, whether $CD8^+$ T cells can be detected in close contact to PTECs, three mouse models for glomerulonephritis were used to obtain sections of differently severe inflamed kidneys, which were analyzed using immunohistochemistry.

To identify $CD8^+$ T cells in renal tissue, immunohistochemical stainings for CD8 and CD3 were established in the course of this study. CD8 is closely associated with the TCR of $CD8^+$ T cells and restricts the interaction of their TCRs to MHC-I (Pishesha et al., 2022). Since CD8 can also be expressed by DCs (Shortman and Heath, 2010), the detection of it alone is not enough to unambiguously identify $CD8^+$ T cells. Therefore, an additional staining for CD3 was established. CD3 is a surface protein, that is closely associated with the TCR and thus can be used to identify T cells in general (Dong et al., 2019). Serial kidney sections of 2 µm width were stained for CD3 and CD8 using the protocol, that is described above (see chapter 2.2.10). Locally coinciding signals in both section stages were interpreted as $CD8^+$ $CD3^+$ T cells.

To assess the sensitivity and specificity of the established CD3 staining, kidney sections of naïve C57BL/6 mice without renal inflammation (negative control) and spleen sections of C57BL/6 mice (positive control) were stained for CD3 with counterstaining with hemalum. As the naïve C57BL/6 mice had no renal inflammation and thus no appreciable infiltration by T cells, only very rare signals were expected in kidney sections of these mice from a specific staining. Spleen sections of C57BL/6 mice were used to test the sensitivity of the CD3 staining, as the centers of the lymph follicles within the spleen are rich in T cells, which are $CD3^+$ and can confirm the

sensitivity by a strong signal in these areas. To assess the sensitivity and specificity of the established CD8 staining, kidney sections of *Cd8a*$^{-/-}$ mice (negative control) and spleen sections of C57BL/6 (positive control) mice were stained for CD8 without counterstaining with hemalum. Because the *Cd8a*$^{-/-}$ mice lack CD8, no signals were expected in sections from these mice from a specific staining. Additionally, the kidney sections examined from the *Cd8a*$^{-/-}$ mice were from animals with NTS-induced cGN. This has the advantage that tissue changes occurring due to renal inflammation can also be better taken into account when assessing specificity. The T cell rich follicles in the spleen of WT mice, that also contain CD8^{+} T cells, were again used to confirm sensitivity. The established final staining protocols for CD3 and CD8 satisfied these quality criteria as seen in the Figures 10 and 11.

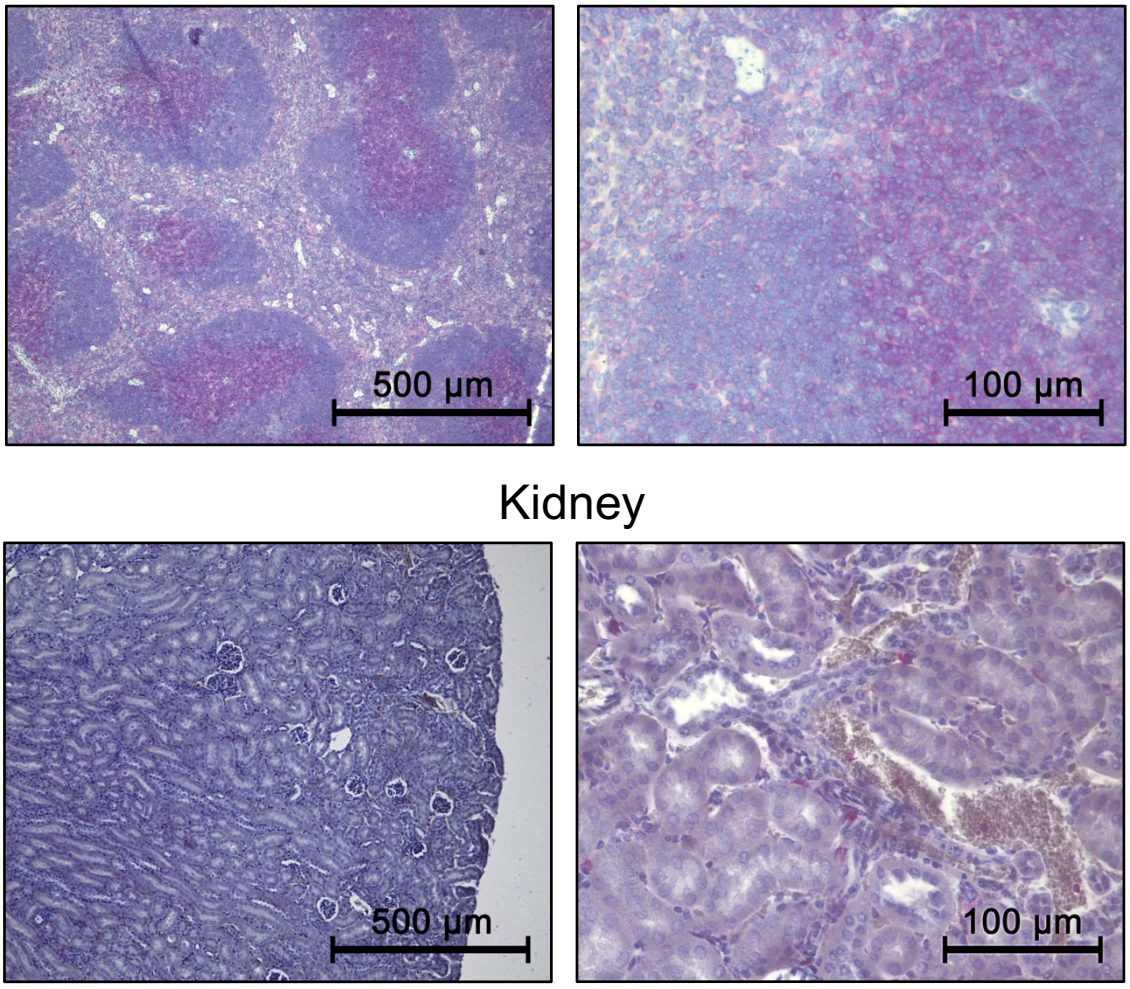

Figure 10: Sensitivity and specificity of the CD3 staining
Staining for CD3 with counterstaining with hemalum of a spleen section of a C57BL/6 mouse and of a kidney section of a naïve C57BL/6 mouse without renal inflammation in two different magnifications each.

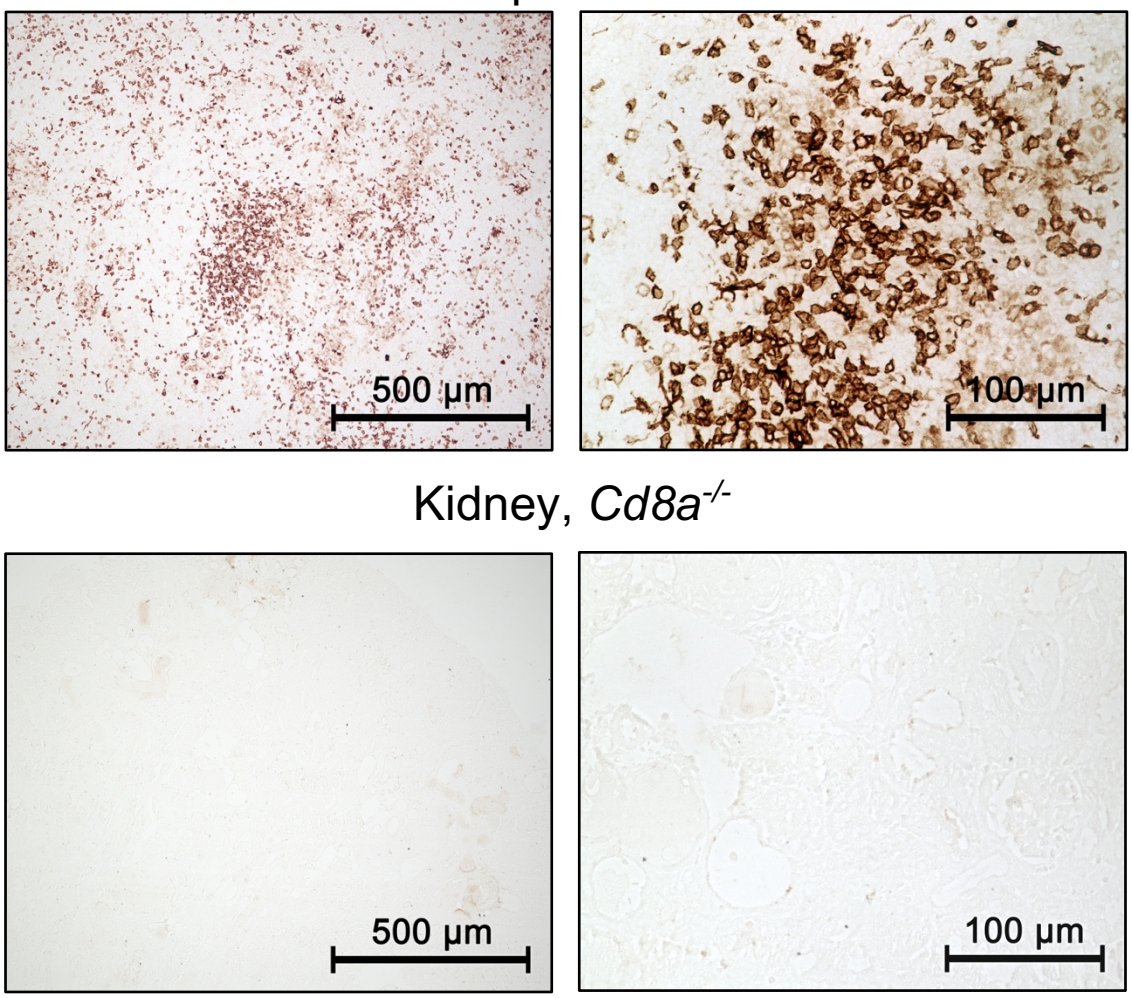

Figure 11: Sensitivity and specificity of the established CD8 staining

Staining for CD8 without counterstaining with hemalum of a spleen section of a C57BL/6 WT mouse and a kidney section of a C57BL/6 *Cd8a*$^{-/-}$ mouse in different magnifications each.

4.3.2 Significant, predominantly tubulointerstitial, infiltration by $CD8^+$ T cells in NTS-treated mice with crescentic glomerulonephritis

After establishing the staining and analysis method for $CD8^+$ T cells, number and localization of $CD8^+$ T cells were firstly analyzed in NTS-treated C57BL/6 mice. Mice, that are injected with NTS, develop an antibody mediated inflammatory reaction against the GBM, which leads to a severe cGN.

The NTS-treated mice were sacrificed at day 8 after disease induction, and the kidneys were collected for the following histological analyses. Two serial kidney sections of 2 µm thickness were stained for CD3 and CD8, respectively, using the established immunohistochemical staining protocol. As described above, five corresponding HPFs were randomly marked in the cortices of the kidneys and the $CD3^+$ $CD8^+$ cells were counted. The cells were divided according to their location into intraglomerular and tubulointerstitial located $CD3^+$ $CD8^+$ cells. To assess the extent of the infiltration by $CD8^+$ T cells during inflammation, the mice with cGN were compared to naïve age-matched, C57BL/6 mice, which were analyzed in the same way.

Representative images of two HPFs from consecutive kidney sections from mice with cGN and naïve mice each are shown in Figure 12A. Cortices of mice with cGN showed significantly more $CD8^+$ T cells in the tubulointerstitial compartment in comparison to the untreated mice (15.1/5HPF ± 4.5/5HPF vs. 170.4/5HPF ± 24.1/5HPF) (Figure 12B). The mice with cGN had also more intraglomerularly located (0/5HPF ± 0/5HPF vs. 1.0/5HPF ± 0.5/5HPF) and total cortical (15.1/5HPF ± 4.5/5HPF vs. 171.4/5HPF ± 24.4/5HPF) $CD8^+$ T cells (Figure 12C and 12D). Thus, there was a significant infiltration by $CD8^+$ T cells detectable in mice with NTS-induced cGN, the vast majority of which was located in the tubulointerstitium.

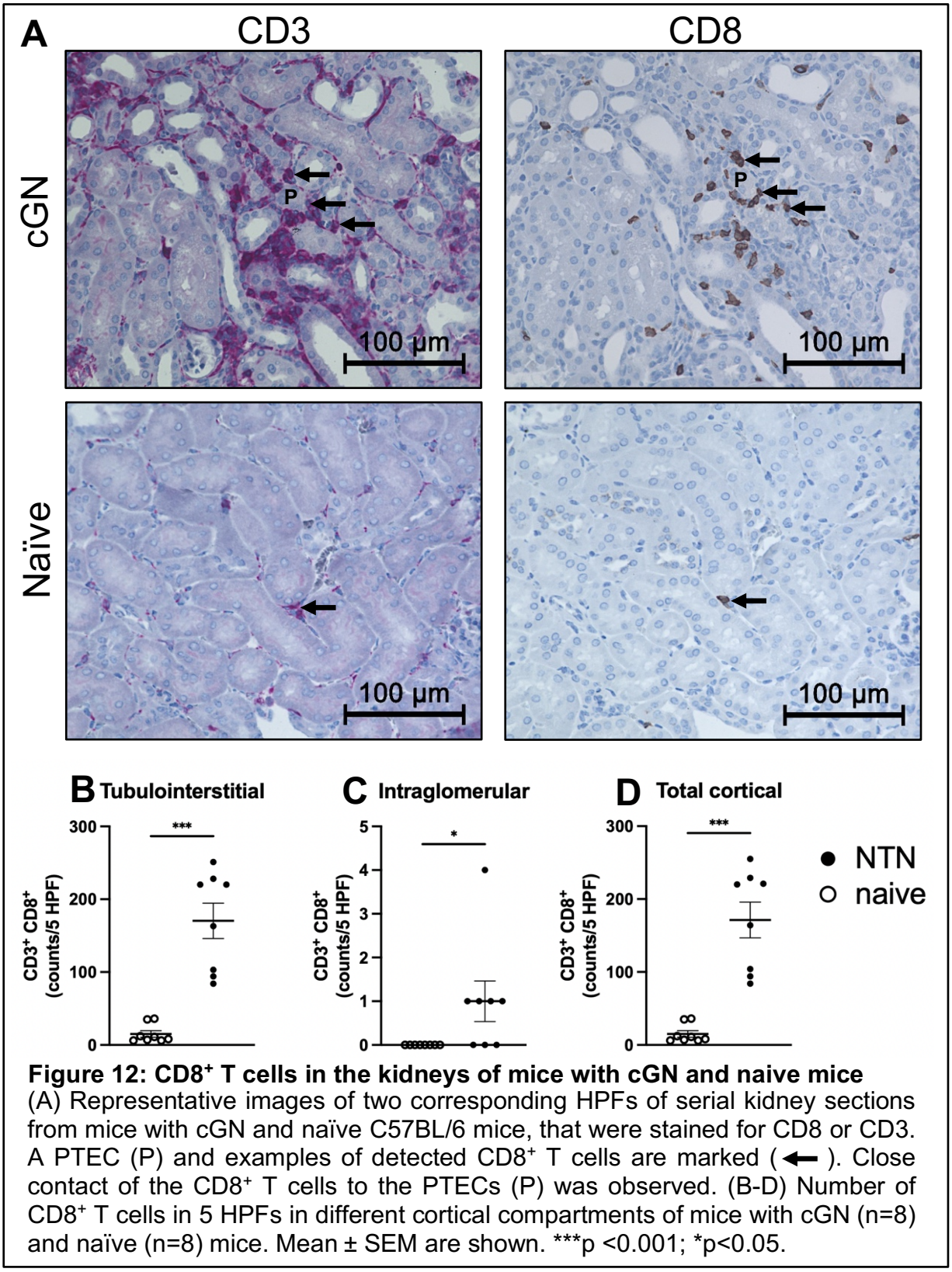

Figure 12: CD8⁺ T cells in the kidneys of mice with cGN and naive mice
(A) Representative images of two corresponding HPFs of serial kidney sections from mice with cGN and naïve C57BL/6 mice, that were stained for CD8 or CD3. A PTEC (P) and examples of detected CD8⁺ T cells are marked (←). Close contact of the CD8⁺ T cells to the PTECs (P) was observed. (B-D) Number of CD8⁺ T cells in 5 HPFs in different cortical compartments of mice with cGN (n=8) and naïve (n=8) mice. Mean ± SEM are shown. ***p <0.001; *p<0.05.

4.3.3 Significant, predominantly tubulointerstitial, infiltration by $CD8^+$ T cells in MRL/MpJ-Fas^{lpr} mice with severe glomerulonephritis

After analyzing the infiltration by $CD8^+$ T cells in the cortices of mice with NTS-induced cGN, next kidney sections of MRL-lpr mice were analyzed using the same method. Mice of the MRL-lpr strain develop a variety of lupus-like symptoms, including a severe lupus glomerulonephritis, which is the leading cause of death in experiments with MRL-lpr mice (Andrews et al., 1978, Dixon et al., 1978). Although the lupus glomerulonephritis is severe, the formation of crescents can only be found occasionally in these mice (Andrews et al., 1978). As controls the MRL mice were used as they share the same genetic background but did not develop lupus nephritis.

Representative imagines of HPFs of kidney sections from MRL-lpr and MRL mice are shown in Figure 13A. Similarly to the results obtained in the comparison of mice with cGN and age-matched, naïve mice, cortices of MRL-lpr mice compared to those of MRL mice had significantly higher numbers of $CD8^+$ T cells in the tubulointerstitial compartment (18.4/5HPF ± 3.2/5HPF vs. 127.6/5HPF ± 60.9/5HP) (Figure 13B). Also, MRL-lpr mice had more $CD8^+$ T cells, that were located intraglomerularly (0.5/5HPF ± 0.2/5HPF vs. 8.4/5HPF ± 2.5/5HP) (Figure 13C) and in total (18.9/5HPF ± 3.3/5HPF vs. 136.0/5HPF ± 62.4/5HP) (Figure 13D) compared to the MRL mice. Again, it could be shown, that there was a significant infiltration by $CD8^+$ T cells into the cortices of inflamed kidneys, which was predominantly tubulointerstitially located.

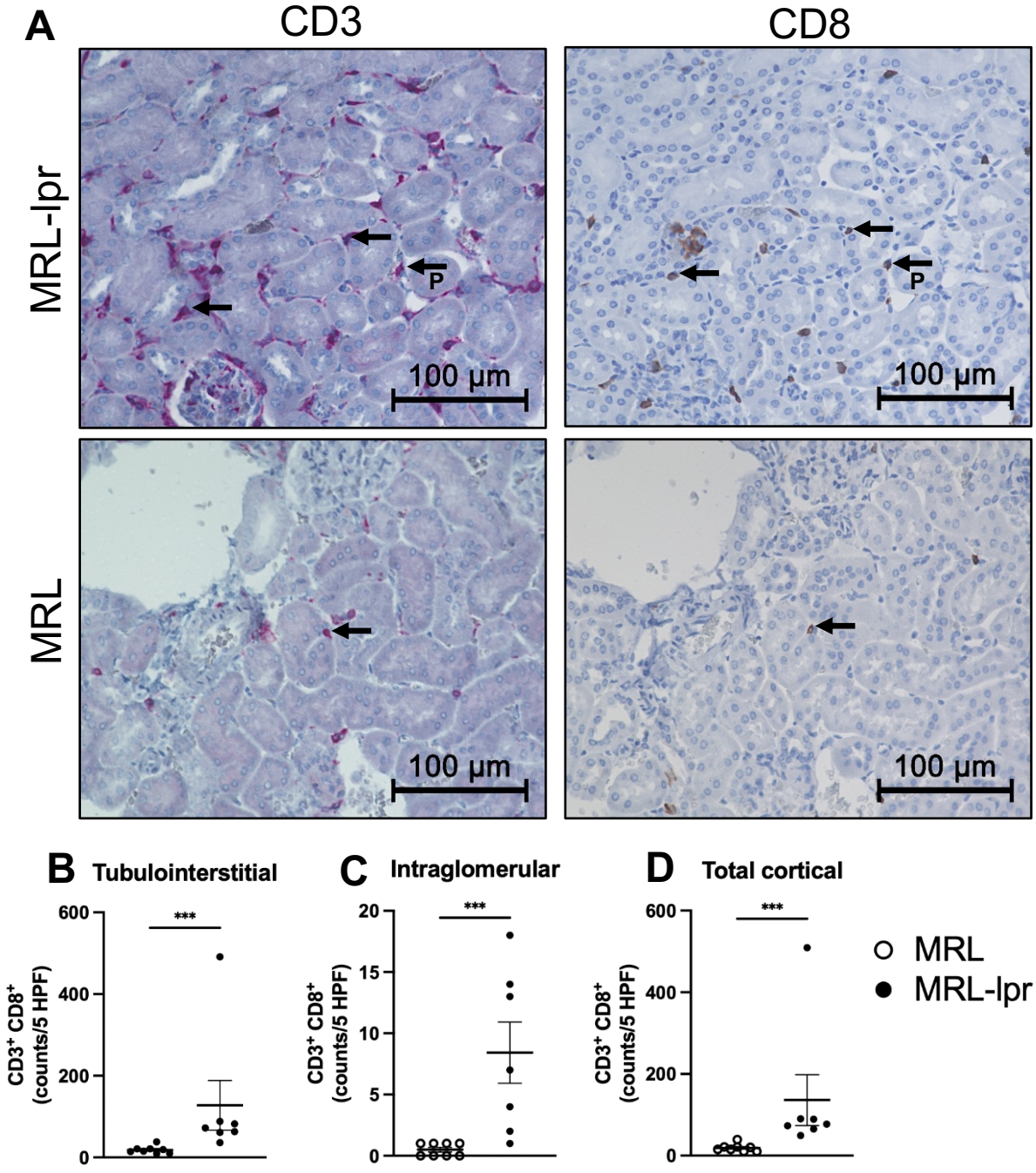

Figure 13: CD8⁺ T cells in the kidneys of MRL-lpr and MRL mice

(A) Representative images of two HPFs of serial kidney sections from MRL-lpr and MRL mice, that were stained for CD8 or CD3. A PTEC (P) and examples of detected $CD8^+$ T cells are marked (←). (B-D) Number of $CD8^+$ T cells in 5 HPFs in different cortical compartments of MRL-lpr (n=7) and MRL (n=8) mice. Mean ± SEM are shown. ***p<0.001.

4.3.4 No significant infiltration by $CD8^+$ T cells in pristane-treated mice with mild glomerulonephritis

After analyzing the infiltration by $CD8^+$ T cells in the cortices of a mouse model for cGN and in MRL-lpr mice, which also exhibit severe glomerulonephritis, the infiltration by $CD8^+$ T cells in pristane-treated mice was studied. As described above, pristane-treated mice develop anti-nuclear antibodies, which induce lupus-like symptoms, including glomerulonephritis (Satoh and Reeves, 1994, Satoh et al., 1995). However, the induced glomerulonephritis is relatively mild and is usually not the cause of death for pristane-treated mice (McGaha and Madaio, 2014).

C57BL/6 mice were injected with pristane and sacrificed after 9 months for histological analyses of the kidneys using immunohistochemistry as described above. Age-matched naïve C57BL/6 mice were used as controls. Representative images of pristane-treated and naïve mice are shown in Figure 14A. In these analyses, the two groups showed no significant difference, neither regarding the number of cortical $CD8^+$ T in the tubulointerstitium (37.0/5HPF ± 6.8/5HPF vs. 29.0/5HPF ± 9.3/5HP), nor inside of glomeruli (1.4/5HPF ± 0.5/5HPF vs. 1.5/5HPF ± 0.6/5HPF) or overall (38.4/5HPF ± 6.9/5HPF vs. 30.5/5HPF ± 9.5/5HPF) (Figure 14B-D).

A substantial part of the data, that was shown in this results section, was published in Cells in 2022 (Linke and Cicek et al., 2022).

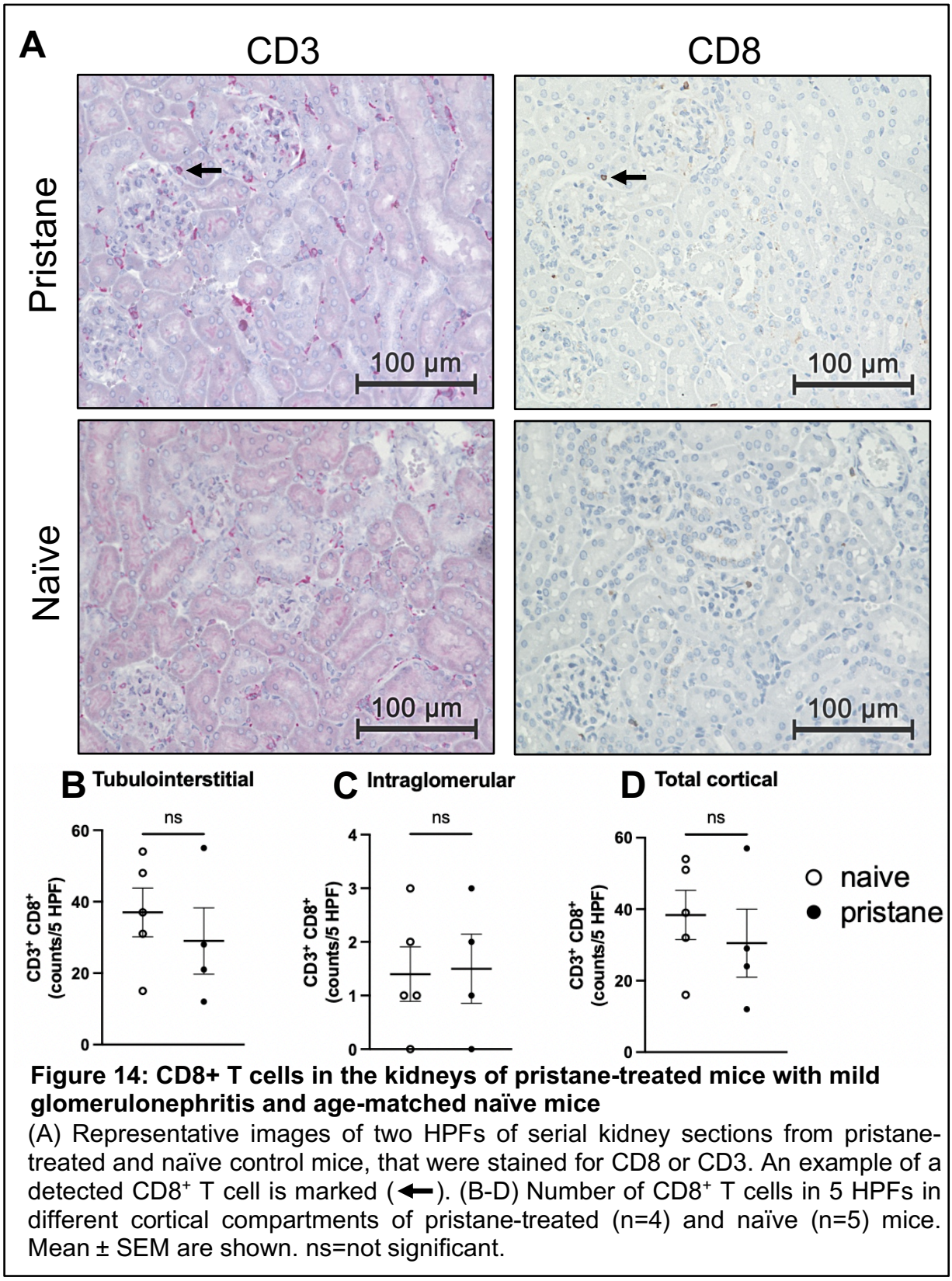

Figure 14: CD8+ T cells in the kidneys of pristane-treated mice with mild glomerulonephritis and age-matched naïve mice

(A) Representative images of two HPFs of serial kidney sections from pristane-treated and naïve control mice, that were stained for CD8 or CD3. An example of a detected $CD8^+$ T cell is marked (←). (B-D) Number of $CD8^+$ T cells in 5 HPFs in different cortical compartments of pristane-treated (n=4) and naïve (n=5) mice. Mean ± SEM are shown. ns=not significant.

5 Discussion

5.1 PTECs express proteins, that are associated with cross-presentation

Glomerulonephritides are autoimmune-mediated glomerular diseases with so far only poorly understood mechanisms. Previous studies show an infiltration by cytotoxic $CD8^+$ T cells during glomerulonephritides such as ANCA-associated glomerulonephritis, lupus nephritis and Goodpasture's disease in patients as well as in animal models. The correlation of these infiltrates with disease severity indicates a pathophysiologic contribution of $CD8^+$ T cells in glomerulonephritis (Kawasaki et al., 1992, Merkel et al., 1996, Reynolds et al., 2002, Couzi et al., 2007, Hu et al., 2016, Chang et al., 2017, Kidder et al., 2017, Chen et al., 2018, Mueller et al., 2023). Furthermore, tubulointerstitial injury, which is associated with many glomerular diseases was shown to be related to renal T cell infiltration (Lai et al., 2007). Additionally, previous studies were able to show, that kidney intrinsic DCs contribute as APCs to the renal infiltration of $CD8^+$ T cells not only by activating $CD8^+$ T cells, but also by mediating the persistence of the infiltration (Heymann et al., 2009, Hochheiser et al., 2011, Chen et al., 2021). APC functions encompass the presentation of exogenous antigen, either on MHC-II or via cross-presentation on MHC-I, and the expression of co-stimulatory molecules, which are upregulated during inflammation and transduce co-stimulatory signals, that are necessary for full T cell activation. Although APC functions are classically associated with leukocytes, it was discovered, that also structural cells are able to function as APCs, which are thus referred to as non-professional APCs (Krausgruber et al., 2020, Harryvan et al., 2021). Accordingly, it could be shown recently, that PTECs are able to induce a proinflammatory phenotype in naïve $CD4^+$ T cells, and thus the PTECs were identified as non-professional APCs regarding $CD4^+$ T cells (Breda et al., 2019). In this study, immunomodulatory properties of PTECs as non-professional APCs towards $CD8^+$ T cells were analyzed.

Because APCs are not necessarily also infected during infections or alter themselves when malignancy occurs, the capability of APCs to present exogenous antigens is essential for effective activation of T cells (Sigal et al., 1999, den Haan and Bevan, 2001). TCRs of $CD8^+$ T cells interact with peptide-presenting MHC-I and since usually the pathway of antigen presentation on MHC-I is restricted to endogenous antigens, distinct APCs possess an additional mechanism, that enables them to present exogenous antigen on MHC-I, which is termed cross-presentation (Sigal et al., 1999, den Haan and Bevan, 2001). Thus, to investigate the immunomodulatory properties of

PTECs towards $CD8^+$ T cells, it was the first aim of this study to determine whether PTECs have the capability to conduct antigen cross-presentation. For this, in a first series of experiments the mRNA expression levels of target genes, that are associated with the endosome-to-cytosol pathway of cross-presentation, were determined in PTECs using reverse transcription and qRT-PCR. As DCs are described as professional (Banchereau and Steinman, 1998) and LSECs as non-professional APCs (Knolle et al., 1999, Limmer et al., 2000, Diehl et al., 2008, Kruse et al., 2009, Tiegs and Lohse, 2010, Shetty et al., 2018), these cell populations were used for comparison. Most notably, in these mRNA expression analyses the PTECs expressed every analyzed target gene. In comparison to DCs, the PTECs had only significantly lower expression levels of *Mrc1* and *Cybb*, which are genes encoding for proteins, that mediate antigen internalization and stabilization after internalization, respectively. Similar results were seen when the PTECs were compared to the non-professional APC population of LSECs, where the LSECs had similar levels of *Cybb*, but higher levels of *Sec61a1*, encoding for one of the subunits of the Sec61 translocon and *Mrc1*. Having shown, that mRNA of target genes, that are associated with the endosome-to-cytosol pathway of cross-presentation, is expressed in PTECs, the next aim was to determine the abundance of the respective proteins in PTECs compared to DCs and LSECs using western blot analyses. As the translation of RNA into proteins can vary as well as the half-life of the translated proteins, the detection of protein levels is a more direct indicator of the functional capabilities of a cell. In the conducted western blot analyses, the PTECs expressed almost every target protein on at least the same level as DCs or LSECs. Interestingly, in comparison to DCs, the PTECs had higher expression levels of the two proteins TAP and SEC61, that are associated with antigen translocation out of and into endosomes. Furthermore, NOX2, which mediates the endosomal alkalization and thereby facilitates antigen stability, was expressed on a higher level in PTECs compared to DCs. All other analyzed proteins had similar expression levels in PTECs and DCs, except for the mannose receptor, of which only low levels were expressed in the PTECs. In the comparison to LSECs, PTECs expressed every analyzed protein on a similar level, again with the exception of the mannose receptor. With this data so far, this study could show, that PTECs express proteins, that mediate the translocation of antigen out of endosomes, transport of antigen back into endosomes, endosomal alkalization and peptide trimming, all of which are described as necessary steps in antigen cross-presentation (Embgenbroich

and Burgdorf, 2018). However, because the PTECs showed low levels of the mannose receptor, the data raised the question, if the PTECs are capable of targeted antigen internalization. The mannose receptor is especially important for cross-presentation as it not only mediates the internalization of antigen, which is the first step of cross-presentation, but also traffics the internalized antigens into the proper endosomal compartments for cross-presentation with low lysosomal activity, which is essential for antigen stabilization and subsequent antigen cross-presentation (Burgdorf et al., 2007, Chatterjee et al., 2012).

Comparing the mRNA and protein data, there was discrepancy in the expression levels. While the protein analyses showed abundances of almost all analyzed proteins in the PTECs, the mRNA expressions did not reflect this trend. This difference is consistent with previous observations, that show various factors affecting the relationship between mRNA and protein levels such as the translation rate, which depends on the mRNA itself (Wethmar et al., 2010) and can be regulated by proteins or micro RNAs (Barrett et al., 2012), and variations in protein half-life by modulation of the ubiquitin-proteasome pathway (Tang and Amon, 2013, Liu et al., 2016). Proteins determine the capability of cells to conduct certain functions, and the mRNA data can only give a hint to the protein expression, which ultimately provides information about the phenotype and functions of a cell.

Another finding worthy of further consideration is the comparatively low expression of SEC61a1, TAP1, and NOX2 in the DCs. In this regard, it should be mentioned that the detection of low protein levels does not necessarily mean the absence of the respective protein function. For example, as it will be discussed below, PTECs have the capacity for mannose receptor-mediated antigen uptake, although only low protein levels of the mannose receptor were detected in PTECs in the assays performed in this study. Furthermore, the possibility of alternative mechanisms has to be addressed. Although it is generally accepted, that the translocation of internalized antigens out of endosomes is ERAD-dependent (Ackerman et al., 2003, Imai et al., 2005, Ackerman et al., 2006, Goldszmid et al., 2009), the question of the exact translocon has not yet been solved. Although strong evidence points out the role of SEC61 (Koopmann et al., 2000, Imai et al., 2005, Ackerman et al., 2006, Zehner et al., 2015), Sec61-independent transport has also been reported (Dingjan et al., 2016, Grotzke et al., 2017). A similar argument can be made with respect to the low levels of TAP in the DCs, where TAP-dependence has been described in many studies, but TAP-independent

transendosomal antigen transport with a possible as yet undiscovered transporter has also been postulated (Kovacsovics-Bankowski and Rock, 1995, Ackerman et al., 2003, Burgdorf et al., 2008, Lawand et al., 2016). Low levels of NOX2 could lead to the argument that antigen stability important for cross-presentation could be missing in DCs. However, it has been previously shown that DCs can store antigen in a prolonged manner in compartments, that were identified as late endosomal or lysosomal. This antigen storage allows DCs to present exogenous antigen to T cells for a longer period of time, thereby activating them more efficiently (van Montfoort et al., 2009). Therefore, it is not plausible to assume low antigen stability in DCs although low levels of NOX2. A possible explanation for antigen stability in the endosomal compartments of DCs despite a possible low degree of alkalization by NOX2 can be the fact that endosomes in DCs have already less proteolytic activity than endosomes in other cell populations. Interestingly, it could be shown, that endosomes in DCs are poor of proteases (Delamarre et al., 2005) and that the protease activity in DCs is reduced after activation by pathogen-associated molecular patterns (Lennon-Duménil et al., 2002).

The abundances of NOX2, Sec61a1 and TAP in PTECs in comparison to DCs could indicate a greater relevance of these proteins for cross-presentation in PTECs in contrast to DCs. Since the DCs are leukocytic cell populations, it is not far-fetched to assume that DCs have additional mechanisms or different requirements in protein abundance than the epithelial PTECs. It is all the more interesting that PTECs and LSECs, which are also structural cells with resorptive functions and are described as non-professional APCs, show similar protein expression profiles.

As mentioned above, the PTECs expressed low levels of the mannose receptor, which raised the question, if the PTECs are capable of receptor-mediated, directed internalization of antigens in the context of cross-presentation as the mannose receptor is reported to be especially relevant for this pathway (Burgdorf et al., 2007). However, other antigen receptors have also been reported to mediate efficient cross-presentation such as langerin, DC-SIGN, Dectin-1 and DEC-205 (Bonifaz et al., 2002, Weck et al., 2008, Unger et al., 2012, Fehres et al., 2017). To answer the question, if the PTECs are capable to internalize exogenous antigen, the antigen uptake by PTECs was analyzed with fluorescently labelled OVA protein and flow cytometry. Here, the data showed, that PTECs actively internalize antigen as the antigen uptake was time and concentration dependent and most importantly energy dependent. Furthermore, this data laid the groundwork for further experiments, that were published in

association with this study, in which the question of the exact receptor was investigated in more detail. In that study, the mannose receptor was blocked using the polysaccharide mannan. Since the mannose receptor-mediated internalization is dependent on clathrin-coated vesicles, the effect of the clathrin-inhibitor chlorpromazine was also studied using flow cytometry. In both cases, the capabilities of PTECs to internalize fluorescently labelled OVA protein decreased significantly, whereas the internalization was not affected by the addition of D-galactose, which does not inhibit the mannose receptor (Linke and Cicek et al., 2022). That data gave evidence, that the mannose receptor provides a substantial contribution to antigen internalization by PTECs. However, since there was still internalization by PTECs after inhibition by mannan or chlorpromazine, the data suggested, that other receptors are also involved in antigen internalization by PTECs. Additional experiments with inhibition of other endocytic receptors could shed light on this question.

Furthermore, as the observations regarding the protein abundance of the mannose receptor and its functionality in PTECs show, protein expression levels do not necessarily reflect the presents of the respective function. Thus, to identify more clearly, which cellular functions the PTECs could use for cross-presentation, coculture experiments with $CD8^+$ T cells and PTECs could be conducted with specific blockage of the associated proteins to determine an effect on cross-presentation by PTECs. An example for such a study was published recently, in which the Sec61 translocon in DCs was blocked using an intrabody (Zehner et al., 2015). Such a functional analysis of protein dependency in the cross-presentation pathway for PTECs was also conducted in the paper, that is associated with the present study. In that paper, the inhibitor of the LMP7 subunit of the immunoproteasome ONX 0914 was used to pre-treat PTECs before co-culture with $CD8^+$ T cells (Linke and Cicek et al., 2022). As discussed previously, the immunoproteasome is associated with antigen degradation into peptides during cross-presentation and generates more immunodominant peptides than the regular proteasome (Aki et al., 1994, Chen et al., 2001, Palmowski et al., 2006, Guimarães et al., 2018). Preliminary results from the present study [data not shown] could show, that, similar to the mannose receptor, PTECs expressed low levels of the immunoproteasome subunit LMP7 in comparison to DCs and LSECs. Yet, the mentioned experiments using ONX 0914 could show inhibited cross-presentation indicating, that the PTECs use the immunoproteasome to conduct cross-presentation

(Linke and Cicek et al., 2022). However, the phenotype, that is induced in $CD8^+$ T cells by PTECs should be discussed in more detail in the next chapter.

5.2 The PTECs as non-professional APCs

Emerging evidence shows that APC functions are not limited to leukocytes, but can also be conducted by structural endothelial, epithelial or stromal cells, which are referred to as non-professional APCs (Krausgruber et al., 2020, Harryvan et al., 2021). Non-professional APCs are identified as such by the capability to present exogenous antigen on MHC-II or via cross-presentation on MHC-I, and regulated expression of co-stimulatory or co-inhibitory molecules, which taken together enables them to modulate T cell responses and induce tolerance or immunity(Krausgruber et al., 2020, Harryvan et al., 2021). Previously, Breda et al. studied the phenotype, that is induced in $CD4^+$ T cells by antigen presenting PTECs, using in vitro coculture analyses with OVA-specific $CD4^+$ T cells and OVA peptide. In that analyses the PTECs induced the production of the type 1 cytokines IL-2, IFN-γ and TNF-α by $CD4^+$ T cells as well as the upregulation of the activation marker CD25 and proliferation, which showed, that PTECs induce a proinflammatory phenotype in $CD4^+$ T cells. However, in comparison to DCs, that were also cocultured with $CD4^+$ T cells, the PTECs were less potent in inducing the proinflammatory phenotype and were thus identified as less potent non-professional APCs regarding $CD4^+$ T cells (Breda et al., 2019). An analogous approach was chosen in the publication, that is associated with this study, where the PTECs were cocultured with OVA-specific $CD8^+$ T cells in the presence of peptide free OVA protein. In these analyses the PTECs induced the production of the proinflammatory cytokines IL-2, -17A, -6, TNF-α and IFN-γ, increased the expression of the activation markers CD25 and CD44, induced proliferation and the expression of the cytotoxic enzyme Gzmb and the degranulation marker CD107a in $CD8^+$ T cells, showing that PTECs induce a cytotoxic phenotype in $CD8^+$ T cells. Interestingly, whilst some of the expression levels of these markers for a cytotoxic phenotype varied in comparison between in vitro PTEC- or DC-activated $CD8^+$ T cells, no clear trend of DCs as more potent inducers of cytotoxicity in $CD8^+$ T cells could be observed (Linke and Cicek et al., 2022). Especially interesting in the context of cross-presentation is also the use of peptide free OVA protein in these conducted coculture experiments. As MHC-I molecules present peptides, that are derived by degradation from proteins, and are not able to present whole proteins, the induction of cytotoxicity in $CD8^+$ T cells requires the

PTECs to internalize the OVA protein present in the coculture, degrade it into peptides and present it on MHC-I, which is cross-presentation. Furthermore, the cytotoxicity of the PTEC-activated $CD8^+$ T cells could be shown in functional experiments using P815 target cells, in which killing of the target cells by the PTEC-activated $CD8^+$ T cells could be shown (Linke and Cicek et al., 2022).

These analyses could show, that PTECs induce cytotoxicity in $CD8^+$ T cells in vitro by cross-presenting exogenous antigen. However, the outcome of stimulation of $CD8^+$ T cells by PTECs in vivo and the possible contribution of PTECs as non-professional APCs in vivo still remain an open question and thus will be discussed in the next chapter.

5.3 Contribution of PTECs as non-professional APCs in vivo

This study was able to show, that PTECs express proteins, that are associated with the endosome-to-cytosol pathway of antigen cross-presentation and laid the groundwork to further identify PTECs as non-professional APCs able to activate $CD8^+$ T cells (Linke and Cicek et al., 2022), which included the use of in vitro assays. In vivo, the contribution of professional as well as non-professional APCs has been studied previously. In vivo studies with DCs describe the induction of tolerance as well as immunity in T cells, depending on the activation status of DCs, which can be changed by pathogen or danger associated molecular patterns, that induce DC maturation with a DC phenotype, which induces immunity. Furthermore, the ability to migrate allows DCs to enter lymph nodes to interact with T cells (Banchereau and Steinman, 1998, Banchereau et al., 2000, Hawiger et al., 2001, Théry and Amigorena, 2001, Joffre et al., 2012). In vivo studies with LSECs as non-professional APCs show their strong tolerogenic potential, and interestingly, LSECs do not upregulate the expression of the co-stimulatory molecules CD80 and CD86, even under inflammatory conditions (Knolle et al., 1999, Limmer et al., 2000, Diehl et al., 2008, Kruse et al., 2009, Kern et al., 2010). As the LSECs are endothelial cells, they are continuously in contact with naïve or effector T cells and thereby can fulfill their APC functions. However, in contrast to DCs or LSECs the PTECs are neither migratory cells, nor constantly in direct contact with the blood flow and since there is no considerable infiltration of the kidney with T cells in homeostasis, it is unlikely, that the PTECs have a relevant contribution to the modulation of T cell responses in homeostasis. However, it would be natural to assume, that PTECs induce tolerance in homeostasis, since the induction of immunity

by APCs usually requires APC maturation, which is dependent on activating signals (Banchereau and Steinman, 1998, Hawiger et al., 2001). Indeed, it has been shown, that PTECs can induce tolerance, which could contribute to allograft tolerability by dampening T cell responses (Starke et al., 2010, Wilkinson et al., 2011, Kassianos et al., 2013, Sampangi et al., 2015). This appears to be in conflict with reports, that suggest a proinflammatory role of PTECs in renal inflammation (Wuthrich et al., 1989, Wu et al., 2004, Breda et al., 2019). However, a similar conflict was also described in relation to the role of DCs during renal inflammation, which acted attenuating in early but aggravating in late disease. This apparent conflict could be solved by the observation, that DCs become activated and thus pathogenic during glomerulonephritis (Heymann et al., 2009, Hochheiser et al., 2011). A similar mechanism could be proposed for PTECs, which can be supported by the finding by Breda et al., that the expression of co-stimulatory molecules by PTECs is downregulated in early but upregulated in later disease during NTS-induced cGN (Breda et al., 2019). Amongst other stimuli, an activating factor for PTECs during renal inflammation could be the exposition of PTECs to excessive amounts of albumin during proteinuric renal diseases, which has been described previously as an activating stimulus towards PTECs and leads to chemokine secretion by PTECs (Zoja et al., 2004, Erkan et al., 2005, Abbate et al., 2006, Nakhoul and Batuman, 2011). The secretion of chemokines by PTECs not only suggests tubulointerstitial infiltration with close contact to PTECs during renal inflammation but would also provide a mechanistical explanation for the occurrence of renal T cell infiltration during inflammation. To analyze the extent and localization of infiltrating $CD8^+$ T cells during glomerulonephritis, an immunohistochemical staining and analysis method to identify $CD3^+$ $CD8^+$ T cells was established in the course of this study and applied to kidney sections of mice with NTS-induced cGN, MRL-lpr mice with severe lupus glomerulonephritis and mice with pristane-induced mild lupus glomerulonephritis. In these analyses a significant infiltration by $CD8^+$ T cells was observed in mice with experimental cGN and in the MRL-lpr mice, which was predominantly tubulointerstitial localized, whereas no significant infiltration could be detected in pristane-treated mice. These findings are in line with previous studies, that describe an infiltration by $CD8^+$ T cells, also in the anti-GBM Goodpasture's disease and in severe (class III and IV) lupus nephritis, which correlates with disease severity (Kawasaki et al., 1992, Merkel et al., 1996, Reynolds et al., 2002, Couzi et al., 2007, Hu et al., 2016, Chang et al., 2017,

Kidder et al., 2017, Chen et al., 2018, Mueller et al., 2023). The interaction with the tubulointerstitially located $CD8^+$ T cells with activated PTECs could lead to a reactivation of cytotoxic $CD8^+$ T cells and thereby aggravate renal inflammatory disease, which also suggests concominant killing of PTECs by $CD8^+$ T cells. Indeed, it could be shown, that particularly PTECs are positive for cleaved caspase 3 in NTS-induced cGN and that the number of cleaved caspase 3^+ cells and renal impairment can be reduced in *Gzmb*$^{-/-}$ mice, suggesting GzmB-mediated killing of PTECs by cytotoxic $CD8^+$ T cells by cleavage of caspase 3 (Mueller et al., 2023). In the same study, clonal expansion of cytotoxic $CD8^+$ T cells could be observed in patients with ANCA-associated glomerulonephritis as well as in mice with NTS-induced cGN, suggesting an antigen-specific activation of $CD8^+$ T cells (Mueller et al., 2023). This is not suprising, as T cell responses are antigen specific, which is well known in Goodpasture's disease and has been described previously in lupus nephritis (Merkel et al., 1996, Murata et al., 2002). Whilst target antigens are known in glomerular diseases such as part of the alpha 3 type IV collagen in Goodpasture's disease and MPO in ANCA-associated glomerulonephritis, it was also shown previously, that albumine-derived peptides, that are generated by PTECs in proteinuric disease, can act as target antigens in renal inflammation (Macconi et al., 2009). Future studies may further identify the target antigen(s) against which T cells react during glomerulonephritis and that may be presented by PTECs to T cells during disease.

Finally, studies with PTEC-specific delivery of immunosuppressants may help to identify the exact role of PTECs in immune-mediated glomerular disease and may lead to better and more targeted therapies in glomerulonephritis.

6 Summary

Glomerulonephritides are autoimmune-mediated glomerular diseases, the underlying mechanisms of which are the subject of current research. Studies point out the contribution of $CD8^+$ T cells during glomerulonephritis, and their modulation by kidney intrinsic APCs in the development of renal damage. According to previous findings, that also structural cell populations can act as non-professional APCs, it was discovered recently, that the PTECs in the kidney are capable to activate $CD4^+$ T cells, inducing a proinflammatory phenotype. The present study aimed to investigate the immunomodulatory properties of PTECs towards $CD8^+$ T cells and the possible contributions of this postulated immunomodulatory property in vivo.

An important mechanism in APCs is the capability to present exogenous antigen on MHC-I, which is called cross-presentation. In this study mRNA analyses for target genes involved in cross-presentation were conducted, in which PTECs were compared to DCs as professional and LSECs as non-professional APCs. Here, the PTECs expressed mRNA of every target gene. In subsequent comparative protein analyses, PTECs expressed every protein on at least similar levels, except for the mannose receptor. Functional analyses of the antigen internalization by PTECs using fluorescently labelled OVA showed, that despite of low protein levels of the mannose receptor, PTECs were able to internalize exogenous antigen in an active and directed process. To determine the plausibility of the postulated immunomodulatory function of PTECs in vivo, in this study an immunohistochemical staining and analysis method for $CD8^+$ T cells was established and used to analyze kidney sections of three murine models for glomerulonephritis with different severity. Especially in the kidneys with severe glomerulonephritis, an infiltration by $CD8^+$ T cells into the tubulointerstitium could be observed, which enables contact of these infiltrating cells with PTECs.

In conclusion, this study shows, (1) that PTECs express proteins required to conduct the endosome-to-cytosol pathway of cross-presentation, with the limitation of low expression levels of the mannose receptor and (2) that the PTECs are able to internalize exogenous antigen in an active process. (3) As a significant tubulointerstitial infiltration by $CD8^+$ T cells was detected in murine severe, but not in mild glomerulonephritis, contact of $CD8^+$ T cells with PTECs and a thereby mediated T cell activation by PTECs might be a contributing mechanism to cell-mediated autoimmune tissue damage especially in severe forms of glomerulonephritis.

7 Zusammenfassung

Glomerulonephritiden sind autoimmunvermittelte glomeruläre Erkrankungen, deren zugrundeliegende Mechanismen Gegenstand der aktuellen Forschung sind. Studien weisen auf den Beitrag $CD8^+$ T-Zellen bei der Glomerulonephritis, und ihre Modulation durch nierenresidente APCs bei der Entstehung von Nierenschäden hin. Nach früheren Erkenntnissen, dass auch strukturelle Zellpopulationen als nicht-professionelle APCs fungieren können, wurde kürzlich gezeigt, dass die PTECs der Niere $CD4^+$ T-Zellen in vitro aktivieren und einen proinflammatorischen Phänotyp induzieren können. Ziel der vorliegenden Studie war es, die immunmodulatorischen Eigenschaften von PTECs gegenüber $CD8^+$ T-Zellen und die möglichen Einflüsse dieser Interaktion in vivo zu untersuchen. Da die Präsentation von exogenem Antigen auf MHC-I (Kreuz-Präsentation) eine wichtige APC-Fähigkeit ist, wurden in dieser Studie in vergleichenden mRNA-Analysen die PTECs mit DCs als professionelle und LSECs als nicht-professionelle APCs hinsichtlich der Expression daran beteiligter Gene verglichen. Dabei exprimierten die PTECs mRNA für jedes untersuchte Zielgen. In anschließenden vergleichenden Proteinanalysen zeigten die PTECs bis auf den Mannoserezeptor mindestens gleichstarke Expressionsniveaus am Prozess der Kreuzpräsentation beteiligter Proteine. Funktionelle Analysen der Antigeninternalisierung durch PTECs mittels Durchflusszytometrie zeigten, dass PTECs trotz geringer Mannoserezeptorexpression exogenes Antigen in einem aktiven Prozess internalisieren. Nach Etablierung einer immunhistochemischen Färbe- und Analysemethode für $CD8^+$ T-Zellen zeigte sich in Nierenschnitten aus drei Mausmodelle für Glomerulonephritis unterschiedlichen Schweregrades insbesondere in Nieren mit schwerer Glomerulonephritis eine Infiltration von $CD8^+$ T-Zellen in das Tubulointerstitium mit einem somit möglichen Zellkontakt von diesen zu PTECs. Zusammenfassend zeigt diese Studie, (1) dass PTECs Proteine exprimieren, die für die Durchführung des Endosom-zu-Zytosol-Weges der Kreuzpräsentation erforderlich sind, mit der Einschränkung niedriger Mannoserezeptorexpression, und (2) dass die PTECs in der Lage sind, exogenes Antigen in einem aktiven Prozess zu internalisieren. (3) Der Nachweis tubulointerstitieller Infiltration durch $CD8^+$ T-Zellen bei schwerer, aber nicht bei leichter, Glomerulonephritis zeigt, dass eine durch Zellkontakt zu PTECs vermittelte Aktivierung von $CD8^+$ T-Zellen ein Mechanismus sein könnte, der zur zellvermittelten autoimmunen Gewebeschädigung während Glomerulonephritis, insbesondere bei schweren Formen, beiträgt.

8. References

ABBATE, M., ZOJA, C. & REMUZZI, G. 2006. How does proteinuria cause progressive renal damage? *J Am Soc Nephrol,* 17**,** 2974-84.

ACKERMAN, A. L., GIODINI, A. & CRESSWELL, P. 2006. A role for the endoplasmic reticulum protein retrotranslocation machinery during crosspresentation by dendritic cells. *Immunity,* 25**,** 607-17.

ACKERMAN, A. L., KYRITSIS, C., TAMPÉ, R. & CRESSWELL, P. 2003. Early phagosomes in dendritic cells form a cellular compartment sufficient for cross presentation of exogenous antigens. *Proc Natl Acad Sci U S A,* 100**,** 12889-94.

ADACHI, M., WATANABE-FUKUNAGA, R. & NAGATA, S. 1993. Aberrant transcription caused by the insertion of an early transposable element in an intron of the Fas antigen gene of lpr mice. *Proc Natl Acad Sci U S A,* 90**,** 1756-60.

AKI, M., SHIMBARA, N., TAKASHINA, M., AKIYAMA, K., KAGAWA, S., TAMURA, T., TANAHASHI, N., YOSHIMURA, T., TANAKA, K. & ICHIHARA, A. 1994. Interferon-gamma induces different subunit organizations and functional diversity of proteasomes. *J Biochem,* 115**,** 257-69.

ALCHI, B. & JAYNE, D. 2010. Membranoproliferative glomerulonephritis. *Pediatr Nephrol,* 25**,** 1409-18.

ALMAANI, S., MEARA, A. & ROVIN, B. H. 2017. Update on Lupus Nephritis. *Clin J Am Soc Nephrol,* 12**,** 825-835.

ALSHARHAN, L. & BECK, L. H., JR. 2021. Membranous Nephropathy: Core Curriculum 2021. *American Journal of Kidney Diseases,* 77**,** 440-453.

ANDREWS, B. S., EISENBERG, R. A., THEOFILOPOULOS, A. N., IZUI, S., WILSON, C. B., MCCONAHEY, P. J., MURPHY, E. D., ROTHS, J. B. & DIXON, F. J. 1978. Spontaneous murine lupus-like syndromes. Clinical and immunopathological manifestations in several strains. *J Exp Med,* 148**,** 1198-215.

ARYA, M., SHERGILL, I. S., WILLIAMSON, M., GOMMERSALL, L., ARYA, N. & PATEL, H. R. H. 2005. Basic principles of real-time quantitative PCR. *Expert Review of Molecular Diagnostics,* 5**,** 209-219.

BANCHEREAU, J., BRIERE, F., CAUX, C., DAVOUST, J., LEBECQUE, S., LIU, Y. J., PULENDRAN, B. & PALUCKA, K. 2000. Immunobiology of dendritic cells. *Annu Rev Immunol,* 18**,** 767-811.

BANCHEREAU, J. & STEINMAN, R. M. 1998. Dendritic cells and the control of immunity. *Nature,* 392**,** 245-252.

BARRETT, L. W., FLETCHER, S. & WILTON, S. D. 2012. Regulation of eukaryotic gene expression by the untranslated gene regions and other non-coding elements. *Cell Mol Life Sci,* 69**,** 3613-34.

BARRY, M. & BLEACKLEY, R. C. 2002. Cytotoxic T lymphocytes: all roads lead to death. *Nature Reviews Immunology,* 2**,** 401-409.

BECK, L. H., JR., BONEGIO, R. G., LAMBEAU, G., BECK, D. M., POWELL, D. W., CUMMINS, T. D., KLEIN, J. B. & SALANT, D. J. 2009. M-type phospholipase A2 receptor as target antigen in idiopathic membranous nephropathy. *N Engl J Med,* 361**,** 11-21.

BENSON, E. M., COLVIN, R. B. & RUSSELL, P. S. 1985. Induction of IA antigens in murine renal transplants. *The Journal of Immunology,* 134**,** 7-9.

BERDEN, A. E., FERRARIO, F., HAGEN, E. C., JAYNE, D. R., JENNETTE, J. C., JOH, K., NEUMANN, I., NOËL, L. H., PUSEY, C. D., WALDHERR, R., BRUIJN, J. A. & BAJEMA, I. M. 2010. Histopathologic classification of ANCA-associated glomerulonephritis. *J Am Soc Nephrol,* 21**,** 1628-36.

BERTHOUX, F. C., MOHEY, H. & AFIANI, A. 2008. Natural History of Primary IgA Nephropathy. *Seminars in Nephrology,* 28**,** 4-9.

BONIFAZ, L., BONNYAY, D., MAHNKE, K., RIVERA, M., NUSSENZWEIG, M. C. & STEINMAN, R. M. 2002. Efficient targeting of protein antigen to the dendritic cell receptor DEC-205 in the steady state leads to antigen presentation on major histocompatibility complex class I products and peripheral CD8+ T cell tolerance. *J Exp Med,* 196**,** 1627-38.

BOOTS, A. M., WIMMERS-BERTENS, A. J. & RIJNDERS, A. W. 1994. Antigen-presenting capacity of rheumatoid synovial fibroblasts. *Immunology,* 82**,** 268-74.

BOUCHER, A., DROZ, D., ADAFER, E. & NOËL, L. H. 1987. Relationship between the integrity of Bowman's capsule and the composition of cellular crescents in human crescentic glomerulonephritis. *Lab Invest,* 56**,** 526-33.

BRADFORD, M. M. 1976. A rapid and sensitive method for the quantitation of microgram quantities of protein utilizing the principle of protein-dye binding. *Anal Biochem,* 72**,** 248-54.
BREDA, P. C., WIECH, T., MEYER-SCHWESINGER, C., GRAHAMMER, F., HUBER, T., PANZER, U., TIEGS, G. & NEUMANN, K. 2019. Renal proximal tubular epithelial cells exert immunomodulatory function by driving inflammatory CD4(+) T cell responses. *Am J Physiol Renal Physiol,* 317**,** F77-F89.
BURGDORF, S., KAUTZ, A., BÖHNERT, V., KNOLLE, P. A. & KURTS, C. 2007. Distinct Pathways of Antigen Uptake and Intracellular Routing in CD4 and CD8 T Cell Activation. *Science,* 316**,** 612-616.
BURGDORF, S., SCHÖLZ, C., KAUTZ, A., TAMPÉ, R. & KURTS, C. 2008. Spatial and mechanistic separation of cross-presentation and endogenous antigen presentation. *Nat Immunol,* 9**,** 558-66.
CANENE-ADAMS, K. 2013. General PCR. *Methods Enzymol,* 529**,** 291-8.
CHADBAN, S. J. & ATKINS, R. C. 2005. Glomerulonephritis. *Lancet,* 365**,** 1797-806.
CHANG, J., EGGENHUIZEN, P., O'SULLIVAN, K. M., ALIKHAN, M. A., HOLDSWORTH, S. R., OOI, J. D. & KITCHING, A. R. 2017. CD8+ T Cells Effect Glomerular Injury in Experimental Anti-Myeloperoxidase GN. *J Am Soc Nephrol,* 28**,** 47-55.
CHATTERJEE, B., SMED-SÖRENSEN, A., COHN, L., CHALOUNI, C., VANDLEN, R., LEE, B. C., WIDGER, J., KELER, T., DELAMARRE, L. & MELLMAN, I. 2012. Internalization and endosomal degradation of receptor-bound antigens regulate the efficiency of cross presentation by human dendritic cells. *Blood,* 120**,** 2011-20.
CHEN, A., LEE, K., D'AGATI, V. D., WEI, C., FU, J., GUAN, T. J., HE, J. C., SCHLONDORFF, D. & AGUDO, J. 2018. Bowman's capsule provides a protective niche for podocytes from cytotoxic CD8+ T cells. *J Clin Invest,* 128**,** 3413-3424.
CHEN, T., CAO, Q., WANG, R., ZHENG, G., AZMI, F., WANG, J., LEE, V. W., WANG, Y. M., YU, H., PATEL, M., P'NG C, H., ALEXANDER, S. I., ROGERS, N. M., WANG, Y. & HARRIS, D. C. H. 2021. Conventional Type 1 Dendritic Cells (cDC1) in Human Kidney Diseases: Clinico-Pathological Correlations. *Front Immunol,* 12**,** 635212.
CHEN, W., NORBURY, C. C., CHO, Y., YEWDELL, J. W. & BENNINK, J. R. 2001. Immunoproteasomes shape immunodominance hierarchies of antiviral CD8(+) T cells at the levels of T cell repertoire and presentation of viral antigens. *J Exp Med,* 193**,** 1319-26.
CHO, M. H., HONG, E. H., LEE, T. H. & KO, C. W. 2007. Pathophysiology of minimal change nephrotic syndrome and focal segmental glomerulosclerosis. *Nephrology (Carlton),* 12 Suppl 3**,** S11-4.
COUSER, W. G. 2017. Primary Membranous Nephropathy. *Clin J Am Soc Nephrol,* 12**,** 983-997.
COUZI, L., MERVILLE, P., DEMINIÈRE, C., MOREAU, J. F., COMBE, C., PELLEGRIN, J. L., VIALLARD, J. F. & BLANCO, P. 2007. Predominance of CD8+ T lymphocytes among periglomerular infiltrating cells and link to the prognosis of class III and class IV lupus nephritis. *Arthritis Rheum,* 56**,** 2362-70.
CUNNINGHAM, M. A., RONDEAU, E., CHEN, X., COUGHLIN, S. R., HOLDSWORTH, S. R. & TIPPING, P. G. 2000. Protease-activated receptor 1 mediates thrombin-dependent, cell-mediated renal inflammation in crescentic glomerulonephritis. *J Exp Med,* 191**,** 455-62.
D'AMICO, F., SKARMOUTSOU, E. & STIVALA, F. 2009. State of the art in antigen retrieval for immunohistochemistry. *J Immunol Methods,* 341**,** 1-18.
DELAMARRE, L., PACK, M., CHANG, H., MELLMAN, I. & TROMBETTA, E. S. 2005. Differential lysosomal proteolysis in antigen-presenting cells determines antigen fate. *Science,* 307**,** 1630-4.
DEN HAAN, J. M. & BEVAN, M. J. 2001. Antigen presentation to CD8+ T cells: cross-priming in infectious diseases. *Curr Opin Immunol,* 13**,** 437-41.
DIEHL, L., SCHURICH, A., GROCHTMANN, R., HEGENBARTH, S., CHEN, L. & KNOLLE, P. A. 2008. Tolerogenic maturation of liver sinusoidal endothelial cells promotes B7-homolog 1-dependent CD8+ T cell tolerance. *Hepatology,* 47**,** 296-305.
DINGJAN, I., VERBOOGEN, D. R., PAARDEKOOPER, L. M., REVELO, N. H., SITTIG, S. P., VISSER, L. J., MOLLARD, G. F., HENRIET, S. S., FIGDOR, C. G., TER BEEST, M. & VAN DEN BOGAART, G. 2016. Lipid peroxidation causes endosomal antigen release for cross-presentation. *Sci Rep,* 6**,** 22064.
DIXON, F. J., ANDREWS, B. S., EISENBERG, R. A., MCCONAHEY, P. J., THEOFILOPOULOS, A. N. & WILSON, C. B. 1978. Etiology and pathogenesis of a spontaneous lupus-like syndrome in mice. *Arthritis Rheum,* 21**,** S64-7.

DONG, D., ZHENG, L., LIN, J., ZHANG, B., ZHU, Y., LI, N., XIE, S., WANG, Y., GAO, N. & HUANG, Z. 2019. Structural basis of assembly of the human T cell receptor–CD3 complex. *Nature,* 573**,** 546-552.

DRISCOLL, W. C. 1996. Robustness of the ANOVA and Tukey-Kramer statistical tests. *Computers & Industrial Engineering,* 31**,** 265-268.

DUSTIN, M. L. 2014. The immunological synapse. *Cancer Immunol Res,* 2**,** 1023-33.

EMBGENBROICH, M. & BURGDORF, S. 2018. Current Concepts of Antigen Cross-Presentation. *Front Immunol,* 9**,** 1643.

ERKAN, E., GARCIA, C. D., PATTERSON, L. T., MISHRA, J., MITSNEFES, M. M., KASKEL, F. J. & DEVARAJAN, P. 2005. Induction of renal tubular cell apoptosis in focal segmental glomerulosclerosis: roles of proteinuria and Fas-dependent pathways. *J Am Soc Nephrol,* 16**,** 398-407.

FEHRES, C. M., DUINKERKEN, S., BRUIJNS, S. C., KALAY, H., VAN VLIET, S. J., AMBROSINI, M., DE GRUIJL, T. D., UNGER, W. W., GARCIA-VALLEJO, J. J. & VAN KOOYK, Y. 2017. Langerin-mediated internalization of a modified peptide routes antigens to early endosomes and enhances cross-presentation by human Langerhans cells. *Cell Mol Immunol,* 14**,** 360-370.

FERVENZA, F. C., SETHI, S. & GLASSOCK, R. J. 2012. Idiopathic membranoproliferative glomerulonephritis: does it exist? *Nephrology Dialysis Transplantation,* 27**,** 4288-4294.

FLOEGE, J. & AMANN, K. 2016. Primary glomerulonephritides. *Lancet,* 387**,** 2036-48.

FRANÇOIS, M., ROMIEU-MOUREZ, R., STOCK-MARTINEAU, S., BOIVIN, M.-N., BRAMSON, J. L. & GALIPEAU, J. 2009. Mesenchymal stromal cells cross-present soluble exogenous antigens as part of their antigen-presenting cell properties. *Blood,* 114**,** 2632-2638.

FURIE, R., ROVIN, B. H., HOUSSIAU, F., MALVAR, A., TENG, Y. K. O., CONTRERAS, G., AMOURA, Z., YU, X., MOK, C. C., SANTIAGO, M. B., SAXENA, A., GREEN, Y., JI, B., KLEOUDIS, C., BURRISS, S. W., BARNETT, C. & ROTH, D. A. 2020. Two-Year, Randomized, Controlled Trial of Belimumab in Lupus Nephritis. *N Engl J Med,* 383**,** 1117-1128.

GASTL, G., EBERT, T., FINSTAD, C. L., SHEINFELD, J., GOMAHR, A., AULITZKY, W. & BANDER, N. H. 1996. Major histocompatibility complex class I and class II expression in renal cell carcinoma and modulation by interferon gamma. *J Urol,* 155**,** 361-7.

GOEL, A., BHADAURIA, D. S. & AGGARWAL, R. 2018. Hepatitis C virus infection and chronic renal disease: A review. *Indian J Gastroenterol,* 37**,** 492-503.

GOLDSZMID, R. S., COPPENS, I., LEV, A., CASPAR, P., MELLMAN, I. & SHER, A. 2009. Host ER-parasitophorous vacuole interaction provides a route of entry for antigen cross-presentation in Toxoplasma gondii-infected dendritic cells. *J Exp Med,* 206**,** 399-410.

GROSS, A., SCHOENDUBE, J., ZIMMERMANN, S., STEEB, M., ZENGERLE, R. & KOLTAY, P. 2015. Technologies for Single-Cell Isolation. *International Journal of Molecular Sciences,* 16**,** 16897-16919.

GROTZKE, J. E., KOZIK, P., MOREL, J. D., IMPENS, F., PIETROSEMOLI, N., CRESSWELL, P., AMIGORENA, S. & DEMANGEL, C. 2017. Sec61 blockade by mycolactone inhibits antigen cross-presentation independently of endosome-to-cytosol export. *Proc Natl Acad Sci U S A,* 114**,** E5910-e5919.

GUERMONPREZ, P., SAVEANU, L., KLEIJMEER, M., DAVOUST, J., VAN ENDERT, P. & AMIGORENA, S. 2003. ER-phagosome fusion defines an MHC class I cross-presentation compartment in dendritic cells. *Nature,* 425**,** 397-402.

GUIMARÃES, G., GOMES, M. T. R., CAMPOS, P. C., MARINHO, F. V., DE ASSIS, N. R. G., SILVEIRA, T. N. & OLIVEIRA, S. C. 2018. Immunoproteasome Subunits Are Required for CD8(+) T Cell Function and Host Resistance to Brucella abortus Infection in Mice. *Infect Immun,* 86.

HAMMER, G. E. & MA, A. 2013. Molecular control of steady-state dendritic cell maturation and immune homeostasis. *Annu Rev Immunol,* 31**,** 743-91.

HARRYVAN, T. J., DE LANGE, S., HAWINKELS, L. & VERDEGAAL, E. M. E. 2021. The ABCs of Antigen Presentation by Stromal Non-Professional Antigen-Presenting Cells. *Int J Mol Sci,* 23.

HAWIGER, D., INABA, K., DORSETT, Y., GUO, M., MAHNKE, K., RIVERA, M., RAVETCH, J. V., STEINMAN, R. M. & NUSSENZWEIG, M. C. 2001. Dendritic cells induce peripheral T cell unresponsiveness under steady state conditions in vivo. *J Exp Med,* 194**,** 769-79.

HELLMARK, T. & SEGELMARK, M. 2014. Diagnosis and classification of Goodpasture's disease (anti-GBM). *J Autoimmun,* 48-49**,** 108-12.

HEUBERGER, D. M. & SCHUEPBACH, R. A. 2019. Protease-activated receptors (PARs): mechanisms of action and potential therapeutic modulators in PAR-driven inflammatory diseases. *Thromb J,* 17**,** 4.

HEYMANN, F., MEYER-SCHWESINGER, C., HAMILTON-WILLIAMS, E. E., HAMMERICH, L., PANZER, U., KADEN, S., QUAGGIN, S. E., FLOEGE, J., GRÖNE, H. J. & KURTS, C. 2009. Kidney dendritic cell activation is required for progression of renal disease in a mouse model of glomerular injury. *J Clin Invest,* 119**,** 1286-97.

HILLER, M. M., FINGER, A., SCHWEIGER, M. & WOLF, D. H. 1996. ER Degradation of a Misfolded Luminal Protein by the Cytosolic Ubiquitin-Proteasome Pathway. *Science,* 273**,** 1725-1728.

HOCHHEISER, K., ENGEL, D. R., HAMMERICH, L., HEYMANN, F., KNOLLE, P. A., PANZER, U. & KURTS, C. 2011. Kidney Dendritic Cells Become Pathogenic during Crescentic Glomerulonephritis with Proteinuria. *J Am Soc Nephrol,* 22**,** 306-16.

HOPFER, H., HOLZER, J., HÜNEMÖRDER, S., PAUST, H. J., SACHS, M., MEYER-SCHWESINGER, C., TURNER, J. E., PANZER, U. & MITTRÜCKER, H. W. 2012. Characterization of the renal CD4+ T-cell response in experimental autoimmune glomerulonephritis. *Kidney Int,* 82**,** 60-71.

HORNUNG, V., BAUERNFEIND, F., HALLE, A., SAMSTAD, E. O., KONO, H., ROCK, K. L., FITZGERALD, K. A. & LATZ, E. 2008. Silica crystals and aluminum salts activate the NALP3 inflammasome through phagosomal destabilization. *Nat Immunol,* 9**,** 847-56.

HU, S. Y., JIA, X. Y., LI, J. N., ZHENG, X., AO, J., LIU, G., CUI, Z. & ZHAO, M. H. 2016. T cell infiltration is associated with kidney injury in patients with anti-glomerular basement membrane disease. *Sci China Life Sci,* 59**,** 1282-1289.

HUANG, S., WU, J., GAO, X., ZOU, S., CHEN, L., YANG, X., SUN, C., DU, Y., ZHU, B., LI, J., YANG, X., FENG, X., WU, C., SHI, C., WANG, B., LU, Y., LIU, J., ZHENG, X., GONG, F., LU, M. & YANG, D. 2018. LSECs express functional NOD1 receptors: A role for NOD1 in LSEC maturation-induced T cell immunity in vitro. *Mol Immunol,* 101**,** 167-175.

HUANG, X. R., HOLDSWORTH, S. R. & TIPPING, P. G. 1994. Evidence for delayed-type hypersensitivity mechanisms in glomerular crescent formation. *Kidney Int,* 46**,** 69-78.

HUTTON, A. J., POLAK, M. E., SPALLUTO, C. M., WALLINGTON, J. C., PICKARD, C., STAPLES, K. J., WARNER, J. A. & WILKINSON, T. M. 2017. Human Lung Fibroblasts Present Bacterial Antigens to Autologous Lung Th Cells. *J Immunol,* 198**,** 110-118.

IKING-KONERT, C., VOGL, T., PRIOR, B., WAGNER, C., SANDER, O., BLECK, E., OSTENDORF, B., SCHNEIDER, M., ANDRASSY, K. & HÄNSCH, G. M. 2008. T lymphocytes in patients with primary vasculitis: expansion of CD8+ T cells with the propensity to activate polymorphonuclear neutrophils. *Rheumatology (Oxford),* 47**,** 609-16.

IMAI, J., HASEGAWA, H., MARUYA, M., KOYASU, S. & YAHARA, I. 2005. Exogenous antigens are processed through the endoplasmic reticulum-associated degradation (ERAD) in cross-presentation by dendritic cells. *Int Immunol,* 17**,** 45-53.

INABA, K., INABA, M., ROMANI, N., AYA, H., DEGUCHI, M., IKEHARA, S., MURAMATSU, S. & STEINMAN, R. M. 1992. Generation of large numbers of dendritic cells from mouse bone marrow cultures supplemented with granulocyte/macrophage colony-stimulating factor. *J Exp Med,* 176**,** 1693-702.

JENSEN, E. C. 2012. The basics of western blotting. *Anat Rec (Hoboken),* 295**,** 369-71.

JOFFRE, O. P., SEGURA, E., SAVINA, A. & AMIGORENA, S. 2012. Cross-presentation by dendritic cells. *Nature Reviews Immunology,* 12**,** 557-569.

KAISSLING, B. & LE HIR, M. 1994. Characterization and distribution of interstitial cell types in the renal cortex of rats. *Kidney Int,* 45**,** 709-20.

KASSIANOS, A. J., SAMPANGI, S., WANG, X., ROPER, K. E., BEAGLEY, K., HEALY, H. & WILKINSON, R. 2013. Human proximal tubule epithelial cells modulate autologous dendritic cell function. *Nephrol Dial Transplant,* 28**,** 303-12.

KAWASAKI, K., YAOITA, E., YAMAMOTO, T. & KIHARA, I. 1992. Depletion of CD8 positive cells in nephrotoxic serum nephritis of WKY rats. *Kidney Int,* 41**,** 1517-26.

KERN, M., POPOV, A., SCHOLZ, K., SCHUMAK, B., DJANDJI, D., LIMMER, A., EGGLE, D., SACHER, T., ZAWATZKY, R., HOLTAPPELS, R., REDDEHASE, M. J., HARTMANN, G., DEBEY-PASCHER, S., DIEHL, L., KALINKE, U., KOSZINOWSKI, U., SCHULTZE, J. & KNOLLE, P. A. 2010. Virally infected mouse liver endothelial cells trigger CD8+ T-cell immunity. *Gastroenterology,* 138**,** 336-46.

KHALIGHI, M. A., WANG, S., HENRIKSEN, K. J., BOCK, M., KESWANI, M., MEEHAN, S. M. & CHANG, A. 2016. Revisiting post-infectious glomerulonephritis in the emerging era of C3 glomerulopathy. *Clinical Kidney Journal,* 9**,** 397-402.

KIDDER, D., BRAY, S. E. & FLEMING, S. 2017. Differences in the frequency of macrophage and T cell markers between focal and crescentic classes of anti-neutrophil cytoplasmic antibody (ANCA)-associated glomerulonephritis. *J Nephropathol,* 6**,** 97-102.

KITCHING, A. R. & HOLDSWORTH, S. R. 2011. The Emergence of Th17 Cells as Effectors of Renal Injury. *Journal of the American Society of Nephrology,* 22.

KNOLLE, P. A., SCHMITT, E., JIN, S., GERMANN, T., DUCHMANN, R., HEGENBARTH, S., GERKEN, G. & LOHSE, A. W. 1999. Induction of cytokine production in naive CD4⁺ T cells by antigen-presenting murine liver sinusoidal endothelial cells but failure to induce differentiation toward T_{h1} cells. *Gastroenterology,* 116**,** 1428-1440.

KOOPMANN, J. O., ALBRING, J., HÜTER, E., BULBUC, N., SPEE, P., NEEFJES, J., HÄMMERLING, G. J. & MOMBURG, F. 2000. Export of antigenic peptides from the endoplasmic reticulum intersects with retrograde protein translocation through the Sec61p channel. *Immunity,* 13**,** 117-27.

KOVACSOVICS-BANKOWSKI, M. & ROCK, K. L. 1995. A phagosome-to-cytosol pathway for exogenous antigens presented on MHC class I molecules. *Science,* 267**,** 243-6.

KRAUSGRUBER, T., FORTELNY, N., FIFE-GERNEDL, V., SENEKOWITSCH, M., SCHUSTER, L. C., LERCHER, A., NEMC, A., SCHMIDL, C., RENDEIRO, A. F., BERGTHALER, A. & BOCK, C. 2020. Structural cells are key regulators of organ-specific immune responses. *Nature,* 583**,** 296-302.

KRSHNAN, L., VAN DE WEIJER, M. L. & CARVALHO, P. 2022. Endoplasmic Reticulum-Associated Protein Degradation. *Cold Spring Harb Perspect Biol,* 14.

KRUSE, N., NEUMANN, K., SCHRAGE, A., DERKOW, K., SCHOTT, E., ERBEN, U., KÜHL, A., LODDENKEMPER, C., ZEITZ, M., HAMANN, A. & KLUGEWITZ, K. 2009. Priming of CD4+ T cells by liver sinusoidal endothelial cells induces CD25low forkhead box protein 3- regulatory T cells suppressing autoimmune hepatitis. *Hepatology,* 50**,** 1904-13.

LAEMMLI, U. K. 1970. Cleavage of Structural Proteins during the Assembly of the Head of Bacteriophage T4. *Nature,* 227**,** 680-685.

LAI, K. N., LEUNG, J. C., CHAN, L. Y., GUO, H. & TANG, S. C. 2007. Interaction between proximal tubular epithelial cells and infiltrating monocytes/T cells in the proteinuric state. *Kidney Int,* 71**,** 526-38.

LAMBA, P., NAM, K. H., CONTRACTOR, J. & KIM, A. 2020. Nephritic Syndrome. *Prim Care,* 47**,** 615-629.

LAN, H. Y., NIKOLIC-PATERSON, D. J. & ATKINS, R. C. 1992. Involvement of activated periglomerular leukocytes in the rupture of Bowman's capsule and glomerular crescent progression in experimental glomerulonephritis. *Lab Invest,* 67**,** 743-51.

LAWAND, M., ABRAMOVA, A., MANCEAU, V., SPRINGER, S. & VAN ENDERT, P. 2016. TAP-Dependent and -Independent Peptide Import into Dendritic Cell Phagosomes. *J Immunol,* 197**,** 3454-3463.

LE HIR, M. & BESSE-ESCHMANN, V. 2003. A novel mechanism of nephron loss in a murine model of crescentic glomerulonephritis. *Kidney Int,* 63**,** 591-9.

LECH, M. & ANDERS, H. J. 2013. The pathogenesis of lupus nephritis. *J Am Soc Nephrol,* 24**,** 1357-66.

LENNON-DUMÉNIL, A. M., BAKKER, A. H., MAEHR, R., FIEBIGER, E., OVERKLEEFT, H. S., ROSEMBLATT, M., PLOEGH, H. L. & LAGAUDRIÈRE-GESBERT, C. 2002. Analysis of protease activity in live antigen-presenting cells shows regulation of the phagosomal proteolytic contents during dendritic cell activation. *J Exp Med,* 196**,** 529-40.

LILLEY, B. N. & PLOEGH, H. L. 2004. A membrane protein required for dislocation of misfolded proteins from the ER. *Nature,* 429**,** 834-40.

LIMMER, A., OHL, J., KURTS, C., LJUNGGREN, H.-G., REISS, Y., GROETTRUP, M., MOMBURG, F., ARNOLD, B. & KNOLLE, P. A. 2000. Efficient presentation of exogenous antigen by liver endothelial cells to CD8+ T cells results in antigen-specific T-cell tolerance. *Nature Medicine,* 6**,** 1348-1354.

LINKE, A., CICEK, H., MÜLLER, A., MEYER-SCHWESINGER, C., MELDERIS, S., WIECH, T., WEGSCHEID, C., RIDDER, J., STEINMETZ, O. M., DIEHL, L., TIEGS, G. & NEUMANN, K. 2022. Antigen Cross-Presentation by Murine Proximal Tubular Epithelial Cells Induces Cytotoxic and Inflammatory CD8(+) T Cells. *Cells,* 11.

LIU, J., JIANG, M., MA, Z., DIETZE, K. K., ZELINSKYY, G., YANG, D., DITTMER, U., SCHLAAK, J. F., ROGGENDORF, M. & LU, M. 2013. TLR1/2 ligand-stimulated mouse liver endothelial cells secrete IL-12 and trigger CD8+ T cell immunity in vitro. *J Immunol,* 191**,** 6178-90.

LIU, Y., BEYER, A. & AEBERSOLD, R. 2016. On the Dependency of Cellular Protein Levels on mRNA Abundance. *Cell,* 165**,** 535-50.

LIVAK, K. J. & SCHMITTGEN, T. D. 2001. Analysis of relative gene expression data using real-time quantitative PCR and the 2(-Delta Delta C(T)) Method. *Methods,* 25**,** 402-8.

LUKACS-KORNEK, V., BURGDORF, S., DIEHL, L., SPECHT, S., KORNEK, M. & KURTS, C. 2008. The kidney-renal lymph node-system contributes to cross-tolerance against innocuous circulating antigen. *J Immunol,* 180**,** 706-15.

MACCONI, D., CHIABRANDO, C., SCHIAREA, S., AIELLO, S., CASSIS, L., GAGLIARDINI, E., NORIS, M., BUELLI, S., ZOJA, C., CORNA, D., MELE, C., FANELLI, R., REMUZZI, G. & BENIGNI, A. 2009. Proteasomal processing of albumin by renal dendritic cells generates antigenic peptides. *J Am Soc Nephrol,* 20**,** 123-30.

MAGAKI, S., HOJAT, S. A., WEI, B., SO, A. & YONG, W. H. 2019. An Introduction to the Performance of Immunohistochemistry. *Methods Mol Biol,* 1897**,** 289-298.

MANN, H. B. & WHITNEY, D. R. 1947. On a Test of Whether one of Two Random Variables is Stochastically Larger than the Other. *The Annals of Mathematical Statistics,* 18**,** 50-60, 11.

MANTEGAZZA, A. R., SAVINA, A., VERMEULEN, M., PÉREZ, L., GEFFNER, J., HERMINE, O., ROSENZWEIG, S. D., FAURE, F. & AMIGORENA, S. 2008. NADPH oxidase controls phagosomal pH and antigen cross-presentation in human dendritic cells. *Blood,* 112**,** 4712-22.

MASTERS, J. R. & STACEY, G. N. 2007. Changing medium and passaging cell lines. *Nature Protocols,* 2**,** 2276-2284.

MAYRHOFER, G. & SCHON-HEGRAD, M. A. 1983. Ia antigens in rat kidney, with special reference to their expression in tubular epithelium. *J Exp Med,* 157**,** 2097-109.

MCGAHA, T. L. & MADAIO, M. P. 2014. Lupus Nephritis: Animal Modeling of a Complex Disease Syndrome Pathology. *Drug Discov Today Dis Models,* 11**,** 13-18.

MELLMAN, I. & STEINMAN, R. M. 2001. Dendritic cells: specialized and regulated antigen processing machines. *Cell,* 106**,** 255-8.

MÉNAGER, J., EBSTEIN, F., OGER, R., HULIN, P., NEDELLEC, S., DUVERGER, E., LEHMANN, A., KLOETZEL, P. M., JOTEREAU, F. & GUILLOUX, Y. 2014. Cross-presentation of synthetic long peptides by human dendritic cells: a process dependent on ERAD component p97/VCP but Not sec61 and/or Derlin-1. *PLoS One,* 9**,** e89897.

MERAD, M., SATHE, P., HELFT, J., MILLER, J. & MORTHA, A. 2013. The dendritic cell lineage: ontogeny and function of dendritic cells and their subsets in the steady state and the inflamed setting. *Annu Rev Immunol,* 31**,** 563-604.

MERKEL, F., KALLURI, R., MARX, M., ENDERS, U., STEVANOVIC, S., GIEGERICH, G., NEILSON, E. G., RAMMENSEE, H. G., HUDSON, B. G. & WEBER, M. 1996. Autoreactive T-cells in Goodpasture's syndrome recognize the N-terminal NC1 domain on alpha 3 type IV collagen. *Kidney Int,* 49**,** 1127-33.

MERZOUGUI, N., KRATZER, R., SAVEANU, L. & VAN ENDERT, P. 2011. A proteasome-dependent, TAP-independent pathway for cross-presentation of phagocytosed antigen. *EMBO Rep,* 12**,** 1257-64.

MORONI, G. & PONTICELLI, C. 2014. Rapidly progressive crescentic glomerulonephritis: Early treatment is a must. *Autoimmun Rev,* 13**,** 723-9.

MUELLER, A., ZHAO, Y., CICEK, H., PAUST, H. J., SIVAYOGANATHAN, A., LINKE, A., WEGSCHEID, C., WIECH, T., HUBER, T. B., MEYER-SCHWESINGER, C., BONN, S., PRINZ, I., PANZER, U., TIEGS, G., KREBS, C. F. & NEUMANN, K. 2023. Transcriptional and Clonal Characterization of Cytotoxic T Cells in Crescentic Glomerulonephritis. *J Am Soc Nephrol*.

MUELLER, D. L., JENKINS, M. K. & SCHWARTZ, R. H. 1989. Clonal expansion versus functional clonal inactivation: a costimulatory signalling pathway determines the outcome of T cell antigen receptor occupancy. *Annu Rev Immunol,* 7**,** 445-80.

MURATA, H., MATSUMURA, R., KOYAMA, A., SUGIYAMA, T., SUEISHI, M., SHIBUYA, K., TSUTSUMI, A. & SUMIDA, T. 2002. T cell receptor repertoire of T cells in the kidneys of patients with lupus nephritis. *Arthritis Rheum,* 46**,** 2141-7.

MURPHY, E. D. A single gene model for massive lymphoproliferation with immune complex disease in new mouse strain MRL. Proceedings of the 16th International Congress of Hematology, 1976. Excerpta Medica.

NAKHOUL, N. & BATUMAN, V. 2011. Role of proximal tubules in the pathogenesis of kidney disease. *Contrib Nephrol,* 169**,** 37-50.

NIEMANN-MASANEK, U., MUELLER, A., YARD, B. A., WALDHERR, R. & VAN DER WOUDE, F. J. 2002. B7-1 (CD80) and B7-2 (CD 86) expression in human tubular epithelial cells in vivo and in vitro. *Nephron,* 92**,** 542-56.

PALMOWSKI, M. J., GILEADI, U., SALIO, M., GALLIMORE, A., MILLRAIN, M., JAMES, E., ADDEY, C., SCOTT, D., DYSON, J., SIMPSON, E. & CERUNDOLO, V. 2006. Role of Immunoproteasomes in Cross-Presentation1. *The Journal of Immunology,* 177**,** 983-990.

PICKERING, M. C., D'AGATI, V. D., NESTER, C. M., SMITH, R. J., HAAS, M., APPEL, G. B., ALPERS, C. E., BAJEMA, I. M., BEDROSIAN, C., BRAUN, M., DOYLE, M., FAKHOURI, F., FERVENZA, F. C., FOGO, A. B., FRÉMEAUX-BACCHI, V., GALE, D. P., GOICOECHEA DE JORGE, E., GRIFFIN, G., HARRIS, C. L., MICHAEL HOLERS, V., JOHNSON, S., LAVIN, P. J., MEDJERAL-THOMAS, N., PAUL MORGAN, B., NAST, C. C., NOEL, L.-H., KEITH PETERS, D., RODRÍGUEZ DE CÓRDOBA, S., SERVAIS, A., SETHI, S., SONG, W.-C., TAMBURINI, P., THURMAN, J. M., ZAVROS, M. & TERENCE COOK, H. 2013. C3 glomerulopathy: consensus report. *Kidney International,* 84**,** 1079-1089.

PINCHUK, I. V., BESWICK, E. J., SAADA, J. I., BOYA, G., SCHMITT, D., RAJU, G. S., BRENMOEHL, J., ROGLER, G., REYES, V. E. & POWELL, D. W. 2011. Human colonic myofibroblasts promote expansion of CD4+ CD25high Foxp3+ regulatory T cells. *Gastroenterology,* 140**,** 2019-30.

PINCHUK, I. V., SAADA, J. I., BESWICK, E. J., BOYA, G., QIU, S. M., MIFFLIN, R. C., RAJU, G. S., REYES, V. E. & POWELL, D. W. 2008. PD-1 ligand expression by human colonic myofibroblasts/fibroblasts regulates CD4+ T-cell activity. *Gastroenterology,* 135**,** 1228-1237, 1237.e1-2.

PISHESHA, N., HARMAND, T. J. & PLOEGH, H. L. 2022. A guide to antigen processing and presentation. *Nature Reviews Immunology,* 22**,** 751-764.

POLITANO, S. A., COLBERT, G. B. & HAMIDUZZAMAN, N. 2020. Nephrotic Syndrome. *Prim Care,* 47**,** 597-613.

PRÓCHNICKI, T., MANGAN, M. S. & LATZ, E. 2016. Recent insights into the molecular mechanisms of the NLRP3 inflammasome activation. *F1000Res,* 5.

REYNOLDS, J., NORGAN, V. A., BHAMBRA, U., SMITH, J., COOK, H. T. & PUSEY, C. D. 2002. Anti-CD8 monoclonal antibody therapy is effective in the prevention and treatment of experimental autoimmune glomerulonephritis. *J Am Soc Nephrol,* 13**,** 359-369.

REYNOLDS, J., TAM, F. W., CHANDRAKER, A., SMITH, J., KARKAR, A. M., CROSS, J., PEACH, R., SAYEGH, M. H. & PUSEY, C. D. 2000. CD28-B7 blockade prevents the development of experimental autoimmune glomerulonephritis. *J Clin Invest,* 105**,** 643-51.

REYNOLDS, J. A. & TANFORD, C. 1970. Binding of dodecyl sulfate to proteins at high binding ratios. Possible implications for the state of proteins in biological membranes. *Proc Natl Acad Sci U S A,* 66**,** 1002-7.

RIO, D. C., ARES, M., JR., HANNON, G. J. & NILSEN, T. W. 2010. Purification of RNA using TRIzol (TRI reagent). *Cold Spring Harb Protoc,* 2010**,** pdb.prot5439.

RONCO, P., BECK, L., DEBIEC, H., FERVENZA, F. C., HOU, F. F., JHA, V., SETHI, S., TONG, A., VIVARELLI, M. & WETZELS, J. 2021. Membranous nephropathy. *Nat Rev Dis Primers,* 7**,** 69.

ROSENBERG, A. Z. & KOPP, J. B. 2017. Focal Segmental Glomerulosclerosis. *Clin J Am Soc Nephrol,* 12**,** 502-517.

ROVIN, B. H., ADLER, S. G., BARRATT, J., BRIDOUX, F., BURDGE, K. A., CHAN, T. M., COOK, H. T., FERVENZA, F. C., GIBSON, K. L., GLASSOCK, R. J., JAYNE, D. R. W., JHA, V., LIEW, A., LIU, Z. H., MEJÍA-VILET, J. M., NESTER, C. M., RADHAKRISHNAN, J., RAVE, E. M., REICH, H. N., RONCO, P., SANDERS, J. F., SETHI, S., SUZUKI, Y., TANG, S. C. W., TESAR, V., VIVARELLI, M., WETZELS, J. F. M., LYTVYN, L., CRAIG, J. C., TUNNICLIFFE, D. J., HOWELL, M., TONELLI, M. A., CHEUNG, M., EARLEY, A. & FLOEGE, J. 2021. Executive summary of the KDIGO 2021 Guideline for the Management of Glomerular Diseases. *Kidney Int,* 100**,** 753-779.

SAMPANGI, S., WANG, X., BEAGLEY, K. W., KLEIN, T., AFRIN, S., HEALY, H., WILKINSON, R. & KASSIANOS, A. J. 2015. Human proximal tubule epithelial cells modulate autologous B-cell function. *Nephrol Dial Transplant,* 30**,** 1674-83.

SATOH, M., KUMAR, A., KANWAR, Y. S. & REEVES, W. H. 1995. Anti-nuclear antibody production and immune-complex glomerulonephritis in BALB/c mice treated with pristane. *Proc Natl Acad Sci U S A,* 92**,** 10934-8.

SATOH, M. & REEVES, W. H. 1994. Induction of lupus-associated autoantibodies in BALB/c mice by intraperitoneal injection of pristane. *J Exp Med,* 180**,** 2341-6.

SAVEANU, L., CARROLL, O., WEIMERSHAUS, M., GUERMONPREZ, P., FIRAT, E., LINDO, V., GREER, F., DAVOUST, J., KRATZER, R., KELLER, S. R., NIEDERMANN, G. & VAN ENDERT, P. 2009. IRAP identifies an endosomal compartment required for MHC class I cross-presentation. *Science,* 325**,** 213-7.

SAVINA, A., JANCIC, C., HUGUES, S., GUERMONPREZ, P., VARGAS, P., MOURA, I. C., LENNON-DUMÉNIL, A.-M., SEABRA, M. C., RAPOSO, G. & AMIGORENA, S. 2006. NOX2 Controls Phagosomal pH to Regulate Antigen Processing during Crosspresentation by Dendritic Cells. *Cell,* 126**,** 205-218.

SAVINOV, A. Y., WONG, F. S., STONEBRAKER, A. C. & CHERVONSKY, A. V. 2003. Presentation of antigen by endothelial cells and chemoattraction are required for homing of insulin-specific CD8+ T cells. *J Exp Med,* 197**,** 643-56.

SCHOLZ, J., LUKACS-KORNEK, V., ENGEL, D. R., SPECHT, S., KISS, E., EITNER, F., FLOEGE, J., GROENE, H. J. & KURTS, C. 2008. Renal dendritic cells stimulate IL-10 production and attenuate nephrotoxic nephritis. *J Am Soc Nephrol,* 19**,** 527-37.

SCHURICH, A., BERG, M., STABENOW, D., BÖTTCHER, J., KERN, M., SCHILD, H. J., KURTS, C., SCHUETTE, V., BURGDORF, S., DIEHL, L., LIMMER, A. & KNOLLE, P. A. 2010. Dynamic regulation of CD8 T cell tolerance induction by liver sinusoidal endothelial cells. *J Immunol,* 184**,** 4107-14.

SCHURICH, A., BÖTTCHER, J. P., BURGDORF, S., PENZLER, P., HEGENBARTH, S., KERN, M., DOLF, A., ENDL, E., SCHULTZE, J., WIERTZ, E., STABENOW, D., KURTS, C. & KNOLLE, P. 2009. Distinct kinetics and dynamics of cross-presentation in liver sinusoidal endothelial cells compared to dendritic cells. *Hepatology,* 50**,** 909-19.

SESSO, R. C., RAMOS, O. L. & PEREIRA, A. B. 1986. Detection of IgG-rheumatoid factor in sera of patients with acute poststreptococcal glomerulonephritis and its relationship with circulating immunecomplexes. *Clin Nephrol,* 26**,** 55-60.

SHEERIN, N. S., SPRINGALL, T., ABE, K. & SACKS, S. H. 2001. Protection and injury: the differing roles of complement in the development of glomerular injury. *Eur J Immunol,* 31**,** 1255-60.

SHEN, L., SIGAL, L. J., BOES, M. & ROCK, K. L. 2004. Important Role of Cathepsin S in Generating Peptides for TAP-Independent MHC Class I Crosspresentation In Vivo. *Immunity,* 21**,** 155-165.

SHETTY, S., LALOR, P. F. & ADAMS, D. H. 2018. Liver sinusoidal endothelial cells — gatekeepers of hepatic immunity. *Nature Reviews Gastroenterology & Hepatology,* 15**,** 555-567.

SHORTMAN, K. & HEATH, W. R. 2010. The CD8+ dendritic cell subset. *Immunol Rev,* 234**,** 18-31.

SIGAL, L. J., CROTTY, S., ANDINO, R. & ROCK, K. L. 1999. Cytotoxic T-cell immunity to virus-infected non-haematopoietic cells requires presentation of exogenous antigen. *Nature,* 398**,** 77-80.

SINCLAIR, G. D., WADGYMAR, A., HALLORAN, P. F. & DELOVITCH, T. L. 1984. Graft-vs-host reactions induce H-2 class II gene transcription in host kidney cells. *Immunogenetics,* 20**,** 503-11.

SMEETS, B., UHLIG, S., FUSS, A., MOOREN, F., WETZELS, J. F., FLOEGE, J. & MOELLER, M. J. 2009. Tracing the origin of glomerular extracapillary lesions from parietal epithelial cells. *J Am Soc Nephrol,* 20**,** 2604-15.

SMITH, R. J., HARRIS, C. L. & PICKERING, M. C. 2011. Dense deposit disease. *Mol Immunol,* 48**,** 1604-10.

STARKE, A., LINDENMEYER, M. T., SEGERER, S., NEUSSER, M. A., RÜSI, B., SCHMID, D. M., COHEN, C. D., WÜTHRICH, R. P., FEHR, T. & WAECKERLE-MEN, Y. 2010. Renal tubular PD-L1 (CD274) suppresses alloreactive human T-cell responses. *Kidney Int,* 78**,** 38-47.

SUMMERS, S. A., STEINMETZ, O. M., LI, M., KAUSMAN, J. Y., SEMPLE, T., EDGTTON, K. L., BORZA, D. B., BRALEY, H., HOLDSWORTH, S. R. & KITCHING, A. R. 2009. Th1 and Th17 cells induce proliferative glomerulonephritis. *J Am Soc Nephrol,* 20**,** 2518-24.

TANG, S. C. & LAI, K. N. 2013. Hepatitis C virus-associated glomerulonephritis. *Contrib Nephrol,* 181**,** 194-206.
TANG, Y. C. & AMON, A. 2013. Gene copy-number alterations: a cost-benefit analysis. *Cell,* 152**,** 394-405.
THEOFILOPOULOS, A. N. & DIXON, F. J. 1981. Etiopathogenesis of murine SLE. *Immunol Rev,* 55**,** 179-216.
THÉRY, C. & AMIGORENA, S. 2001. The cell biology of antigen presentation in dendritic cells. *Curr Opin Immunol,* 13**,** 45-51.
TIEGS, G. & LOHSE, A. W. 2010. Immune tolerance: what is unique about the liver. *J Autoimmun,* 34**,** 1-6.
TIPPING, P. G., NEALE, T. J. & HOLDSWORTH, S. R. 1985. T lymphocyte participation in antibody-induced experimental glomerulonephritis. *Kidney Int,* 27**,** 530-7.
TOMAS, N. M., BECK, L. H., JR., MEYER-SCHWESINGER, C., SEITZ-POLSKI, B., MA, H., ZAHNER, G., DOLLA, G., HOXHA, E., HELMCHEN, U., DABERT-GAY, A. S., DEBAYLE, D., MERCHANT, M., KLEIN, J., SALANT, D. J., STAHL, R. A. K. & LAMBEAU, G. 2014. Thrombospondin type-1 domain-containing 7A in idiopathic membranous nephropathy. *N Engl J Med,* 371**,** 2277-2287.
TOWBIN, H., STAEHELIN, T. & GORDON, J. 1979. Electrophoretic transfer of proteins from polyacrylamide gels to nitrocellulose sheets: procedure and some applications. *Proc Natl Acad Sci U S A,* 76**,** 4350-4.
UNGER, W. W., VAN BEELEN, A. J., BRUIJNS, S. C., JOSHI, M., FEHRES, C. M., VAN BLOOIS, L., VERSTEGE, M. I., AMBROSINI, M., KALAY, H., NAZMI, K., BOLSCHER, J. G., HOOIJBERG, E., DE GRUIJL, T. D., STORM, G. & VAN KOOYK, Y. 2012. Glycan-modified liposomes boost CD4+ and CD8+ T-cell responses by targeting DC-SIGN on dendritic cells. *J Control Release,* 160**,** 88-95.
VAN MONTFOORT, N., CAMPS, M. G., KHAN, S., FILIPPOV, D. V., WETERINGS, J. J., GRIFFITH, J. M., GEUZE, H. J., VAN HALL, T., VERBEEK, J. S., MELIEF, C. J. & OSSENDORP, F. 2009. Antigen storage compartments in mature dendritic cells facilitate prolonged cytotoxic T lymphocyte cross-priming capacity. *Proc Natl Acad Sci U S A,* 106**,** 6730-5.
VANDESOMPELE, J., DE PRETER, K., PATTYN, F., POPPE, B., VAN ROY, N., DE PAEPE, A. & SPELEMAN, F. 2002. Accurate normalization of real-time quantitative RT-PCR data by geometric averaging of multiple internal control genes. *Genome Biol,* 3**,** Research0034.
VINAY, P., GOUGOUX, A. & LEMIEUX, G. 1981. Isolation of a pure suspension of rat proximal tubules. *Am J Physiol,* 241**,** F403-11.
VIVARELLI, M., MASSELLA, L., RUGGIERO, B. & EMMA, F. 2017. Minimal Change Disease. *Clin J Am Soc Nephrol,* 12**,** 332-345.
WALTER, U. & SANTAMARIA, P. 2005. CD8+ T cells in autoimmunity. *Curr Opin Immunol,* 17**,** 624-31.
WATTS, C. 1997. Capture and processing of exogenous antigens for presentation on MHC molecules. *Annu Rev Immunol,* 15**,** 821-50.
WECK, M. M., APPEL, S., WERTH, D., SINZGER, C., BRINGMANN, A., GRÜNEBACH, F. & BROSSART, P. 2008. hDectin-1 is involved in uptake and cross-presentation of cellular antigens. *Blood,* 111**,** 4264-72.
WETHMAR, K., SMINK, J. J. & LEUTZ, A. 2010. Upstream open reading frames: molecular switches in (patho)physiology. *Bioessays,* 32**,** 885-93.
WILKINSON, R., WANG, X., ROPER, K. E. & HEALY, H. 2011. Activated human renal tubular cells inhibit autologous immune responses. *Nephrol Dial Transplant,* 26**,** 1483-92.
WOLTMAN, A. M., DE FIJTER, J. W., ZUIDWIJK, K., VLUG, A. G., BAJEMA, I. M., VAN DER KOOIJ, S. W., VAN HAM, V. & VAN KOOTEN, C. 2007. Quantification of dendritic cell subsets in human renal tissue under normal and pathological conditions. *Kidney Int,* 71**,** 1001-8.
WU, Q., JINDE, K., ENDOH, M. & SAKAI, H. 2004. Clinical significance of costimulatory molecules CD80/CD86 expression in IgA nephropathy. *Kidney Int,* 65**,** 888-96.
WUTHRICH, R. P., YUI, M. A., MAZOUJIAN, G., NABAVI, N., GLIMCHER, L. H. & KELLEY, V. E. 1989. Enhanced MHC class II expression in renal proximal tubules precedes loss of renal function in MRL/lpr mice with lupus nephritis. *Am J Pathol,* 134**,** 45-51.

YE, Y., SHIBATA, Y., YUN, C., RON, D. & RAPOPORT, T. A. 2004. A membrane protein complex mediates retro-translocation from the ER lumen into the cytosol. *Nature,* 429**,** 841-7.

ZEB, Q., WANG, C., SHAFIQ, S. & LIU, L. 2019. Chapter 6 - An Overview of Single-Cell Isolation Techniques. *In:* BARH, D. & AZEVEDO, V. (eds.) *Single-Cell Omics.* Academic Press.

ZEHNER, M., CHASAN, A. I., SCHUETTE, V., EMBGENBROICH, M., QUAST, T., KOLANUS, W. & BURGDORF, S. 2011. Mannose receptor polyubiquitination regulates endosomal recruitment of p97 and cytosolic antigen translocation for cross-presentation. *Proc Natl Acad Sci U S A,* 108**,** 9933-8.

ZEHNER, M., MARSCHALL, A. L., BOS, E., SCHLOETEL, J. G., KREER, C., FEHRENSCHILD, D., LIMMER, A., OSSENDORP, F., LANG, T., KOSTER, A. J., DÜBEL, S. & BURGDORF, S. 2015. The translocon protein Sec61 mediates antigen transport from endosomes in the cytosol for cross-presentation to CD8(+) T cells. *Immunity,* 42**,** 850-63.

ZOJA, C., BENIGNI, A. & REMUZZI, G. 2004. Cellular responses to protein overload: key event in renal disease progression. *Curr Opin Nephrol Hypertens,* 13**,** 31-7.

9 List of figures

10 List of tables

11 Abbreviations

2-ME	2-mercaptoethanol
Actb	beta-actin
ANCA	antineutrophil cytoplasmic antibodies
ANOVA	analysis of variance
AP	alkaline phosphatase
APC	antigen presenting cell
BSA	bovine serum albumin
CD	cluster of differentiation
cDNA	complementary DNA
cGN	crescentic glomerulonephritis
ct	cycle of threshold
Cybb	cytochrome b-245 beta chain
DAB	3,3′-Diaminobenzidine
DC	dendritic cell
DMEM/F12	Dulbecco's Modified Eagle Medium: Nutrient Mixture F12
DNA	deoxyribonucleic acid
dNTP	deoxynucleoside triphosphate
EDTA	ethylenediaminetetraacetic acid
EGFP	enhanced green fluorescent protein
ER	endoplasmic reticulum
ERAD	endoplasmic reticulum-associated degradation
EtOH	ethanol
FACS	fluorescence activated cell sorting
FBS	fetal bovine serum
Fc	fragment crystallizable
FSC	forward scatter
GAPDH	glyceraldehyde 3-phosphate dehydrogenase
GBM	glomerular basement membrane
GM-CSF	granulocyte-macrophage colony-stimulating factor
Gzmb	granzyme B
H2-D	histocompatibility 2, D region locus 1
HBSS	Hank's Balanced Salt Solution
HIER	heat induced epitope retrieval
HPF	high power field
HRP	horseradish peroxidase
i.p.	intraperitoneal
IFN	interferon
Ig	immunoglobulin
IL	interleukin
IRAP	insulin-regulated aminopeptidase

LDS	lithium dodecyl sulfate
LNPEP	leucyl and cystinyl aminopeptidase
LMP	low-molecular-weight protein
LSEC	liver sinusoidal endothelial cell
MACS	magnetic activated cell sorting
MECL	multicatalytic endopeptidase complex subunit
MES	(2-(N-morpholino)ethanesulfonic acid
MHC	major histocompatibility complex
MMR/Mrc1	mannose receptor
MRL	MRL/MpJ
MRL-lpr	MRL/MpJ-*Fas*^{lpr}/J
mRNA	messanger RNA
MPO	myeloperoxidase
NOX2	NADPH oxidase 2
ns	not significant
NTS	nephrotoxic serum
OVA	ovalbumin
PAGE	polyacrylamide gel electrophoresis
PBS	phosphate-buffered saline
PCR	polymerase chain reaction
PD-L1	programmed cell death ligand 1
PMSF	phenylmethylsulfonyl fluoride
Psmb8	Proteasome subunit beta type-8
PTEC	proximal tubular epithelial cell
qRT-PCR	quantitative real-time polymerase chain reaction
RNA	ribonucleic acid
RPMI	Roswell Park Memorial Institute
RT	reverse transcription
SDS	sodium dodecyl sulfate
SEM	standard error mean
SLE	systemic lupus erythematosus
SSC	side scatter
Tap	transporter associated with antigen processing
TBS	tris-buffered saline
TCR	T cell receptor
TGF	transforming growth factor
TMB	3,3′,5,5′-Tetramethylbenzidine
TNF	tumor necrosis factor
VCP	valosin-containing protein
WT	wild-type

12 Acknowledgments

Zuallererst möchte ich Frau Prof. Gisa Tiegs danken für die Möglichkeit, in ihrem Labor als Teil ihres Teams an diesem äußerst interessanten Forschungsthema arbeiten zu dürfen. Ebenso möchte ich Herrn Prof. Ulf Panzer als Sprecher des Sonderforschungsbereichs 1192 „Immune-Mediated Glomerular Diseases“ danken, in dessen Graduiertenkolleg ich eine exzellente Betreuung genießen und in regem Austausch mit anderen Kommiliton:innen, Wissenschaftler:innen und Professor:innen stehen konnte. Weiterhin möchte ich Herrn Prof. Hans-Willi Mittrücker sowie Herrn Prof. Samuel Huber für ihre konstruktiven Ratschläge im Rahmen des Betreuungskommissionstreffens danken. Für die exzellente Organisation des Graduiertenkollegs möchte ich auch Frau Anett Peters danken. Darüber hinaus bin ich der Else Kröner-Fresenius-Stiftung für die Förderung dieser Arbeit im Rahmen eines einjährigen Forschungsstipendiums dankbar.

Besonderer Dank gilt meiner Betreuerin PD Dr. Katrin Neumann. Sie führte mich geduldig an wissenschaftliche Praktiken heran, gab mir Freiraum, eigenständig wissenschaftlich zu arbeiten, und hatte immer Zeit, mir bei Fragen oder Problemen mit klugen Ratschlägen zu helfen. Besonders danken möchte ich ihr auch für das Lesen meiner Disseration, zu der sie mir ausführliche und wertvolle Kommentare sowie Verbesserungsvorschläge gab. Für die technische Unterstützung im Labor möchte ich Carsten Rothkegel und Elena Tasika danken. Ebenso gilt mein Dank PD Dr. Andrea Horst und Ph.D. Kingsley Kumashie, mit denen ich im Labor faszinierenden und unterhaltsamen Austausch genießen konnte.

Spezieller Dank gilt auch meinen Freunden, insbesondere Till Dobner, Lennart Bauditz und Malte Kuehl, die mich während meiner Doktorarbeit wissenschaftlich und vor allem auch freundschaftlich unterstützt haben.
Abschließend möchte ich insbesondere meinen Eltern danken für ihre liebevolle und exzellente Erziehung. Sie legten mir bereits sehr früh die Wichtigkeit von Bildung und wissenschaftlichem Interesse nahe. Ohne sie wäre diese Arbeit nicht möglich gewesen.

13 Publications

Transcriptional and Clonal Characterization of Cytotoxic T cells in Crescentic Glomerulonephritis.
Mueller A, Zhao Y, **Cicek H**, Paust HJ, Sivayoganathan A, Linke A, Wegscheid C, Wiech T, Huber TB, Meyer-Schwesinger C, Bonn S, Prinz I, Panzer U, Tiegs G, Krebs CF, Neumann K.
In: Journal of the American Society of Nephrology. 2023 Mar 13.

Antigen Cross-Presentation by Murine Proximal Tubular Epithelial Cells Induces Cytotoxic and Inflammatory CD8+ T Cells.
Linke A*, **Cicek H***, Müller A, Meyer-Schwesinger C, Melderis S, Wiech T, Wegscheid C, Ridder J, Steinmetz OM, Diehl L, Tiegs G, Neumann K.
In: Cells. 2022 Apr 30;11(9):1510.
*These authors contributed equally to this work

14 Curriculum vitae

Lebenslauf aus datenschutzrechtlichen Gründen nicht enthalten.

15 Eidesstattliche Versicherung

10. Eidesstattliche Versicherung

Ich versichere ausdrücklich, dass ich die Arbeit selbständig und ohne fremde Hilfe verfasst, andere als die von mir angegebenen Quellen und Hilfsmittel nicht benutzt und die aus den benutzten Werken wörtlich oder inhaltlich entnommenen Stellen einzeln nach Ausgabe (Auflage und Jahr des Erscheinens), Band und Seite des benutzten Werkes kenntlich gemacht habe.
Ferner versichere ich, dass ich die Dissertation bisher nicht einem Fachvertreter an einer anderen Hochschule zur Überprüfung vorgelegt oder mich anderweitig um Zulassung zur Promotion beworben habe.
Ich erkläre mich einverstanden, dass meine Dissertation vom Dekanat der Medizinischen Fakultät mit einer gängigen Software zur Erkennung von Plagiaten überprüft werden kann.

Unterschrift: .....